2013

Identification of a target using its natural poles using both frequency and time domain response

Woojin Lee

ABSTRACT

A new methodology for detection and identification of unknown objects in free space or on ground, or under the ground is presented in this dissertation. The Singularity Expansion Method (SEM) is introduced because it is possible to find the natural resonant frequencies of a scatterer from the scattered fields and use the resonant frequencies for identification. Many techniques to extract singularities of the EM response of an object are studied and then the Cauchy and the Matrix Pencil (MP) methods are chosen to carry out the processing. In the first part of the dissertation, a methodology for the computation of the natural poles of an object in the frequency domain is presented. The main advantage of this methodology is that there is no need to differentiate between the early time and the late time response of the object as required in the SEM and the Cauchy method can be applied directly to the frequency domain data to extract the SEM poles. Thus, one can generate a library of poles of various objects using the Cauchy method.

In the second part of the dissertation, the methodology for detecting and identifying an unknown object in the time domain is also presented. For the simulation model, one transmitter and two receivers (dipole antennas) are utilized to obtain the object response. The received currents of the unknown object are computed by using the deconvolving procedure. The MP method is applied for extracting natural poles of the late time response of the unknown object and the Time-Difference-of-Arrival (TDOA) technique is utilized to obtain the location of the objects. Therefore, by generating the pole library using the frequency domain data and simultaneous use of the actual poles computed using the time domain data, the correlation between the two pole sets obtained using totally different methodologies can provide a robust identification procedure.

IDENTIFICATION OF A TARGET USING ITS NATURAL POLES USING BOTH FREQUENCY AND TIME DOMAIN RESPONSE

By

Woojin Lee

B.E., Korea Military Academy (KMA), Republic of Korea, 1998

M.S., Gwangju Institute of Science and Technology (GIST), Republic of Korea, 2003

DISSERTATION

Submitted in partial fulfillment of the requirements for the

Degree of Doctor of Philosophy in Electrical Engineering

in the Graduate School of Syracuse University

June 2013

ACKNOWLEDGEMENT

First of all, I would like to glorify our Lord, Jesus Christ. I have completed one of important tasks of my life with his grace, mercy, and love. Also, I would like to express my deep gratitude to my advisor, Professor Tapan K. Sarkar for his guidance and support in my study. I deeply respect him for his vast knowledge, numerous suggestions, and strong passion. I am also grateful to my co-advisor, Dr. Magdalena Salazar-Palma for her advice on my dissertation.

I am grateful to my dissertation committee, Dr. Jay K. Lee, Dr. Carlos Hartmann, Dr. Fred Schlereth, Dr. Tomislav Bujanovic, and the committee chair, Dr. Jeongmin Ahn for their advice and opinions.

I am also grateful to my colleagues in the CEMLAB, Hongsik Moon, Zicong Mei, Weixin Zhao, Latoya Brown, Walid Dyab, Mohammad Abdallah, Tanawut Tantisopharak, Runzhong Li, Dr. Baek-Ho Jung, Dr. Yongseek Chung, Dr. Ic Pyo Hong, Dr. Yu Zhang, Dr. Santana Burintramart, Dr. Mary C. Taylor, Dr. Arijit De, Dr. Xiaopeng Yang, Dr. Sio W. Ting, Dr. Sai H. Yeung, and especially Dr. Jinhwan Koh for their helpful discussion, assistant, and friendship. I would like to thank all the Korean EECS members for their support and valuable friendship.

I am grateful to my country, Republic of Korea, especially Army for providing a good opportunity to study a Ph.D. program in USA.

Finally, I would like to express my deepest gratitude to my parents and family members, especially my wife, Hyekyung Nah, for their love, support, and prayer. I also would like to express my love to children, Hwanhee and Hwanjoon.

LIST OF CONTENTS

LIST OF TABLES

LIST OF FIGURES

1. INTRODUCTION

1.1. Background

The history of the radar system starts with experiments to verify the theory of Maxwell by Heinrich Hertz in 1886 showed that radio waves could be reflected by metallic and dielectric bodies. Even though several investigators simultaneously had made advancements in the field of a radar prior to World War II, the research and development of the true radar systems spurred during World War II because a radar must both detect a target and provide range information for a target [1]. Thus, the radar system has long been used for detection and identification of objects using the reflected scattered energy from the illuminated target of a radar system. The current problem to solve for the scattered electromagnetic (EM) field is to detect and identify various objects with different shapes, made of composite materials and may be buried underground. Multiple studies to solve these problems have been performed using the resonance phenomena produced by the EM field from an object because it is possible to find its natural resonant frequencies for identification of an object. The Singularity Expansion Method (SEM) introduced by C. E. Baum [2] was to find the natural resonant frequencies of an object from the late time response.

There are the well-known relationships between the resonant signature of an object and its late time response. If we illuminate an object with a plane wave then, the backscattered energy from the object contains important information which can be used for identification. If we consider the mechanisms of backscattering from an object, the backscattered energy is composed of two parts. The first part is the impulsive part corresponding to the early time response, i.e. it is the direct reflection of the incident

wave from the surface of the object. The second part is the oscillatory part corresponding to the late time response, i.e. it consists of surface creeping wave (external resonances) and cavity wave (internal resonances) related to the resonance phenomena. In the case of perfectly conducting objects (PEC), only external resonances exist. Hence, one can obtain object signatures (dimension, shape, constitution, etc.) using the SEM poles. Therefore, the SEM methodology can provide a pair of complex conjugate poles corresponding to the damped sinusoids from typical transient temporal response of various objects (e.g., antennas, canonical objects, and aircrafts).

Many techniques to extract singularities of the EM response of an object have been developed by studying either the impulse response of an object in the time domain or its transfer function in the frequency domain [3]-[27]. In the time domain, the most popular techniques of poles extractions are based on Prony's method [6]-[10] and the Matrix Pencil (MP) method [11]-[15]. Generally, the signal model of the observed late time of an EM scattered response from an object can be represented by a sum of complex exponentials with parameters (poles and residues). Prony's method introduced by R. Prony [6] was based on the fact that the poles are roots of a polynomial whose coefficients satisfy a set of linear prediction equations, whereas the MP method developed by Y. Hua and T. K. Sarkar [11] can directly solve for the poles and residues by using the generalized eigenvalues of a matrix pencil generated from the scattered data. The MP method is more robust to noise present in the sampled data and computationally more efficient than Prony's method [12].

The frequency domain techniques to extract poles and residues can be more advantageous than the time domain techniques because one can directly use the

frequency domain data of an object without transforming the frequency domain data into the time domain data. A. L. Cauchy was the first to propose a rational function approximation to interpolate the signal data [16]. Then it was modified (Cauchy method) to extract poles and residues based on the approximation of the given data by a transfer function consisting of a ratio of two polynomials [17]-[20]. Also, many papers have been published for its application in signal modeling, filter design, analysis of scattering from an object [21]-[25] and so on.

Each of the technique has advantages and disadvantages. The advantage of the frequency domain techniques is that it is not necessary to identify the early time and the late time region. The disadvantage of the frequency domain techniques is that one can get only the object signature. It means one cannot get any information where the object is located. The time domain techniques can provide us with the location of a detected object using the Time-Difference-of-Arrival (TDOA). But the time domain techniques have the restriction that only the late time response can be used to extract natural poles of an object.

1.2. Objectives

The first objective of this dissertation is to illustrate that information about the SEM poles can also be obtained in the frequency domain where the restriction of the late time response to the SEM formulation is non-existent. Therefore we generate the library of poles for different objects entirely in the frequency domain using the Cauchy method. Thus, in this procedure for pole extraction, it is not necessary to identify the early time and the late time regions where the SEM formulation has this requirement. The Cauchy method is based on the approximation of a transfer function of a Linear Time Invariant System (LTI) in the frequency domain using a rational function approximation. The computations of the poles are carried out using the Cauchy method by approximating the transfer function as a ratio of two polynomials. This is different from the usual way of obtaining the SEM poles by applying the MP method to the late time response. The unique feature of the Cauchy method is that it is not necessary to distinguish between the early and the late time responses as all the computations are carried out in the time domain and this may make this procedure accurate and efficient. Thus, one can generate a library of poles of various objects using the Cauchy method.

The second objective is to describe that by observing the complete impulse response, the presence of a single object or multiple objects can be determined. Then the MP method can be applied to the late time response of this transient temporal impulse response. In the time domain it is relatively easier to locate the late time response corresponding to the resonant region. The MP method approximates a time domain function by a sum of complex exponentials and this approximation is valid only for the late time response. By generating the pole library using the frequency domain data and

the actual poles computed using the time domain data, we illustrate that the correlation between the two pole sets obtained using totally different methodologies provide a robust identification procedure [26], [27]. The poles using responses from data generated in different domains can be used for comparison purposes. It is important to note that in the time domain one has to be careful about the early time and the late time response, only the late time domain response data can be utilized.

The third objective is to illustrate a procedure to obtain the accurate coordinates (radial distance and azimuthal angle) of an unknown object using the time difference between the impulses from two receivers. The specific time of each impulse represents the time delay from each receiver for the unknown object, which has the information of the distance of the illuminated surface of the object from each receiver.

Hence, the goal of this research is to propose the use of a robust methodology to generate a library of poles of various objects and then these signatures can now be compared by using data from the time domain to replicate essentially the same results. Therefore, one can not only identify the number of unknown objects to be discriminated but also the coordinates of the location of the objects using the proposed robust identification procedure.

1.3. The Scope of the Dissertation

The dissertation is divided into six chapters. The first chapter provides a short background including a survey of the present state of knowledge about the use of the frequency and time domain techniques to extract the SEM poles for various objects.

The second chapter presents the Cauchy method and illustrates its use for generating a library of poles of various objects (a wire, a disk, an ellipsoid, a cone, two spheres, and a cylinder). Simulation examples illustrate this novel and accurate way for finding the SEM poles. Each example is selected considering the characteristic size. It also addresses criteria needed for the extraction of the SEM poles.

The third chapter discusses a proposed methodology for detecting and identifying the unknown object based on the MP method and the TDOA in the time domain. It also presents different criteria needed for an object identification using a simulation example.

The fourth chapter deals entirely with a proposed methodology for simultaneous identification of multiple PEC objects in free space. Various examples of multiple objects for identification are presented and discussed.

The fifth chapter deals with identification of a single object located on an urban ground. It shows that the proposed methodology can be applied not only to characterize unknown objects in free space but also detects an unknown object on ground. This chapter also discusses the proposed methodology for identification of an unknown object under the ground. Some simulation examples related to identification of an object are presented. The sixth chapter provides a conclusion to the current research.

2. PROCEDURE TO MAKE A LIBRARY OF POLES OF OBJECTS IN THE FREQUENCY DOMAIN

2.1. Overview

The procedure to make a library of poles of objects based on the Cauchy method is presented in this chapter. The Cauchy method is a well-known technique for interpolation and extrapolation of data using a ratio of two polynomials. The origin of the Cauchy method starts from interpolating data with a ratio of two polynomials (numerator and denominator polynomials) [16]. This concept is then extended to extrapolate and/or interpolate the wide-band response of Electromagnetic (EM) systems using narrow-band data [17]-[18]. It means that the Cauchy method can be used to speed up the numerical computations of parameters (residues and poles) related to the impedance, currents, and the scattering data from any linear time-invariant (LTI) EM systems.

From the basic methodology of the Cauchy method, one can find poles of the EM response using denominator polynomials in the frequency domain. The extracted poles from denominator polynomials are directly related to the resonance characteristics of the object. Thus, one methodology to find the natural poles of an object is to use the Cauchy method in the frequency domain. The important advantage of the Cauchy method is that since the computation of the SEM poles is carried out in the frequency domain, there is no need to differentiate between the early time and the late time response of the object.

This chapter starts with the procedure of the Cauchy method and then explains how to extract the natural poles of the PEC sphere. Finally, this chapter shows a library of poles of various objects obtained by applying this technique..

2.2. Application of the Cauchy Method to Find Natural Poles

The Cauchy method starts by assuming that the parameter of interest which is to be extrapolated and/or interpolated, as a function of frequency, can be performed using a ratio of two polynomials. This procedure holds for an LTI system [28]. Let us assume that the system response is from an LTI system. The transfer function $H(f)$ for the LTI system, as a rational function of frequency, can be characterized by

$$H(f_i) \approx \frac{A(f_i)}{B(f_i)} = \frac{\sum_{k=0}^{P} a_k f_i^k}{\sum_{k=0}^{Q} b_k f_i^k}, \qquad i = 1, 2, \cdots N \tag{2.1}$$

where the numerator and denominator polynomials are given by $A(f)$ and $B(f)$, respectively. For convenience and computational simplicity, we assume

$$Q = P + 1 \tag{2.2}$$

where P is the order of the numerator polynomial and Q is the order of the denominator polynomial. As seen from (2.1), the unknown coefficients a_k and b_k can be put into the following form:

$$[A]_{N\times(P+1)}\, a_{(P+1)\times 1} = [B]_{N\times(Q+1)}\, b_{(Q+1)\times 1} \tag{2.3}$$

or

$$[A \quad -B]_{N\times(P+Q+2)} \begin{bmatrix} a \\ b \end{bmatrix}_{(P+Q+2)\times 1} = 0 \quad \Rightarrow \quad [C]_{N\times(P+Q+2)} \begin{bmatrix} a \\ b \end{bmatrix}_{(P+Q+2)\times 1} = 0 \tag{2.4}$$

where

$$[a] = \left[a_0, a_1, a_2, \cdots, a_P\right]^T \tag{2.5}$$

$$[b] = \left[b_0, b_1, b_2, \cdots, b_Q\right]^T \tag{2.6}$$

and

$$[C]=\underbrace{\begin{bmatrix}1 & f_1 & \cdots & f_1^P\\ 1 & f_2 & \cdots & f_2^P\\ \vdots & \vdots & \ddots & \vdots\\ 1 & f_N & \cdots & f_N^P\end{bmatrix}}_{[A]}\underbrace{\begin{bmatrix}-H(f_1) & -H(f_1)f_1 & \cdots & -H(f_1)f_1^Q\\ -H(f_2) & -H(f_2)f_2 & \cdots & -H(f_2)f_2^Q\\ \vdots & \vdots & \ddots & \vdots\\ -H(f_N) & -H(f_N)f_N & & -H(f_N)f_N^Q\end{bmatrix}}_{[-B]} \tag{2.7}$$

Here, the superscript T denotes the transpose of a matrix. The size of the matrix $[C]$ is $N\times(P+Q+2)$, so the solution of $[a]$ and $[b]$ are unique only if the total number of the frequency sample points are greater than or equal to the number of unknown coefficients $P+Q+2$.

$$N\geq P+Q+2 \tag{2.8}$$

The singular value decomposition (SVD) [29] of the matrix $[C]$ will give us an estimate for the required values of P and Q. A SVD of the matrix $[C]$ results in

$$[U][\Sigma][V]^H\begin{bmatrix}a\\ b\end{bmatrix}=0 \tag{2.9}$$

where the matrices $[U]$ and $[V]$ are unitary matrices, i.e.,

$$\begin{aligned}[U]^H[U]&=[I]\\ [V]^H[V]&=[I]\end{aligned} \tag{2.10}$$

The superscript H denotes the conjugate transpose of a matrix. $[\Sigma]$ is a diagonal matrix with the singular values of the matrix $[C]$ in descending order as its entries.

$$\Sigma=\begin{bmatrix}\sigma_1 & & & & & \\ & \sigma_2 & & & & \\ & & \ddots & & & \\ & & & \sigma_R & & \\ & & & & 0 & \\ & & & & & \ddots\end{bmatrix}\qquad \sigma_1\geq\sigma_2\geq\cdots\sigma_R>0 \tag{2.11}$$

The columns of the matrix [U] are the left singular vectors of the matrix [C] or the eigenvectors of the matrix [C][C]^H. The columns of the matrix [V] are the right singular vectors of matrix [C] or the eigenvectors of the matrix [C]^H[C]. The singular values are the square roots of the eigenvalues of the matrix [C]^H[C]. Therefore, the singular values of any matrix are real and positive. The number of nonzero singular values of the matrix [C] is the rank (R) of the matrix [C] and they contain the information content of the system transfer function $H(f)$. Therefore, the knowledge of the number of nonzero singular values does provide useful information for the rank of the system.

For the validation of this approximation given by (2.4), the smallest singular value should be less than or equal to the number of accurate significant decimal digits of the data. It means that if the data is corrupted by additive noise including numerical noise, the parameters P and Q are estimated by observing the ratio of the various singular values to the largest one as defined by [30]

$$\frac{\sigma_R}{\sigma_{\max}} \approx 10^{-w} \tag{2.12}$$

where w is the number of accurate significant decimal digits of the system response data. Based on w, one can choose the required parameters P and Q to interpolate or extrapolate the data. The computed number of nonzero singular values from the selected parameter P and Q is the rank of the matrix in (2.9), so it provides an idea about the information in this system of simultaneous equations. Since the rank R is the number of nonzero singular values, the dimension of the right null space of [C] is $P+Q+2-R$. The solution vector belongs to this null space. Therefore, to make this solution unique, one needs to make the dimension of this null space approximately 1 so that only one vector defines this space. Hence, P and Q must satisfy the relation

$$R+1=P+Q+2 \tag{2.13}$$

Using (2.13), better estimates for the parameter P and Q are obtained. Letting P and Q represent these new estimates of the polynomial orders, one can regenerate the matrix $[C]$ using (2.7) resulting in

$$[C]_{N\times(P+Q+2)}\begin{bmatrix} a \\ b \end{bmatrix}_{(P+Q+2)\times 1} = [A \quad -B]_{N\times(P+Q+2)}\begin{bmatrix} a \\ b \end{bmatrix}_{(P+Q+2)\times 1} = 0 \tag{2.14}$$

where matrix $[C]$ is a rectangular matrix with more rows than columns. The above equation can be solved by using the total least squares (TLS) method [31]. In the matrix equation of (2.14), the submatrix $[A]$ is a function of the frequency only, and does not depend on the data being observed or measured as illustrated in (2.7). Hence, this matrix is not affected by measurement errors and noise. However, the submatrix $[B]$ is affected by the measurement and computational errors in the evaluation of the transfer function. To take this non-uniformity of noise in the data into account, we first need to perform a QR decomposition [29] of the matrix $[A\ -B]$ up to its first $P+1$ columns. First, we perform a QR decomposition of the submatrix $[A]$ to consider the measurement and computational errors because submatrix $[A]$ is the samples of the frequency variable only and does not include any noise. A QR decomposition of the matrix results in

$$[A]=[Q][R] \tag{2.15}$$

$$[A \quad -B]=Q^T[A \quad -B]=[R \quad -Q^T B] \tag{2.16}$$

$$[R \quad -Q^T B]\begin{bmatrix} a \\ b \end{bmatrix}=\begin{bmatrix} R_{11} & R_{12} \\ 0 & R_{22} \end{bmatrix}\begin{bmatrix} a \\ b \end{bmatrix}=0 \tag{2.17}$$

where Q is a n-by-n orthogonal matrix and R is a n-by-m upper triangular matrix. $[R_{11}]$ is upper triangular matrix and both $[R_{12}]$ and $[R_{22}]$ are affected by the noise in the data. From (2.17), we now equate

$$[R_{22}][b] = 0 \tag{2.18}$$

$$[R_{11}][a] = -[R_{12}][b] \quad \Rightarrow \quad [a] = -[R_{11}]^{-1}[R_{12}][b] \tag{2.19}$$

A SVD of $[R_{22}]$ results in

$$[U'][\Sigma'][V']^H [b] = 0 \tag{2.20}$$

By the theory of TLS, the solution vector $[b]$ is proportional to the last column of the matrix $[V']$ as shown.

$$[b] = [V']_{Q+1} \tag{2.21}$$

This is the optimal solution for the coefficients of the denominator polynomial under the given conditions. Using (2.21) and (2.19), coefficients of the numerator polynomial can be computed and one can interpolate or extrapolate the system response from the numerator and denominator polynomials. Finally, the transfer function $H(f)$ can be rewritten as

$$\begin{aligned} H(f) \approx \frac{A(f)}{B(f)} &= \frac{\sum_{k=0}^{P} a_k f^k}{\sum_{k=0}^{Q} b_k f^k} \\ &\approx \sum_{m=1}^{M} \left(\frac{R_m}{f - \left(\frac{\sigma_m}{j2\pi} + f_m \right)} + \frac{R_m^*}{f - \left(\frac{\sigma_m}{j2\pi} - f_m \right)} \right) \end{aligned} \tag{2.22}$$

where R_m is the residue (R_m^* is the complex conjugate of R_m), σ_m is the damping factor, and f_m is the natural frequency for the mth pole.

2.3. Extracting Natural Poles of a PEC Sphere Using the Cauchy Method

We compute the EM scattering data from a 0.15-m-diameter Perfectly Electric Conductor (PEC) sphere in free space as shown in Figure 2.1 using the Higher Order Basis Based Integral Equation Solver (HOBBIES) simulation program [32]. HOBBIES can be used for solution of various types of electromagnetic field analysis involving electrically large objects of arbitrary shapes composed of complex metallic and dielectric structures in the frequency domain. In this case, a plane wave is applied as an incident wave ($\phi = 0°,\ \theta = 0°,\ E_\phi = 0,\ E_\theta = 1$) and for three different observation angles ($\phi = 0°, \theta = 0°$; $\phi = 0°, \theta = 30°$; and $\phi = 0°, \theta = 60°$). The observed responses are shown in Figure 2.2. In Figure 2.1, the horizontal arrow is the propagation vector corresponding to the incident wave and the vertical arrow is the orientation for the incident E-field vector. The result is generated for the frequency range from 0.01 GHz to 5 GHz (Δf = 0.01 GHz), and the number of samples selected is 500. We used not only the results from the positive frequency data generated by HOBBIES, but also complement it with the response for the negative frequency (conjugate) to reflect its mirror image in the frequency domain.

If we utilize the Cauchy method to get the natural poles of the 0.15-m-diameter PEC sphere without transforming the frequency domain data into the time domain data, we can obtain eight natural poles corresponding to the physical resonances after applying three different criteria to filter out the spurious poles. Perhaps, most of these spurious poles correspond to the early time response of the object.

The first criterion removes the poles having very high damping factors, i.e., ($|\sigma_m| > 8$). A pole having high damping factor implies high radiation energy loss in case

of a perfectly conducting target and it has little contribution to the target response. The second criterion allows one to remove single poles located on the real axis, poles having positive σ, and poles in the frequency range of f_m < 0.01 GHz and f_m > 5 GHz. The natural poles occur in complex conjugate pairs. They generally have a negative damping factor corresponding to a causal and stable system, and since the computed frequency range is from 0.01 GHz to 5 GHz. It means the poles with positive damping factor or single poles have no physical meaning. The third criterion removes the poles having $\left|R_m / \sigma_m\right| < 10^{-4}$ because it has very little contribution to the target response. Figure 2.3 shows the natural poles of the 0.15-m-diameter PEC sphere for three different observation angles using the Cauchy method. One can notice that the poles from these three different realizations corresponding to three different observation angles almost overlap each other because the natural poles are directly related to the late time response (creeping wave) of the PEC object.

Table 2.1 presents the natural poles of the 0.15-m-diameter sphere using the SEM method in the time domain and the Cauchy method in the frequency domain. The natural poles from the SEM and the Cauchy method match very well. Therefore, it is proved that one can use the natural poles of the 0.15-m-diameter PEC sphere using the Cauchy method as a library of poles to identify objects, which does not require any late time characterization of the data.

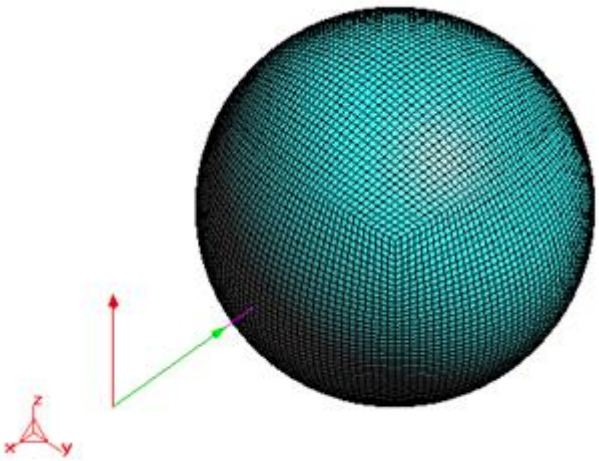

Figure 2.1 HOBBIES simulation model for the 0.15-m-diameter PEC sphere.

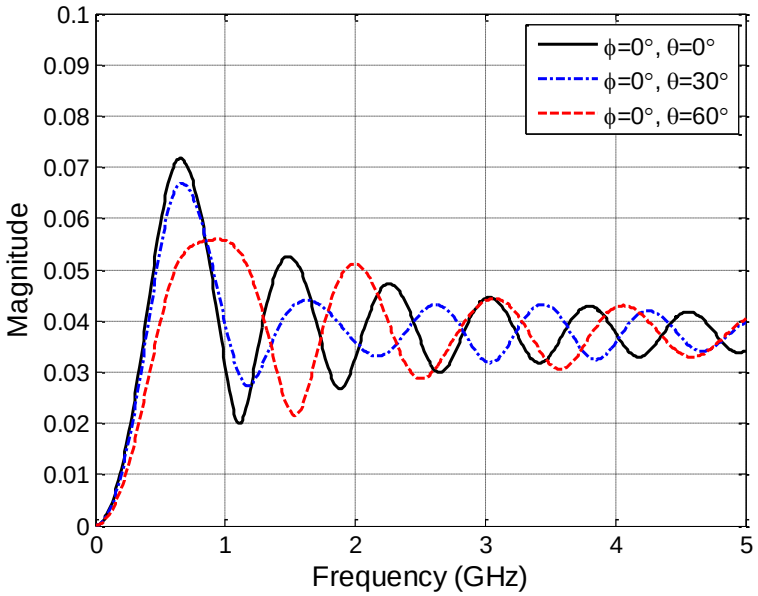

Figure 2.2 Frequency domain response of the HOBBIES model with the 0.15-m-diameter PEC sphere for three observation angles.

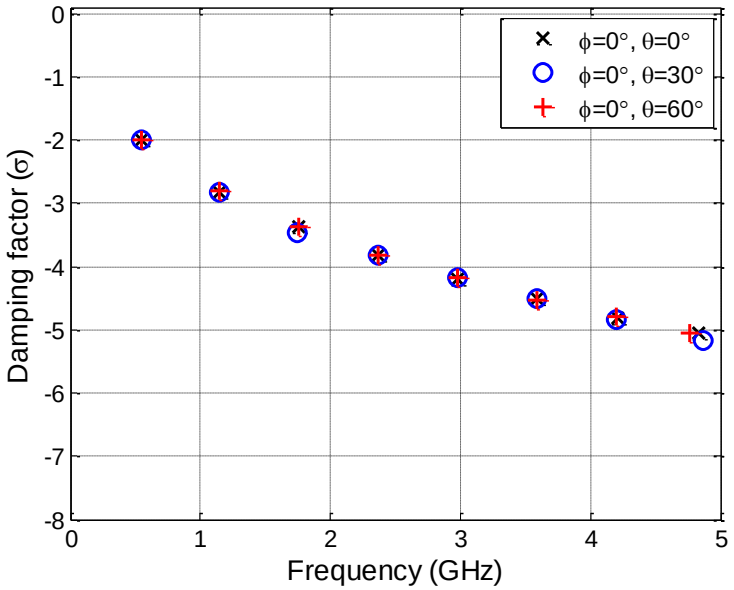

Figure 2.3 Natural poles of the 0.15-m-diameter PEC sphere.

Table 2.1 Natural Poles of the 0.15-m-diameter PEC Sphere from the SEM and the Cauchy Method.

SEM		Cauchy Method	
Damping Factor (σ)	Natural Frequency (GHz)	Damping factor (σ)	Natural Frequency (GHz)
-2.0000	0.5513	-2.0011	0.5504
-2.8080	1.1504	-2.8183	1.1490
-3.3720	1.7558	-3.3758	1.7534
-3.8160	2.3650	-3.8136	2.3638
-4.1920	2.9768	-4.1985	2.9761
-4.5160	3.5918	-4.5086	3.5885
-4.8040	4.2081	-4.8147	4.2081
-5.0680	4.8256	-5.0576	4.8299

2.4. Simulation Examples: Generating a Library of Poles of Objects

Different simulation examples are presented to illustrate the application of this methodology to make a library of poles for different objects. We also generate the EM scattering data from six additional PEC objects, such as a wire, a disk, an ellipsoid, a sphere, a cone, and a cylinder using the HOBBIES simulation program [32]. Each object has the same characteristic size (0.1 m diameter, or length, or height) but they are of different shape as shown in Table 2.2. The thickness of the disk and the ellipsoid are very small. The simulation setup is the same as outlined before. We also apply the same criteria to extract the natural poles of each object.

Figures 2.4, 2.7, 2.10, 2.13, 2.16, and 2.19 show the six HOBBIES simulation models and their frequency domain response for the three observation angles are shown in Figures 2.5, 2.8, 2.11, 2.14, 2.17, and 2.20. From Figures 2.6, 2.9, 2.12, 2.15, and 2.21, it is seen that the poles overlap each other even though the observation angles are different. However, one can see that the higher order poles (3*rd*, 4*th*, and 5*th*) are slightly different when using the frequency domain data than when using the damping factor as shown in Figure 2.18. Perhaps, the damping factor of the higher order poles can fluctuate due to the scattering from various regions of the illuminated surface of the object for the different observation angles. One thing we notice that the first order pole is not changed for the different observation angle because it provides the most significant contribution to the object response.

If we observe the object response, the response of the PEC ellipsoid is very similar to the response of the PEC wire as shown in Figures 2.11 and 2.5. Thus, the resonant frequencies are also very close to each other (PEC ellipsoid: 1.3967, 4.2956,

PEC wire: 1.3339, 4.2265) based on their frequency domain response as shown in Table 2.3. For object identification, one can use not only the first order pole including the damping factor but also the resonant frequencies of the higher order poles.

Figure 2.6 presents the results for a PEC wire, whereas Figure 2.9 provides the data for a PEC disk. The poles for the PEC ellipsoid are presented in Figure 2.12. The poles for a PEC sphere are presented in Figure 2.15 and for a PEC cone in Figure 2.18. The poles for the PEC cylinder are presented in Figure 2.21. The classical SEM poles and the respective resonant frequencies are presented in Table 2.3 for all of these objects. Since the values for the damping factors are not reliable for the higher order poles we present the values only for the imaginary part of the natural poles. From the two spheres of Figures 2.3 and 2.15, one can observe that the resonant frequency of the first order pole decreases and the number of poles increases as the size of the object increases. Notice that for the PEC spheres, if the resonant frequency of the first order pole of a D_1-m-diameter PEC sphere is f_{1D1}, the first order resonant frequency of a D_2-m-diameter PEC sphere (f_{1D2}) can be computed by $f_{1D1} \times D_1 / D_2$ [2], [26]. Therefore, one can also obtain the first order resonant frequency of a 0.15-m-diameter PEC sphere as 0.5511 GHz ($= 0.8267 \times 0.1 / 0.15$) from the first order resonant frequency of a 0.1-m-diameter PEC sphere. Finally, one can identify the unknown object by comparing the pole library with the extracted poles measured from the data in the time domain.

Table 2.2 The Dimension of Each Object.

Target	Dimension
Wire	0.1 m Length, 1 mm radius
Disk	0.1 m Diameter
Ellipsoid	0.02 m Diameter, 0.1 m Length
Sphere	0.1 m Diameter
Cone	0.1 m Diameter, 0.1 m Height
Cylinder	0.1 m Diameter, 0.1 m Height

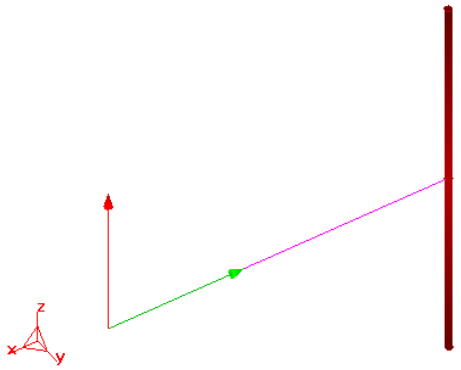

Figure 2.4 HOBBIES simulation model for the 0.1-m-length and 1-mm-radius PEC wire.

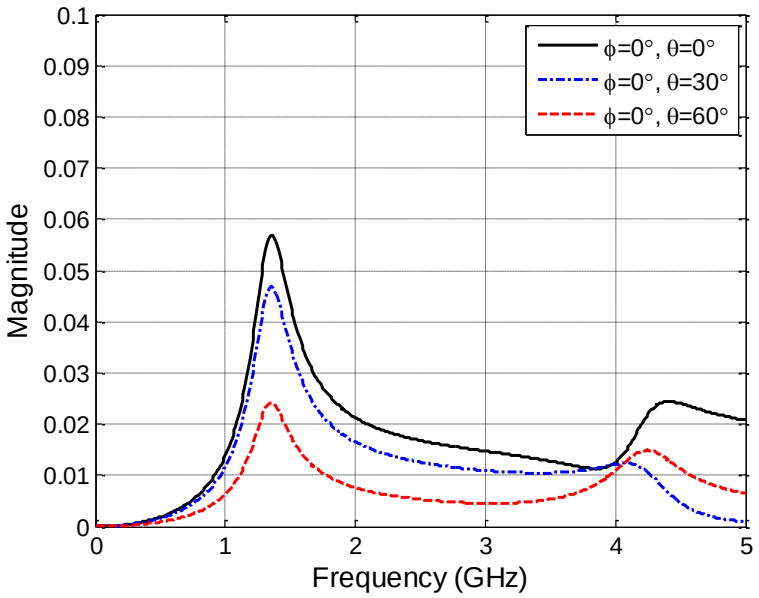

Figure 2.5 Frequency domain response of the HOBBIES model with the 0.1-m-length and 1-mm-radius PEC wire for three observation angles.

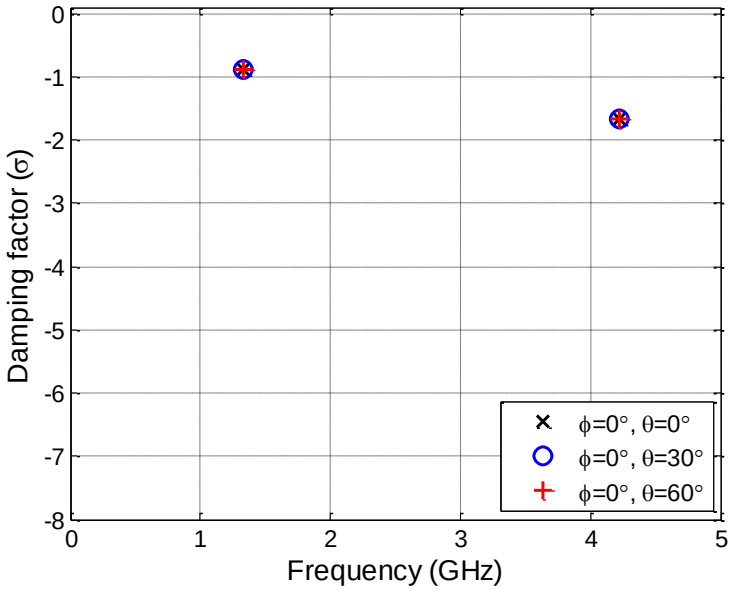

Figure 2.6 Natural poles of the 0.1-m-length and 1-mm-radius PEC wire.

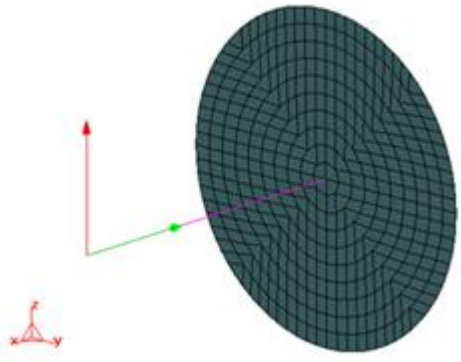

Figure 2.7 HOBBIES simulation model for the 0.1-m-diameter PEC disk.

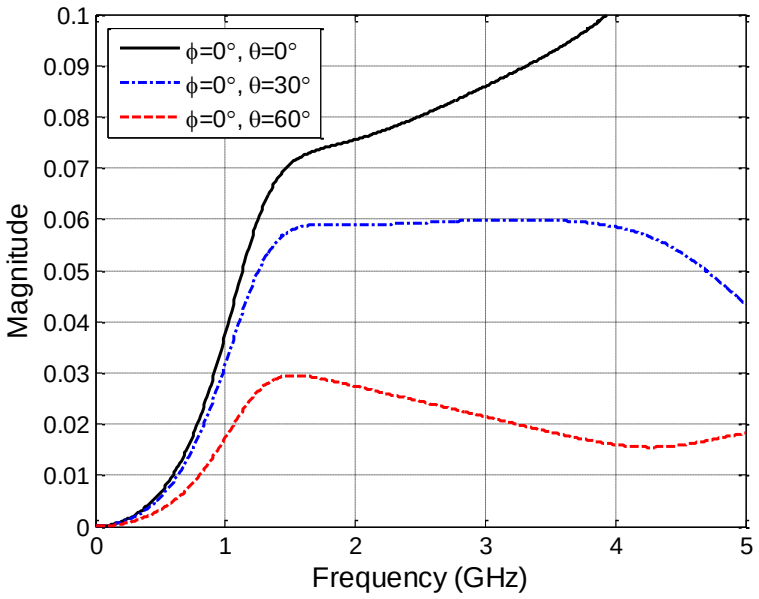

Figure 2.8 Frequency domain response of the HOBBIES model with the 0.1-m-diameter PEC disk for three observation angles.

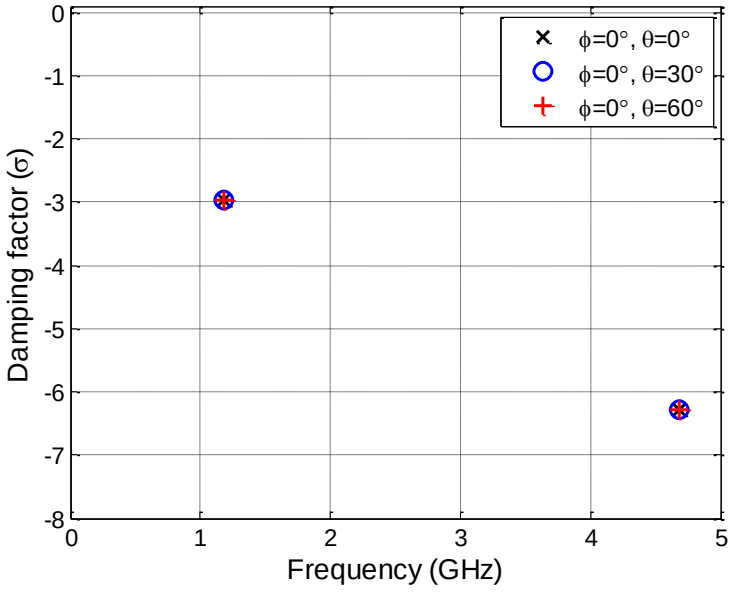

Figure 2.9 Natural poles of the 0.1-m-diameter PEC disk.

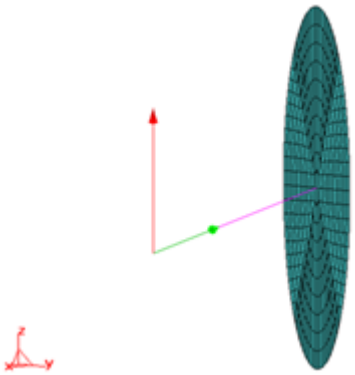

Figure 2.10 HOBBIES simulation model for the 0.02-m-diameter and 0.1-m-length PEC ellipsoid.

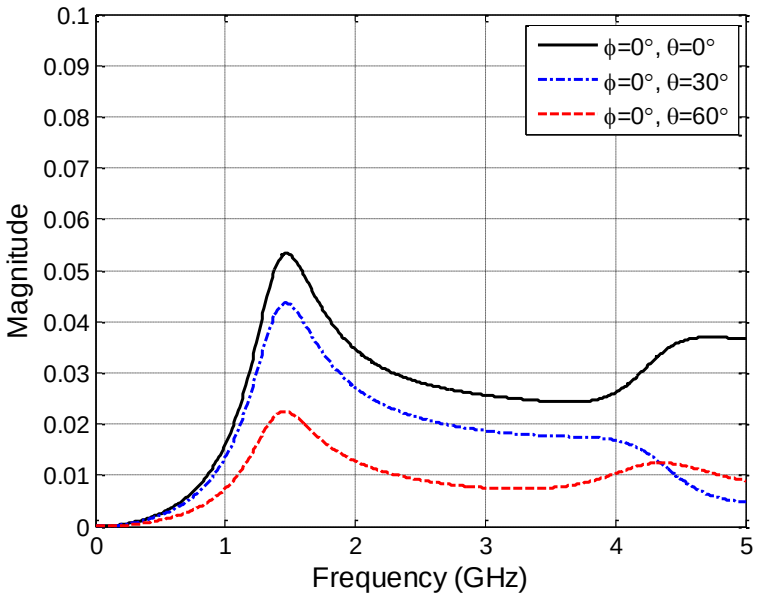

Figure 2.11 Frequency domain response of the HOBBIES model with the 0.02-m-diameter and 0.1-m-length PEC ellipsoid for three observation angles.

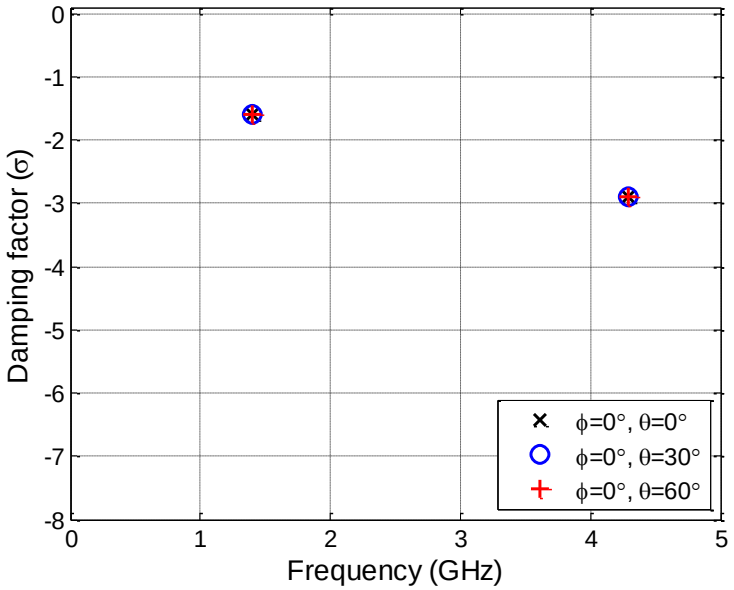

Figure 2.12 Natural poles of the 0.02-m-diameter and 0.1-m-length PEC ellipsoid.

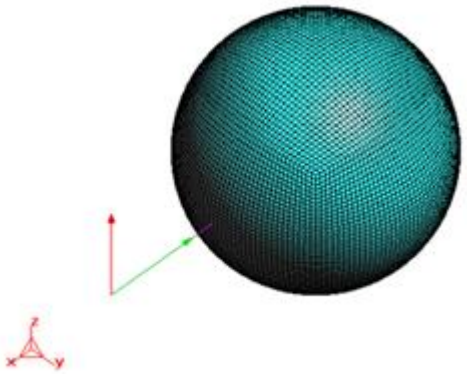

Figure 2.13 HOBBIES simulation model for the 0.1-m-diameter PEC sphere.

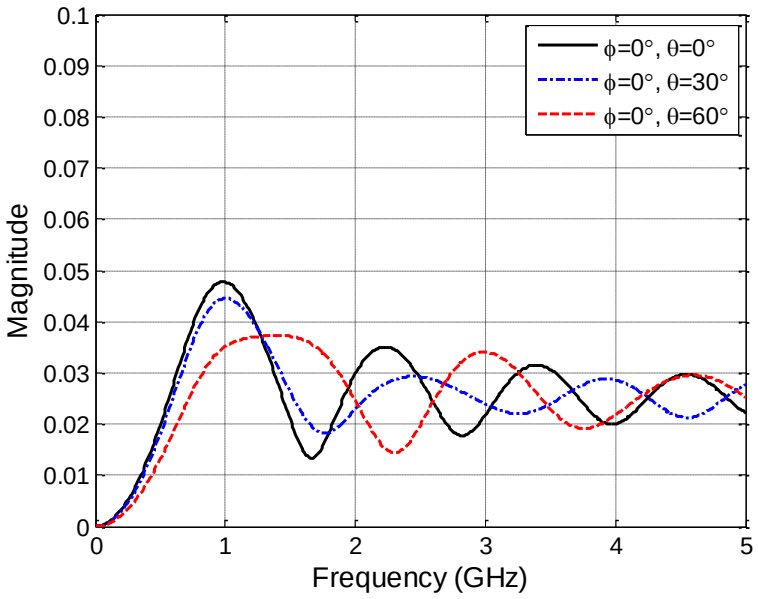

Figure 2.14 Frequency domain response of the HOBBIES model with the 0.1-m-diameter PEC sphere for three observation angles.

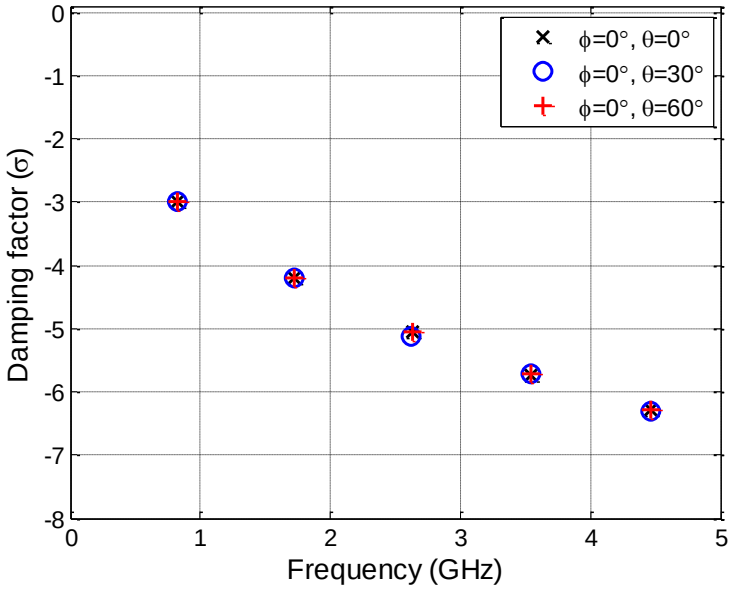

Figure 2.15 Natural poles of the 0.1-m-diameter PEC sphere.

.

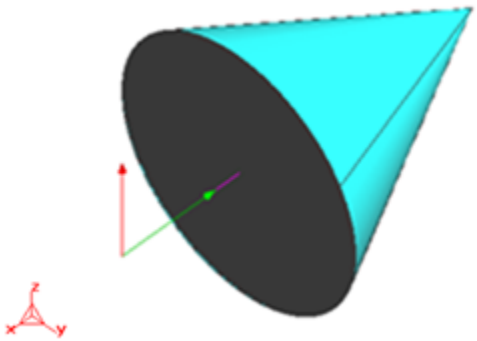

Figure 2.16 HOBBIES simulation model for the 0.1-m-diameter and 0.1-m-height PEC cone.

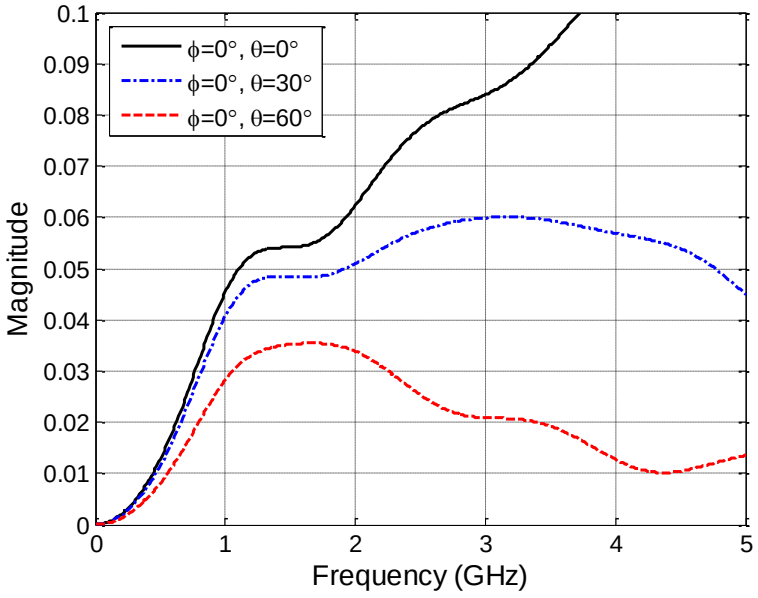

Figure 2.17 Frequency domain response of the HOBBIES model with the 0.1-m-diameter and 0.1-m-height PEC cone for three observation angles.

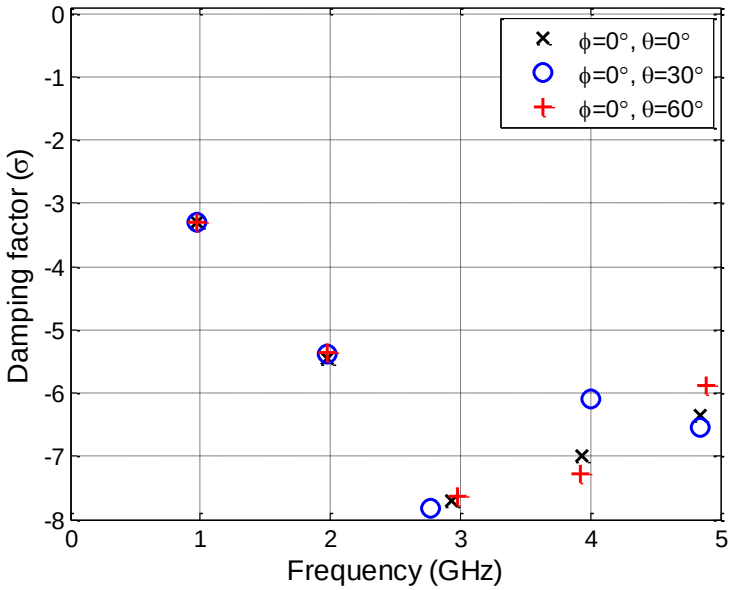

Figure 2.18 Natural poles of the 0.1-m-diameter and 0.1-m-height PEC cone.

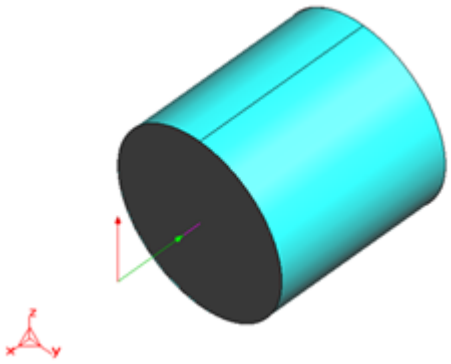

Figure 2.19 HOBBIES simulation model for the 0.1-m-diameter and 0.1-m-height PEC cylinder.

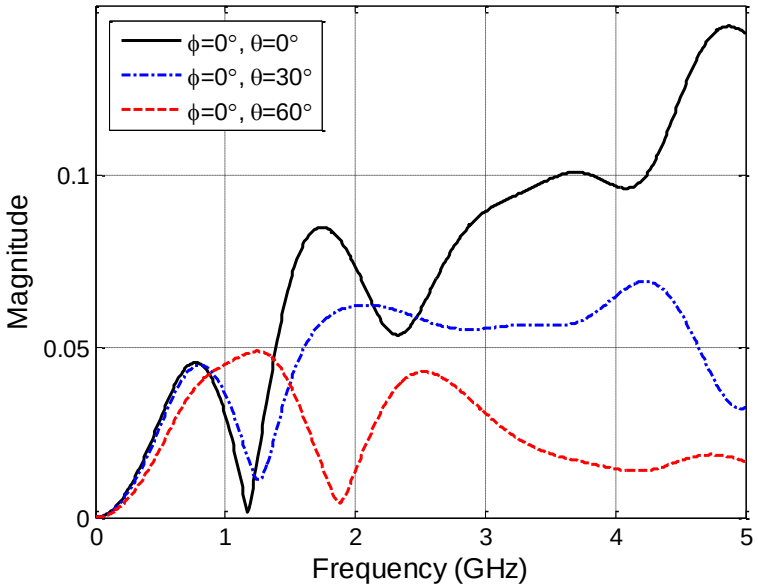

Figure 2.20 Frequency domain response of the HOBBIES model with the 0.1-m-diameter and 0.1-m-height PEC cylinder for three observation angles.

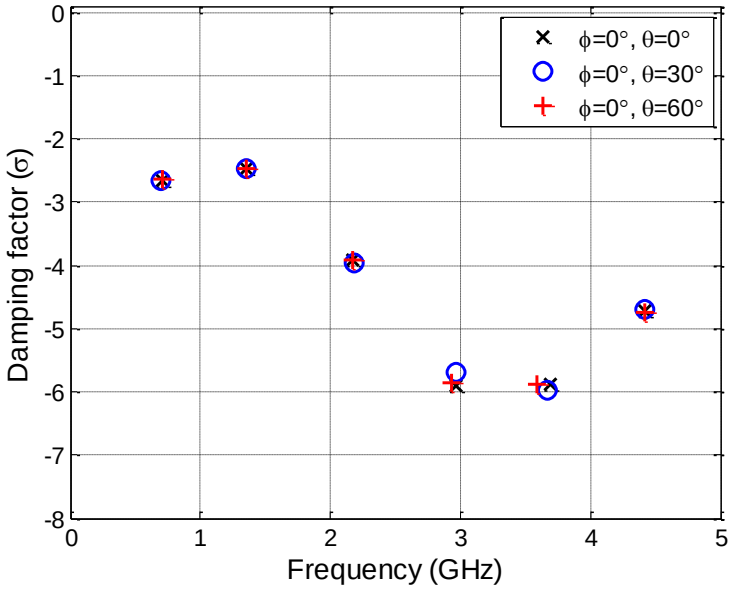

Figure 2.21 Natural poles of the 0.1-m-diameter and 0.1-m-height PEC cylinder.

Table 2.3 Pole Library of the seven PEC Objects.

Object	First Order Pole (σ_1, f_1)	Higher Order Frequency (GHz)
Wire	(-0.8811, 1.3339)	4.2265
Disk	(-2.9610, 1.1775)	4.6855
Ellipsoid	(-1.5828, 1.3967)	4.2956
Cone	(-3.3024, 0.9700)	1.9722, 2.9350, 3.9375, 4.8416
Sphere (D = 0.1 m)	(-2.9988, 0.8267)	1.7243, 2.6322, 3.5454, 4.4602
Cylinder	(-2.6532, 0.7028)	1.3540, 2.1733, 2.9673, 3.6885, 4.4146
Sphere (D = 0.15 m)	(-2.0011, 0.5504)	1.1490, 1.7534, 2.3638, 2.9761, 3.5885, 4.2081, 4.8299

3. PROCEDURE TO INDENTIFY AN UNKNOWN OBJECT

3.1. Overview

This chapter presents a proposed methodology for detecting and identifying an unknown object based on the Matrix Pencil (MP) method and using the Time-Difference-of-Arrival (TDOA) in the time domain. The MP method is well-known not only for interpolation and extrapolation techniques but also for identification of an unknown object using the data in the time domain [11]-[15]. The TDOA technique is also applicable to find the coordinates of an unknown object [33].

This chapter starts with the procedure of the MP method and then an example is presented to validate the proposed methodology for detecting and identifying an unknown object. The MP method is applied to find the natural poles of an unknown object using the late time response of the receiver (dipole antenna). Thus, comparing the natural frequencies by using data from the MP method along with a library of poles obtained using the Cauchy method, one can identify an unknown object with very high accuracy. One can also get the accurate coordinates of an unknown object using the time difference between the complete impulse response of the left and the right receivers, when two receivers are employed to receive the scattered signal from the object.

3.2. Matrix Pencil (MP) Method to Find the Natural Poles of an object

The MP method approximates a time domain function by a sum of complex exponentials and this approximation is valid only for the late time response. In general, the Electromagnetic (EM) transient signal of the observed late time response from an object can be formulated as

$$y(t) = x(t) + n(t) \approx \sum_{i=1}^{M} R_i e^{s_i t} + n(t), \qquad 0 \le t \le T \tag{3.1}$$

Such a model is valid because the scatterer can be treated as a linear time-invariant (LTI) system [28]. It is well-known that for an LTI system, the eigenfunctions of the transfer operator are of the form $e^{s_i t}$ where s_i are the poles of the system. After sampling, the time variable, t, is replaced by kT_s, where T_s is the sampling period. The sequence can be rewritten as

$$y(kT_s) = x(kT_s) + n(kT_s) \approx \sum_{i=1}^{M} R_i z_i^k + n(kT_s), \qquad for\ k = 0,1,\cdots,N-1 \tag{3.2}$$

$$z_i = e^{s_i T_s} = e^{(\alpha_i + j\omega_i)T_s}, \qquad for\ i = 1,2,\cdots,M \tag{3.3}$$

where $y(t)$ = observed time response

$x(t)$ = signal

$n(t)$ = noise in the system

R_i = residue or complex amplitudes of the ith pole

$s_i = \alpha_i + j\omega_i$ (ith pole of the system)

α_i = negative damping factor of the ith pole

ω_i = angular frequency of the ith pole

N = number of data samples

M = number of poles of the signal (Number of singular values)

The transient response from a structure can be characterized by the best estimates of M, R_i, and Z_i using the MP method, especially in the case of noisy data resulting from numerical errors and random noise. For noiseless data, we can define the $(N-L)\times(L+1)$ matrix [Y] as

$$[Y]=\begin{bmatrix} y_0 & y_1 & \cdots & y_L \\ y_1 & y_2 & \cdots & y_{L+1} \\ \vdots & \vdots & \ddots & \vdots \\ y_{N-L-1} & y_{N-L} & \cdots & y_{N-1} \end{bmatrix}_{(N-L)\times(L+1)} \tag{3.4}$$

We can also define matrix [Y] as

$$[Y]=\begin{bmatrix} c_1, & Y_1 \end{bmatrix}=\begin{bmatrix} Y_2, & c_{L+1} \end{bmatrix} \tag{3.5}$$

where c_i represents the ith column of matrix [Y]. These matrices [Y_1] and [Y_2] can be written as

$$[Y_1]=[Z_1][R][Z_0][Z_2] \tag{3.6}$$

$$[Y_2]=[Z_1][R][Z_2] \tag{3.7}$$

where

$$[Z_1]=\begin{bmatrix} 1 & 1 & \cdots & 1 \\ z_1 & z_2 & \cdots & z_M \\ \vdots & \vdots & \ddots & \vdots \\ z_1^{(N-L-1)} & z_2^{(N-L-1)} & \cdots & z_M^{(N-L-1)} \end{bmatrix}_{(N-L)\times M} \tag{3.8}$$

$$[Z_2]=\begin{bmatrix} 1 & z_1 & \cdots & z_1^{L-1} \\ 1 & z_2 & \cdots & z_2^{L-1} \\ \vdots & \vdots & \ddots & \vdots \\ 1 & z_M & \cdots & z_M^{L-1} \end{bmatrix}_{M\times L} \tag{3.9}$$

$$[Z_0] = \begin{bmatrix} z_1 & 0 & \cdots & 0 \\ 0 & z_2 & \cdots & 0 \\ \vdots & \vdots & \ddots & \vdots \\ 0 & 0 & \cdots & z_M \end{bmatrix}_{M \times M} \tag{3.10}$$

$$[R] = \begin{bmatrix} R_1 & 0 & \cdots & 0 \\ 0 & R_2 & \cdots & 0 \\ \vdots & \vdots & \ddots & \vdots \\ 0 & 0 & \cdots & R_M \end{bmatrix}_{M \times M} \tag{3.11}$$

Consider the following matrix pencil

$$[Y_1] - \lambda[Y_2] = [Z_1][R]\{[Z_0] - \lambda[I]\}[Z_2] \tag{3.12}$$

Provided $M \le L \le N - M$, the matrix $[Y_1] - \lambda[Y_2]$ has rank M. However, if $\lambda = z_i$, i=1,2,…,M, the ith row of $[Z_0] - \lambda[I]$ is zero, and the rank of $[Z_0] - \lambda[I]$ will be $M - 1$. Here [I] is the identity matrix. Therefore, the matrix pencil $[Y_1] - \lambda[Y_2]$ will also be reduced in rank to $M - 1$. It implies that z_i's are the generalized eigenvalues of the matrix pair {[Y_1], [Y_2]}. Therefore,

$$[Y_1][r_i] = z_i[Y_2][r_i] \tag{3.13}$$

where r_i is the generalized eigenvector corresponding to z_i. In the equivalent form

$$\left\{[Y_2]^{\dagger}[Y_1] - z_i[I]\right\}[r_i] = 0 \tag{3.14}$$

where $[Y_2]^{\dagger}$ is the Moore-Penrose pseudo-inverse of $[Y_2]$. From (3.14), we can obtain z_i's from the eigenvalues of $[Y_2]^{\dagger}[Y_1]$. Hence, for the MP method, the poles are obtained directly as a one-step process. For efficient noise filtering, the pencil parameter L is chosen between $N/3$ to $N/2$. Define the Singular Value Decomposition (SVD) [29] of matrix [Y] as

$$[Y] = [U][\Sigma][V]^H \tag{3.15}$$

The matrix [U] and [V] are $(N-L)\times(N-L)$ and $(L+1)\times(L+1)$ unitary matrices, respectively. The matrix [Σ] is a $(N-L)\times(L+1)$ diagonal matrix with the singular values of matrix [Y] in descending order. If the given data $y(kT_s)$ were noise free, matrix [Y] would have exactly M nonzero singular values.

However, due to the presence of noise, the zero singular values are perturbed. This results in several small nonzero singular values. This error due to the noise can be suppressed by eliminating these spurious singular values from matrix [Σ]. Define $[\Sigma']$ as a $M\times M$ diagonal matrix with the M largest singular values of [Y] on its main diagonal. Furthermore, define $[U']$ and $[V']$ as submatrices of [U] and [V] corresponding to these singular values:

$$[U'] = [U(:,\ 1:M)] \tag{3.16}$$

$$[V'] = [V(:,\ 1:M)] \tag{3.17}$$

$$[\Sigma'] = [\Sigma(1:M,\ 1:M)] \tag{3.18}$$

$$[Y'] = [U'][\Sigma'][V']^H \tag{3.19}$$

Therefore, using matrix [Y'] instead of matrix [Y] in (3.5) results in filtering the noise in both [Y_1] and [Y_2]. From (3.5) and (3.19), we can write

$$[Y_1] = [U'][\Sigma'][V_1']^H \tag{3.20}$$

$$[Y_2] = [U'][\Sigma'][V_2']^H \tag{3.21}$$

where $[V_1']$ and $[V_2']$ are equal to $[V']$ without the first and the last row, respectively. Using (3.20-3.21), the poles of the signal (eigenvalues of $[Y_2]^{\dagger}[Y_1]$) are given by the nonzero eigenvalues of

$$\{[V_2']\}^{\dagger}[V_1'] \tag{3.22}$$

The number of modes M is chosen by observing the ratio of the various singular values to the largest one as defined by [30]

$$\frac{\sigma_R}{\sigma_{\max}} \approx 10^{-w} \tag{3.23}$$

where w is the number of accurate significant decimal digits of the system response data. Based on w, one can determine the proper values of M for the assumed precision. Using this better choice of M, one can evaluate the poles z_i and the amplitude R_i using the previously detailed approach. Hence, for the matrix pencil method, the poles are obtained from the contaminated data by the noise using the SVD [29] and the TLS method [31].

3.3. Extracting Natural Poles of a PEC Sphere Using the MP Method

Figure 3.1 shows the HOBBIES simulation model. The configuration is with one transmitter (center antenna), two receivers (left and right antennas), and one sphere object located in free space. Using two receivers one can get the coordinates of the unknown object including the radial distance and the azimuthal angle. The specification for each of the antenna for transmitter and receiver are 0.15 m in length and 1.5 mm radius. The diameter of the sphere is 0.15 m. Spacing between the transmitter and the receiver is 2.5 m to fully minimize the effects of the antenna coupling. The target sphere is located at 12.046 m and is oriented by -5° from the axis of the transmitting antenna. The

transmitting antenna is excited by a voltage generator (delta-function generator) with 1 V. The response of the object is computed from 0.01 GHz to 5 GHz (sampling frequency Δf = 0.01 GHz), and the number of samples is 500. To isolate the response of the desired objects at the receiver, the received signals at both the antennas are computed with and without the presence of the object of interest.

By subtracting one response from the other one reduces the coupling between the various antennas. In addition, the antenna impulse response needs to be deconvolved out from the computed total response from both the antennas and the object [34]. Therefore, the deconvolved response $Y(f)$ from the object at each receiver can be represented as

$$Y(f) = \frac{X(f)_{Object} - X(f)_{No-Object}}{R_{Ant}(f)} \tag{3.24}$$

where $X(f)_{Object}$ and $X(f)_{No-Object}$ are the received signal with the object present and the received signal without the object present, respectively. $R_{Ant}(f)$ is the response of a receiving antenna. Figure 3.2 shows the normalized frequency domain response of the dipole antenna. Figures 3.3 and 3.4 show the received signal without the object present and the received signal with the object present in the frequency domain, respectively. Figure 3.5 shows the response of the sphere seen by the left and right receivers in the frequency domain using (3.24). The peak in the object response around 3.5 GHz is due to the antenna response.

For applying the MP method, we need to obtain the time domain response of the object from the frequency domain data (deconvolved response and its complement response) using the inverse fast Fourier transform (IFFT, Matlab function). As expected, one can get exactly the same frequency domain response from the obtained time domain

response using the FFT (Matlab function). Figure 3.6 displays the time domain response of the object (for the left and for the right receivers). From Figure 3.6, one can identify the location of the object with respect to a global coordinate system.

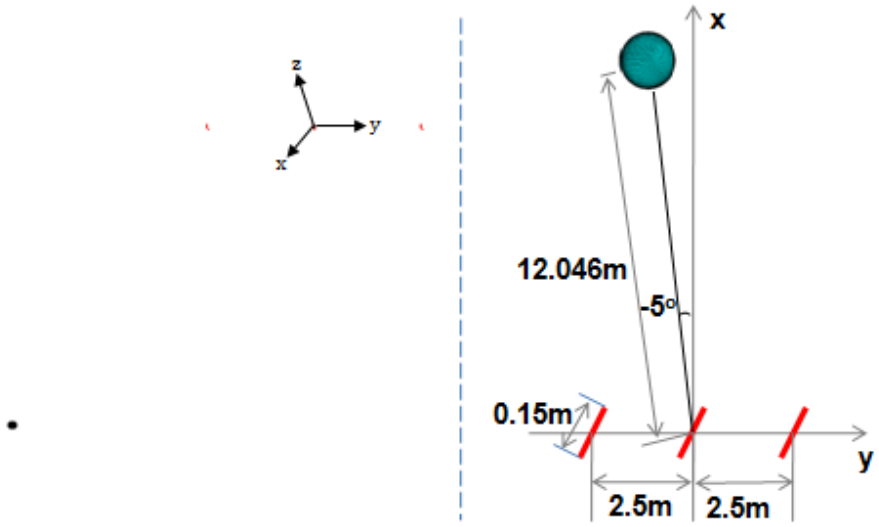

Figure 3.1 HOBBIES simulation model and its configuration using one transmitter, two receivers, and a 0.15-m-diameter PEC sphere.

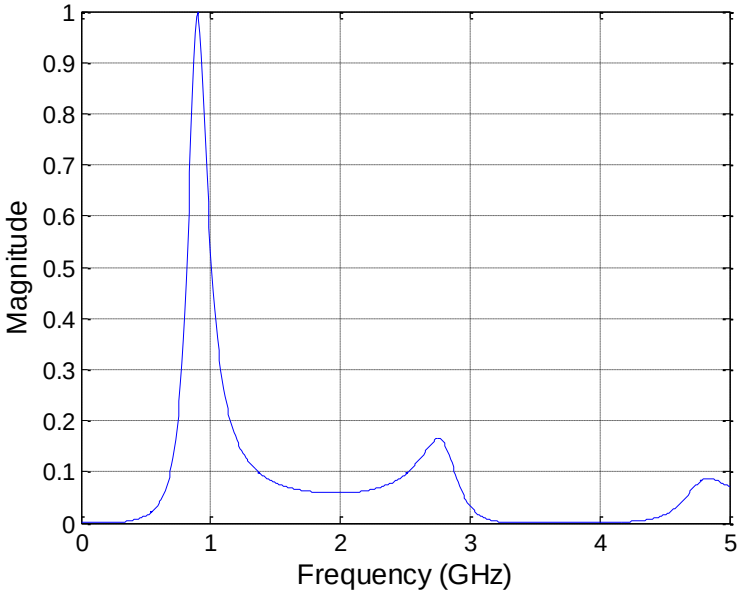

Figure 3.2 Normalized frequency domain response of the dipole antenna.

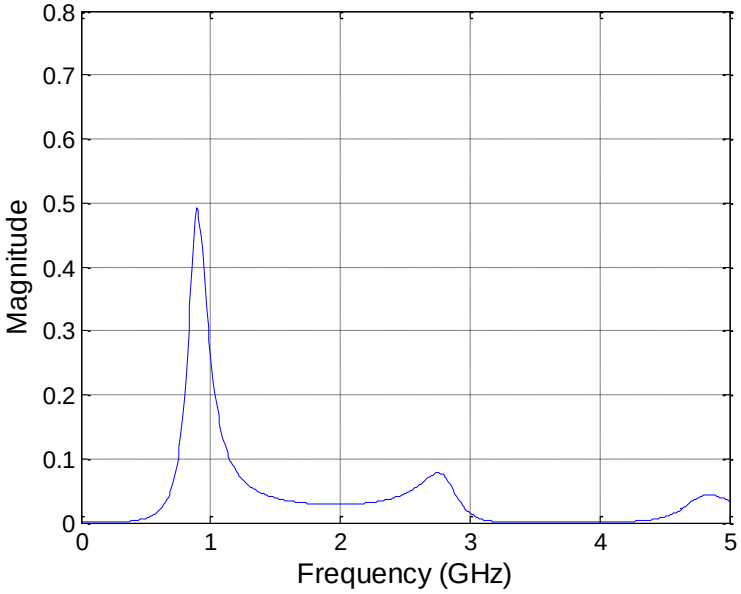

Figure 3.3 Received signal without the object present

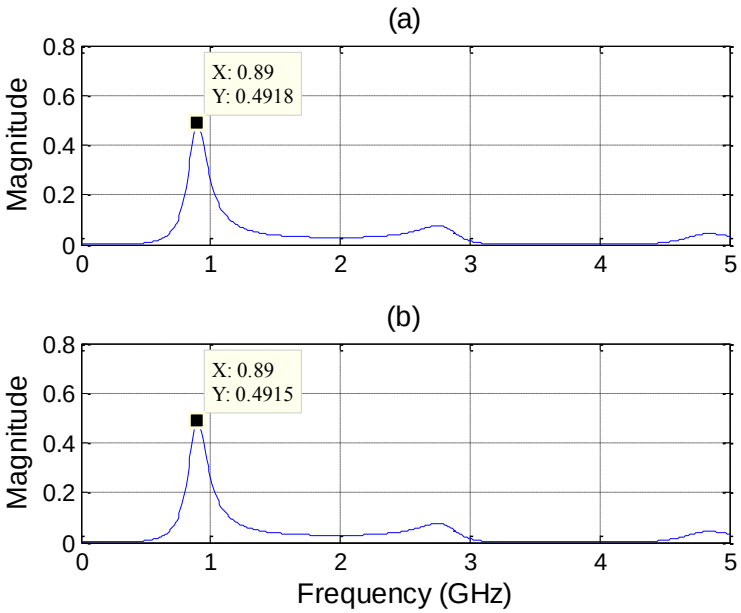

Figure 3.4 Received signal with the object present from (a) left receiver, (b) right receiver.

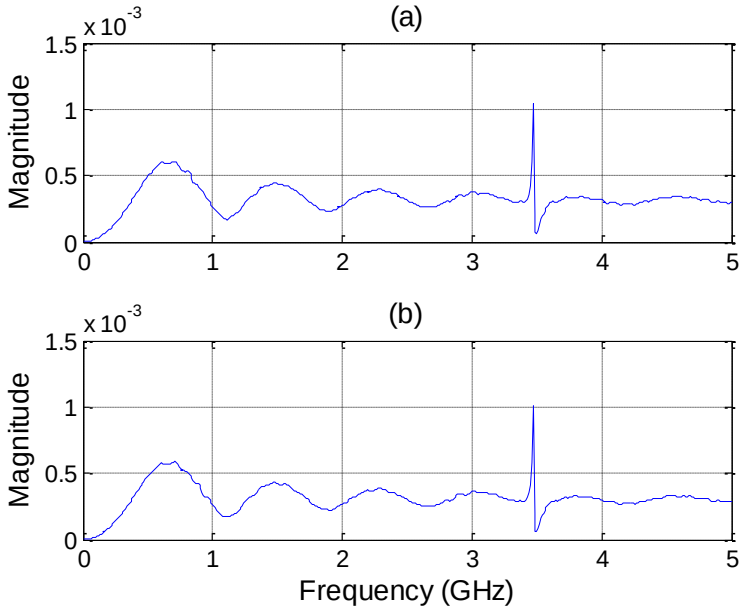

Figure 3.5 Frequency domain response of the 0.15-m-diameter PEC sphere; (a) the left receiver, (b) the right receiver.

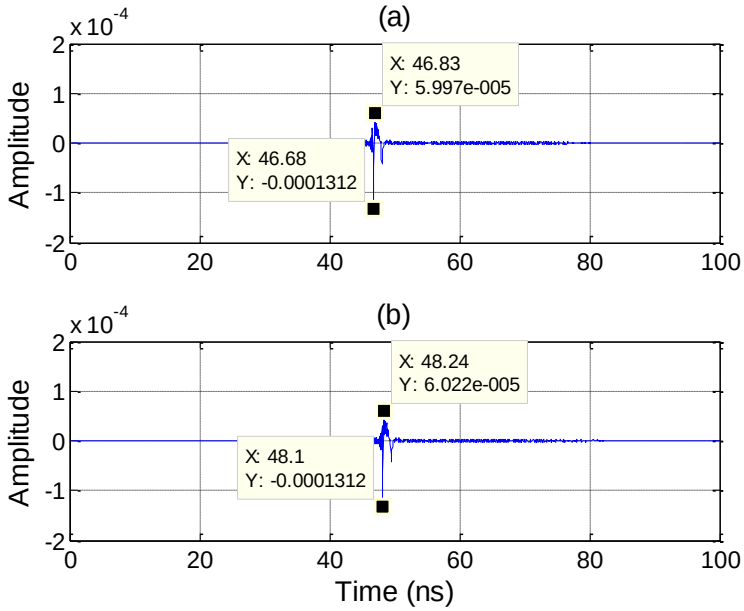

Figure 3.6 Time domain response of the 0.15-m-diameter PEC sphere obtained from (a) the left receiver, (b) the right receiver.

When the object is located on the left hand side of the normal to the line joining the location of all the antennas, the time delay of the signal received at the left receiver is shorter than that from the right receiver. Therefore, one can calculate the distance

between the object and the transmitting antenna using the Time-Difference-of-Arrival (TDOA) [33]. If we assume that the locations of the left receiver, the right receiver, and the object are (0, –*d*, 0), (0, *d*, 0), and (*x*, *y*, *z*), respectively as shown in Figure 3.7, then

$$R_L + R = C_1, \;\; R_R + R = C_2 \tag{3.25}$$

where

$$R_L = \sqrt{x'^2 + (y'+d)^2 + z'^2}, \;\; R_R = \sqrt{x'^2 + (y'-d)^2 + z'^2} \tag{3.26}$$

$$C_1 = T_L \times 3\times 10^8, \;\; C_2 = T_R \times 3\times 10^8 \tag{3.27}$$

$$x' = x - r, \;\; y' = y - r, \;\; z' = z - r \tag{3.28}$$

where R is the radial distance of the illuminated surface of the unknown object from the transmitter. R_L and R_R are the distances of the surface of the object from the left and the right receiver, respectively. T_L and T_R are the time delay (peak of the impulse response) of the left and the right receiver, respectively. r is the distance from the center of the object to the illuminated surface of the object by antennas. Since the distances of the left and the right receiver from the origin are the same, we can get one more formula based on the Pappus's theorem [35].

$$R_L^2 + R_R^2 = 2(R^2 + d^2) \tag{3.29}$$

From (3.25~3.29), one can calculate the radial distance (R)

$$R = C_2 - R_R, \tag{3.30}$$

where

$$R_R = \frac{-C_1^2 + C_2^2 + 2C_1C_2 + 2d^2}{2(C_1 + C_2)} \tag{3.31}$$

We can also estimate the displacement of the object in angle from the direction of the normal using the law of cosine.

$$\phi_{DOA} = \cos^{-1}\left(\frac{d^2 + R^2 - R_L{}^2}{2dR}\right) - 90° \tag{3.32}$$

where ϕ_{DOA} is the azimuthal angle of inclination from the normal.

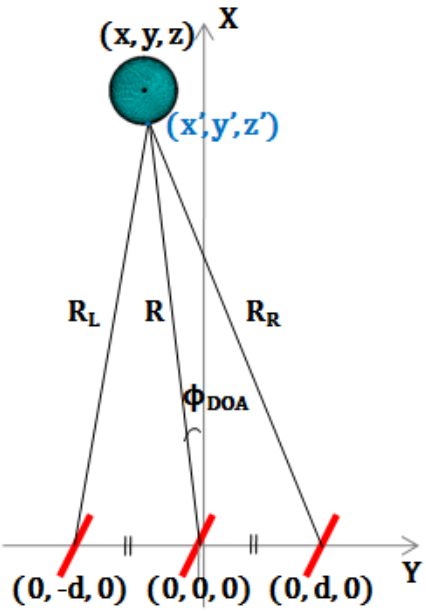

Figure 3.7 Configuration of one transmitter, two receivers, and one object for calculating object coordinates

Notice that we use R (distance from the origin to the front of the object) instead of R' (distance from the origin to the center of the object) considering the TDOA in the time domain. The peak point of the late time response is chosen to compute R_L and R_R. Table 3.1 presents the actual vs. estimated coordinates of the target from the origin. It has an relative error of 0.26 % for the distance R and 0.44 % error for the ϕ_{DOA}.

Table 3.1 Actual vs. Estimated Target Coordinates (0.15-m-diameter Sphere).

	R (m)	Angle (°)
Actual target coordinates	11.971	–5
Estimated target coordinates	12.002	–4.9779

For identification of unknown objects, we need to compute their natural poles. If we consider the mechanisms of backscattering from the object, it can be divided into two parts. The first part is the impulsive part corresponding to the early time response (direct reflection of the incident wave from the surface of the object). The second part is the oscillatory part corresponding to the late time response (resonance phenomena). Therefore, we chose the truncated time domain data from the target between the peak point and its response settling down to zero with respect to the late time response for the receivers as shown in Figures 3.8 and 3.9. Even though the magnitude of the first negative peak is larger than the peak of the truncated data, it is not utilized because the first negative peak is from the first part in the backscattering mechanisms. One should notice that the late time response of the object represents its information. If one truncated very small portion of the late time response of the object, one cannot obtain its correct natural frequencies because of loss of information. Under this consideration, the truncated time domain data should be chosen very carefully. In this case, the truncated time domain data and the number of samples for the left receiver are 3.5594 ns and 73, respectively, whereas the truncated time domain data and the number of samples for the right receiver are 3.5515 ns and 73, respectively as shown in Figures 3.8 and 3.9.

The MP method then is applied to extract the natural poles of the detected object. We apply two criteria to extract the natural poles. The first criterion filters the poles out having very high damping factors ($|\sigma_m| > 7$). The second criterion allows one to remove single poles located on the real axis, poles having positive σ, and poles in the range $f_m <$ 0.01 GHz and f_m > 5 GHz. The last criterion for the Cauchy method is not applied for the MP method because of its initial assumption from (3.2). Table 3.2 presents a list of poles

for the 0.15-m-diameter PEC sphere for the left and the right receivers using the MP method. If we compare these two sets of computed poles from the time domain response of the left and the right receivers, they are almost identical not only the first order pole but also the resonant frequencies of the higher order poles. It means one can extract the SEM poles with high accuracy using the late time response of the detected object irrespective of using which receiver.

To evaluate the performance of this methodology, we compute the *estimated error* of the identification accuracy following the normalized mean square errors (MSEs) using resonance frequencies as

$$E_{est} = \frac{\left\| \hat{f} - f \right\|_2}{\left\| f \right\|_2} \tag{3.33}$$

where $\|\bullet\|_2$ is the L^2-norm of a vector. f and $\hat{f}$ are the resonance frequency of the pole library and extracted resonance frequency, respectively.

Now let us try to indentify this unknown object based on Table 2.3 (pole library of the seven PEC objects) and the computed poles in the time domain. For identification of the unknown object, we need to compare two parameters. The first key parameter is the first order pole and the second parameter is the resonant frequencies. Thus, one can identify the unknown object as the 0.15-m-diameter PEC sphere comparing the pole library with the first order pole and the resonant frequencies of the unknown object. If we consider only the resonance frequencies, the estimated error is 1.97 % for the left receiver and 1.74 % for the right receiver, respectively. Therefore, one can locate the 0.15-m-diameter PEC sphere with approximate 98 % accuracy at 12.002 m radial distance and -4.9779° azimuthal angle.

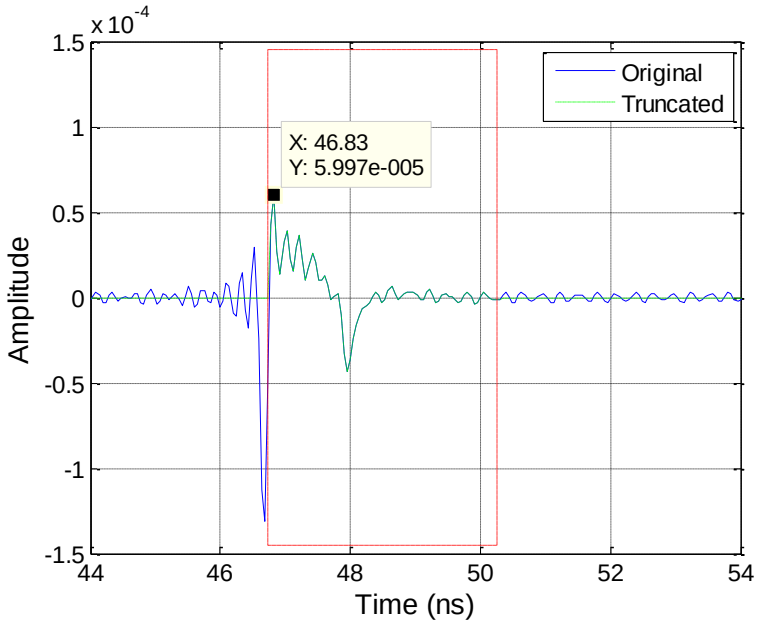

Figure 3.8 Truncated data from the object to apply the MP method from the left receiver (one sphere model).

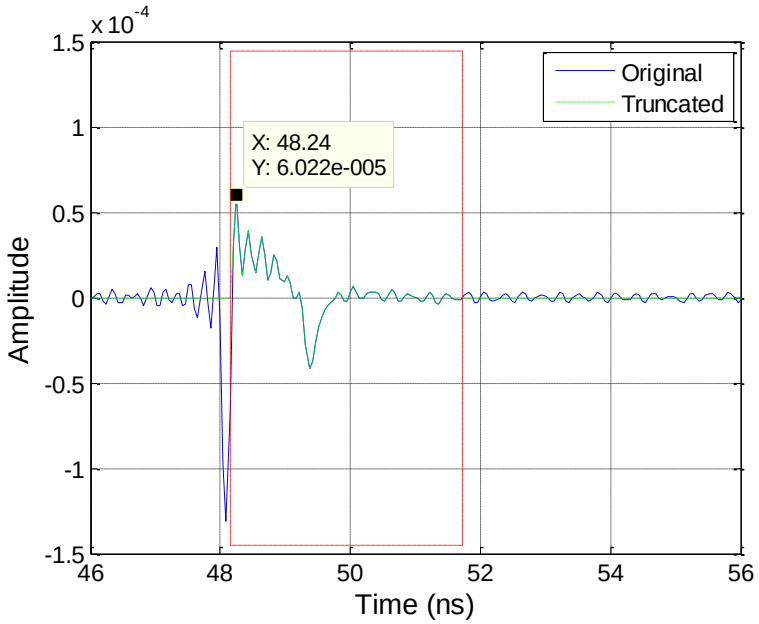

Figure 3.9 Truncated data from the object to apply the MP method from the right receiver (one sphere model).

Table 3.2 Library of Poles of the 0.15-m-diameter PEC Sphere and Computed Natural Poles of the Detected Object Using the MP Method.

Library of pole (0.15-m-diameter PEC Sphere)		Computed poles from the left receiver		Computed poles from the right receiver	
First Order Pole (σ_1, f_1)	Higher Order Frequency (GHz)	First Order Pole (σ_1, f_1)	Higher Order Frequency (GHz)	First Order Pole (σ_1, f_1)	Higher Order Frequency (GHz)
(-2.0011, 0.5504)	1.1490 1.7534 2.3638 2.9761 3.5885 4.2081 4.8299	(-2.0180, 0.5463)	1.1551 1.7685 2.3766 2.9780 3.6901 4.3410 4.8294	(-2.0178, 0.5465)	1.1543 1.7665 2.3741 2.9724 3.6733 4.3290 4.8234

3.4. Object Identification in Noisy Environment

In practice the received data may be contaminated by an additive noise. So the noisy environment is studied where the system has an additive white Gaussian random noise of 30 dB SNR (signal-to-noise ratio). Let the system have a noise floor of 30 dB SNR. Based on the simulation model as shown in Figure 3.1, both $X(f)_{Object}$ (received signal with the object present) and $X(f)_{No-Object}$ (received signal without the object present) are also noise contaminated data with 30 dB SNR. Figure 3.10 shows the time domain response of the 0.15-m-diameter PEC sphere including the noise obtained from the left receiver.

The MP method is a robust pole extraction technique in any noisy environment as mentioned before. Therefore, one can extract natural poles from the noise contaminated data using the proposed methodology. Table 3.3 presents a list of the poles for the 0.15-m-diameter PEC sphere from the left receiver in noisy environment using the MP method.

If we consider only the resonance frequencies, the estimated error is 4.49 %. Even though the accuracy is decreased from 98 % (noiseless data) to 95 % (noisy data), one can identify the detected target as a 0.15-m-diameter PEC sphere comparing the pole library with the first order pole and the resonant frequencies of the detected target.

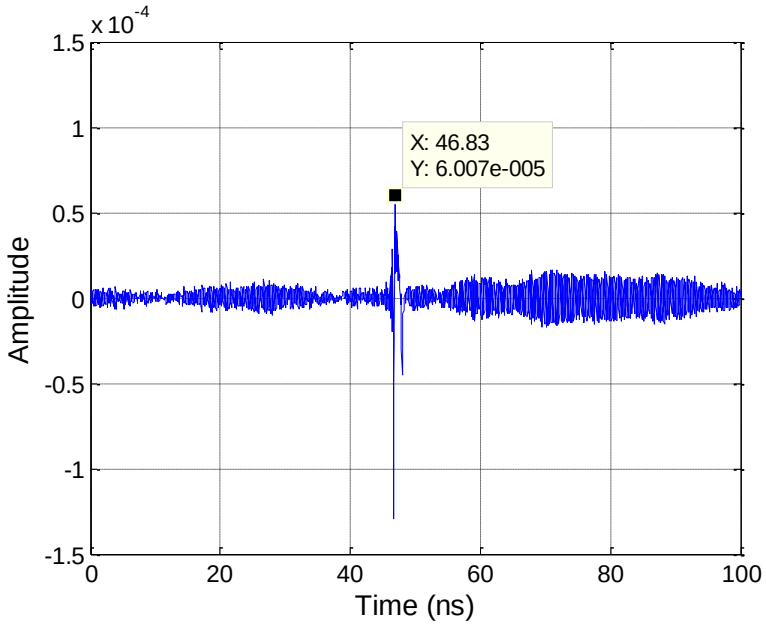

Figure 3.10 Time domain response of the 0.15-m-diameter PEC sphere including the noise obtained from the left receiver

Table 3.3 Library of Poles of the 0.15-m-diameter PEC Sphere and Natural Poles of the Detected Target in Noisy Environment Using the MP Method.

Library of pole (0.1 m diameter PEC Sphere)		Computed poles from the left receiver in Noisy Environment Using MP method	
First Order Pole (σ_1, f_1)	Higher Order Frequency (GHz)	First Order Pole (σ_1, f_1)	Higher Order Frequency (GHz)
(-2.0011, 0.5504)	1.1490	(-2.2049, 0.5690)	1.1980
	1.7534		1.8458
	2.3638		2.5665
	2.9761		3.0119
	3.5885		3.6247
	4.2081		4.5104
	4.8299		4.7951

4. SIMULATION EXAMPLES WITH MULTIPLE TARGETS IN FREE SPACE

4.1. Overview

In this chapter, six different examples are presented to validate the proposed methodology for simultaneous identification of multiple PEC objects in free space. Each example is selected considering different dimensions, different shapes, similar shapes, and interaction effects. For the simulation, we apply the same methodology as described for the PEC sphere example in the specified frequency range as outlined in chapter 3.3.

The first example (4.2. two spheres) illustrates that the natural frequencies of the object are different due to its different dimensions. The second example (4.3. one sphere and one disk) shows their different natural frequencies although the projection of the sphere is the disk. Also we observe the natural frequencies of two objects with similar shape from the third example (4.4. one disk and one ellipsoid). For the fourth example (4.5. one cone and one wire) we identify closely spaced objects in order to identify them even though the cone is larger in shape than the wire. The fifth example (4.6. one cylinder and one sphere) shows their different natural frequencies when two objects have similar dimension. From the last example (4.7. one cone, one wire, and one sphere) we check the interaction effects in case of more than two objects.

4.2. Two Spheres

Figure 4.1 shows the HOBBIES simulation model and its configuration with one transmitter (center), two receivers (left, right), and two PEC spheres of different sizes located in free space. The diameter of the first sphere is 0.1 m. The location of the spheres from the origin (the location of the transmitter) and in angle with respect to the normal joining the three antennas are 10.154 m and 10°. The diameter of the second PEC sphere is 0.15 m and its distance and angle are 12.046 m and -5°, respectively. Figure 4.2 shows the deconvolved response of the two spheres to the left and right receiving antennas in the frequency domain. Figure 4.3 displays the time domain response of the detected objects for the left and right receivers.

Based on the TDOA in the time domain, one can get estimated coordinates of the targets using (3.30) and (3.32). Table 4.1 describes the actual vs. estimated coordinates of the targets (two spheres) from the origin. For the first target, the computed relative error for the location is 0.29 % for the radial distance and a 0.71 % error for the azimuthal angle. For the second target, the corresponding error is 0.26 % for the distance and 0.44 % error for the angle.

For identification, we chose the truncated data as illustrated in Figures 4.4 and 4.5 for both the targets. The record length is selected from the peak value of the waveform in the time domain till it decays down to zero. The MP method is applied to this truncated time domain data of the left receiver as shown in Figures 4.4 and 4.5. Figure 4.6 compares the pole library using the Cauchy method with the computed poles of the unknown targets using the MP method. From Figure 4.6(a), one can clearly identify the unknown targets because the first and the second unknown targets overlap with the

library poles of the 0.1-m-diameter PEC sphere and 0.15-m-diameter PEC sphere, respectively. The estimated errors of the resonant frequency are 1.17 % for the first target and 4.79 % for the second target, respectively as shown in Figure 4.6(b). Therefore, one can locate the 0.1-m-diameter PEC sphere with approximate 99 % accuracy at 10.133 m radial distance, 10.071° azimuthal angle and the 0.15-m-diameter PEC sphere with approximate 95 % accuracy at 12.002 m radial distance, -4.9779° azimuthal angle.

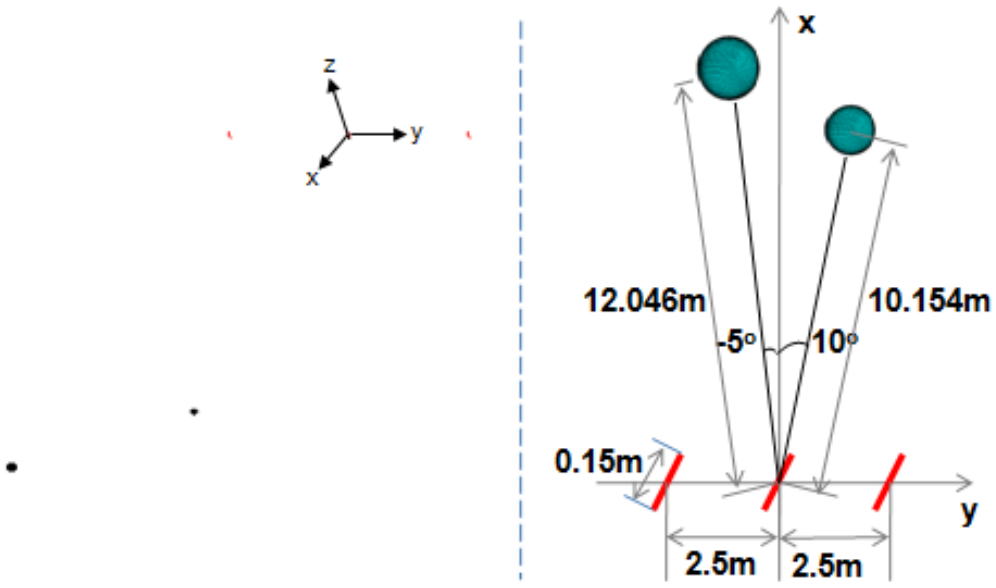

Figure 4.1 HOBBIES simulation model and its configuration with one transmitter, two receivers, a 0.1-m-diameter PEC sphere, and a 0.15-m-diameter PEC sphere.

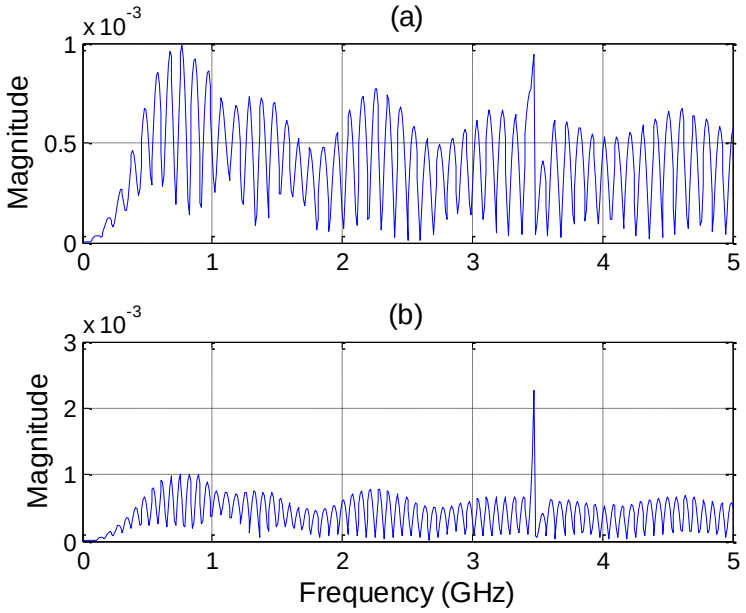

Figure 4.2 Frequency domain response of the 0.1-m and 0.15-m-diameter PEC spheres; (a) the left receiver, (b) the right receiver.

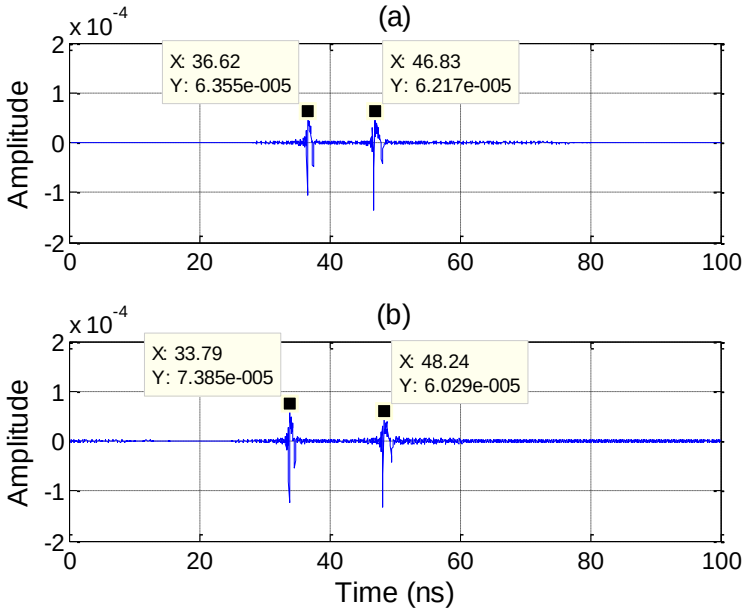

Figure 4.3 Time domain response of the 0.1-m and 0.15-m-diameter PEC spheres; (a) the left receiver, (b) the right receiver.

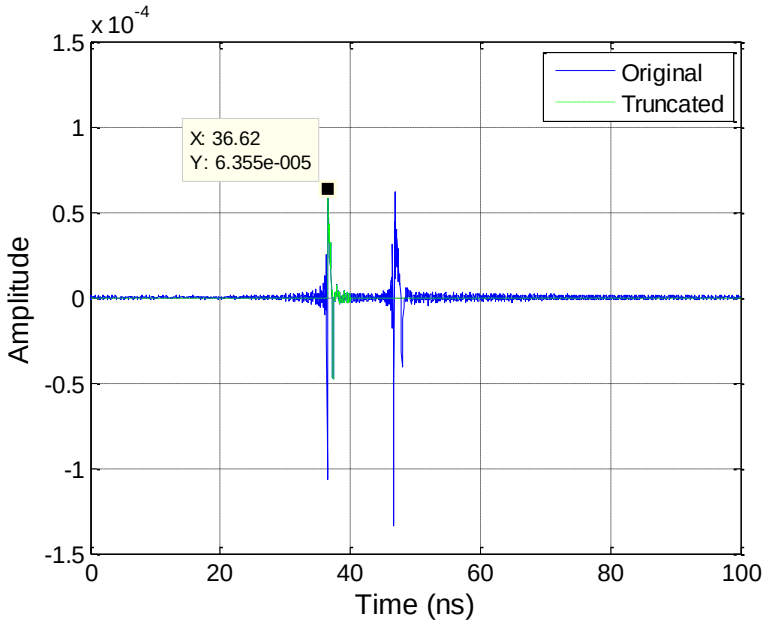

Figure 4.4 Truncated data from the first unknown target to apply the MP method from the left receiver (two spheres model).

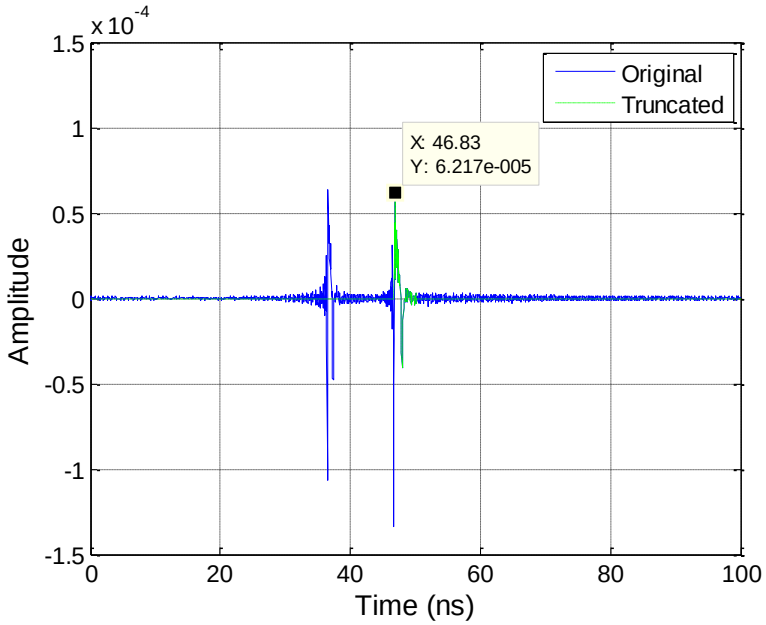

Figure 4.5 Truncated data from the second unknown target to apply the MP method from the left receiver (two spheres model).

Table 4.1 Actual vs. Estimated Target Coordinates (Two Spheres).

	Sphere (D=0.1 m)		Sphere (D=0.15 m)	
	R (m)	Angle (º)	*R* (m)	Angle (º)
Actual target coordinates	10.104	10	11.971	-5
Estimated target coordinates	10.133	10.071	12.002	-4.9779

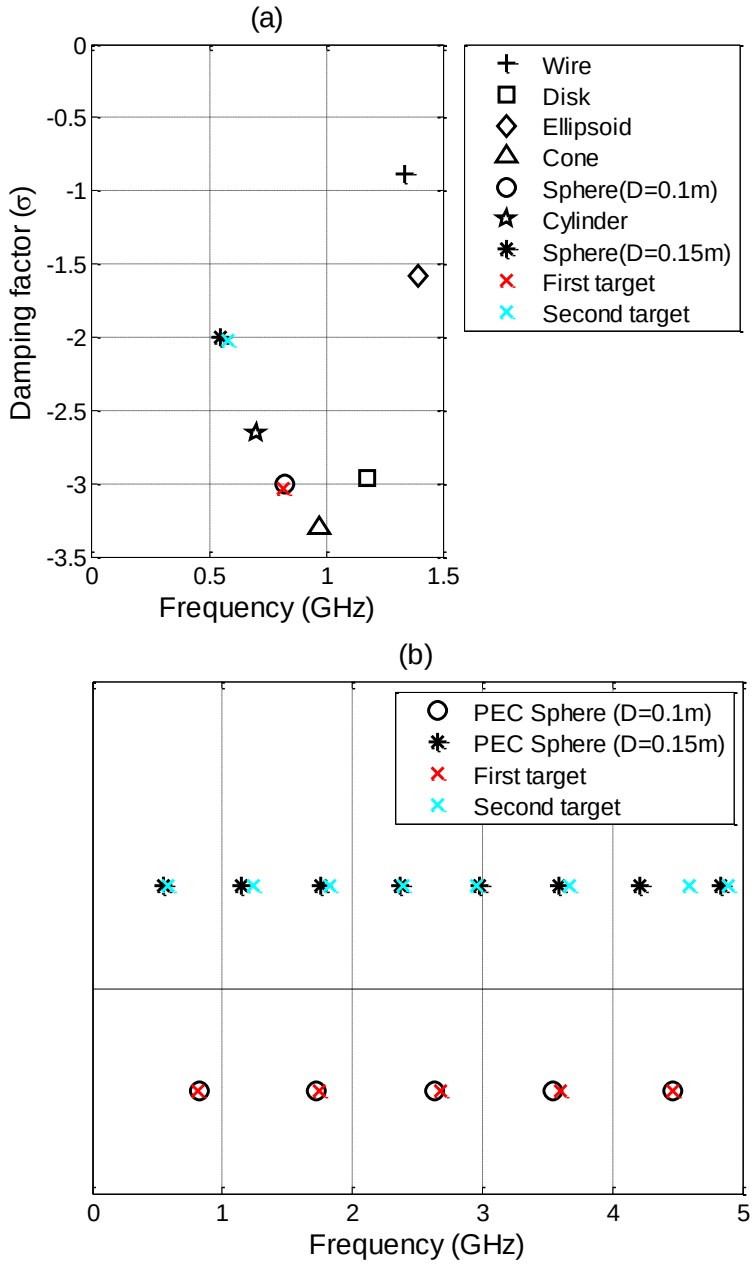

Figure 4.6 Pole Library vs. Computed poles of the unknown targets using the MP method (two spheres model); (a) First order pole, (b) Resonant frequency.

4.3. One Sphere and one Disk

For the next example we consider a PEC sphere and a PEC disk. Figure 4.7 shows the HOBBIES simulation model and its configuration for the case of one PEC sphere and one PEC disk in free space. The diameter of the sphere is 0.1 m. The coordinates of the object from the origin (transmitter) is 10.154 m and 10° respectively. The diameter of the disk is 0.1 m. Its coordinates from the transmitter (the origin) are 12.046 m and -5°, respectively. Figures 4.8-4.9 show the deconvolved response of the sphere and the disk for the left and right receivers in the frequency domain and in the time domain, respectively. Table 4.2 shows the actual vs. estimated coordinates of the targets (sphere and disk) from the origin. For the first target, it has a relative error of 0.29 % for the radial distance and 0.71 % error in the azimuthal angle. For the second target, it has 0.16 % error for the distance and a 2.98 % error for the angle. The MP method is applied to the truncated time domain data of the right receiver as shown in Figures 4.10 and 4.11.

Figure 4.12 compares the pole library along with the computed poles of the unknown targets using the truncated time domain response of the right receiver. Figure 4.12(a) shows that one can identify the unknown targets because the first and the second unknown targets almost overlap with the library poles of the 0.1-m-diameter PEC sphere and 0.1-m-diameter PEC disk, respectively. The estimated errors of the resonant frequency are 2.12 % for the first target and 3.17 % for the second target, respectively as shown in Figure 4.12(b). Therefore, one can locate the 0.1-m-diameter PEC sphere with approximate 98 % accuracy at 10.133 m radial distance, 10.071° azimuthal angle and the 0.1-m-diameter PEC disk with approximate 97 % accuracy at 12.065 m radial distance, -5.1488° azimuthal angle.

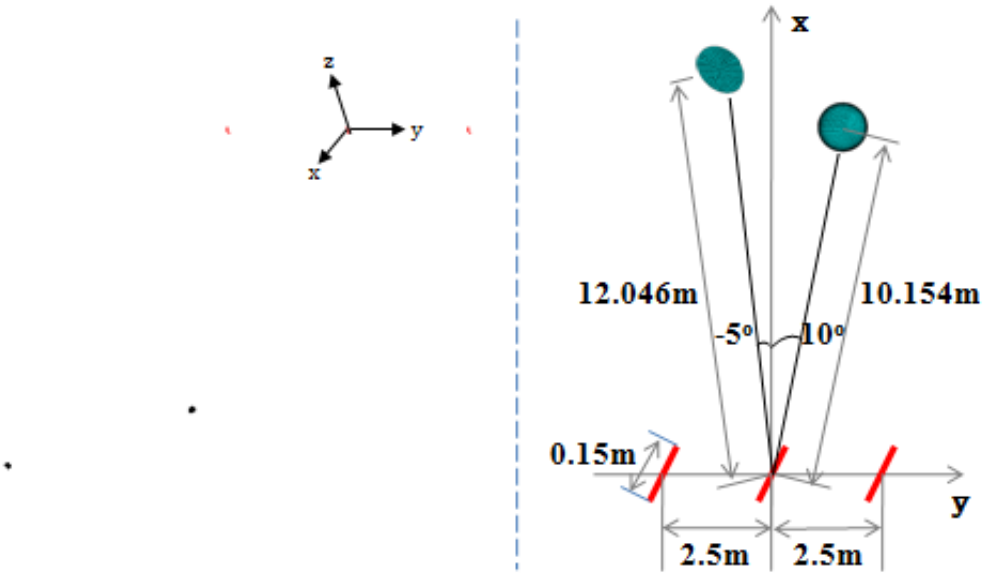

Figure 4.7 HOBBIES simulation model and its configuration with one transmitter, two receivers, a PEC sphere, and a PEC disk.

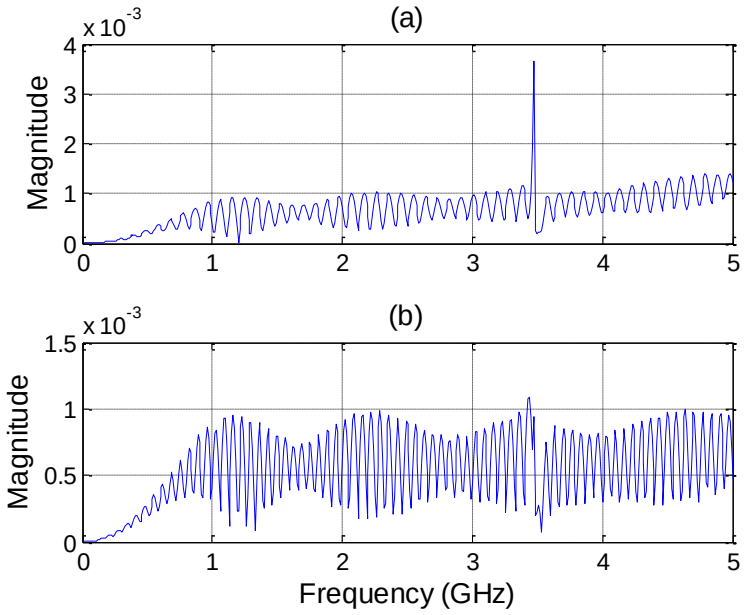

Figure 4.8 Frequency domain response of a PEC sphere and a PEC disk; (a) the left receiver, (b) the right receiver.

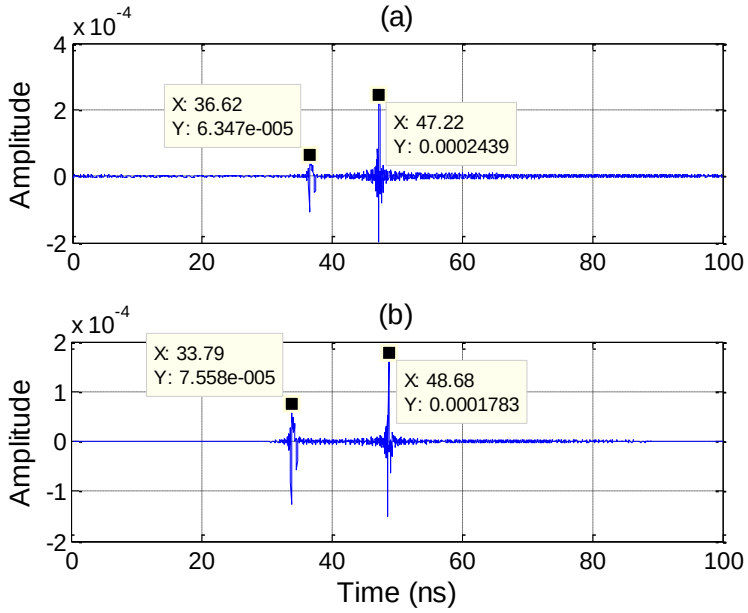

Figure 4.9 Time domain response of a PEC sphere and a PEC disk; (a) the left receiver, (b) the right receiver.

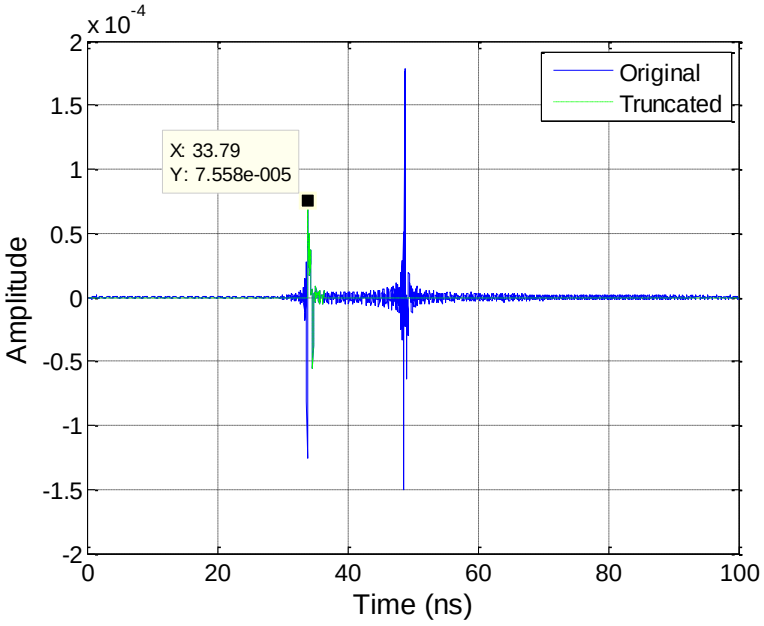

Figure 4.10 Truncated data from the first unknown target to apply the MP method from the right receiver (one sphere and one disk model).

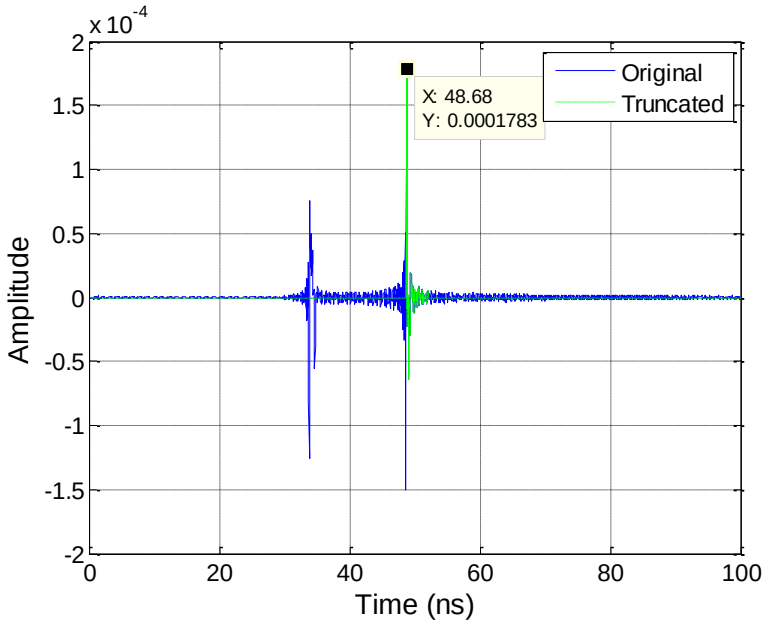

Figure 4.11 Truncated data from the second unknown target to apply the MP method from the right receiver (one sphere and one disk model).

Table 4.2 Actual vs. Estimated Target Coordinates (Sphere and Disk).

	Sphere (D=0.1 m)		Disk (D=0.1 m)	
	R (m)	Angle (º)	*R* (m)	Angle (º)
Actual target coordinates	10.104	10	12.046	–5
Estimated target coordinates	10.133	10.071	12.065	–5.1488

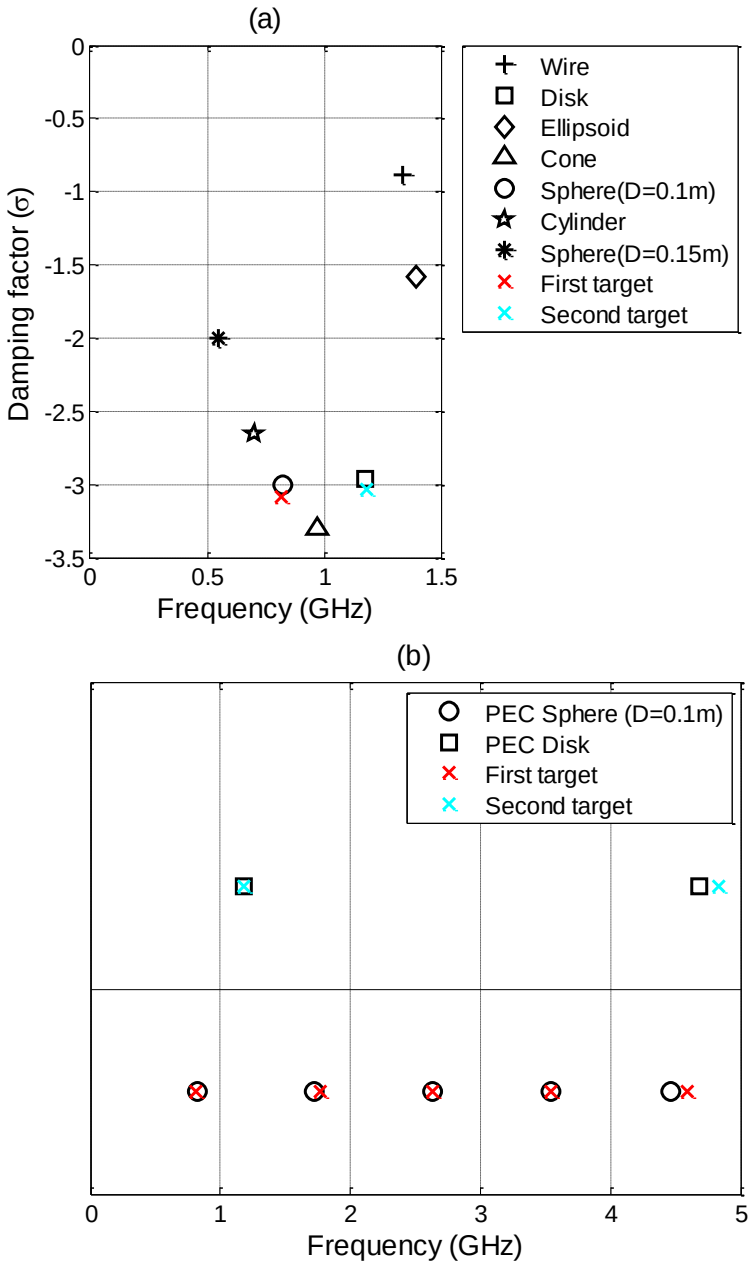

Figure 4.12 Pole Library vs. Computed poles of the unknown targets using the MP method (one sphere and one disk model); (a) First order pole, (b) Resonant frequency.

4.4. One Disk and one Ellipsoid

Figure 4.13 shows the HOBBIES simulation model and its configuration for the case of one PEC disk and one PEC ellipsoid located in free space. The diameter of the disk is 0.1 m. The coordinates of the disk from the origin (transmitter) is 7.2469 m and 15°, respectively. The diameter and length of the ellipsoid is 0.02 m and 0.1 m, respectively. Its coordinates from the origin (transmitter) is 9.2011 m and -12°, respectively. Figure 4.14 shows the computed response of a disk and an ellipsoid to the left and right receivers in the frequency domain, whereas Figure 4.15 shows their time domain response.

Table 4.3 shows the actual vs. estimated coordinates of the targets (disk and ellipsoid) from the origin. For the first target, it has a 0.18 % relative error for the distance and a 0.97 % error for the angle. For the second target, it has a 0.20 % error for the distance and a 0.87 % error in the angle. Figures 4.16-4.17 show the truncated time domain data of the right receiver to apply the MP method. Figure 4.18 shows a pole library of the PEC disk (0.1 m diameter), a PEC ellipsoid (0.02 m diameter, 0.1 m length) and computed poles of the targets. If we compare them, we can clearly identify the two unknown objects. The estimated errors of the resonant frequency are 3.34 % for the first target and 4.9 % for the second target, respectively as shown in Figure 4.18(b). Therefore, one can locate the 0.1-m-diameter PEC disk with approximate 97 % accuracy at 7.2601 m radial distance, 14.855° azimuthal angle and the 0.02-m-diameter, 0.1-m-length PEC ellipsoid with approximate 95 % accuracy at 9.2199 m radial distance, –11.896° azimuthal angle.

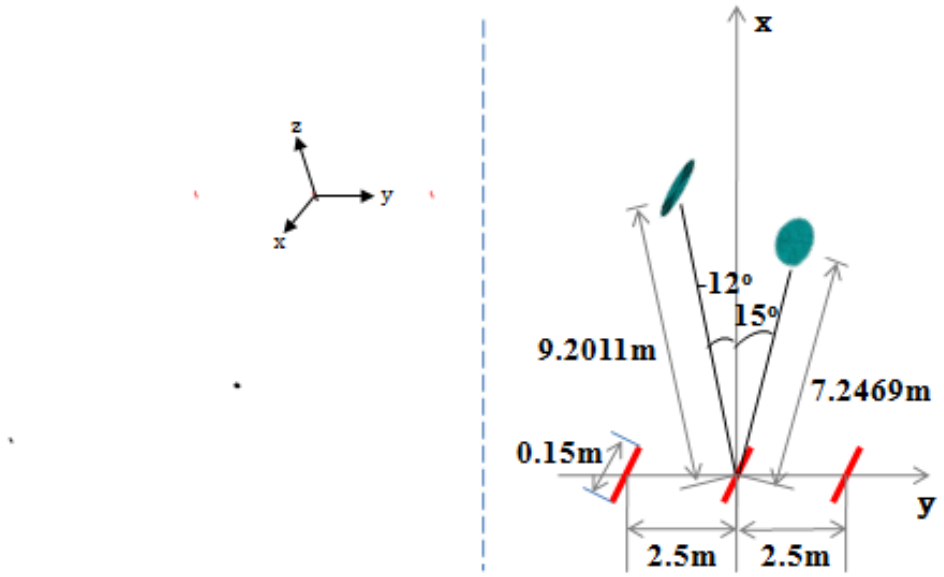

Figure 4.13 HOBBIES simulation model and its configuration with one transmitter, two receivers, a PEC disk, and a PEC ellipsoid.

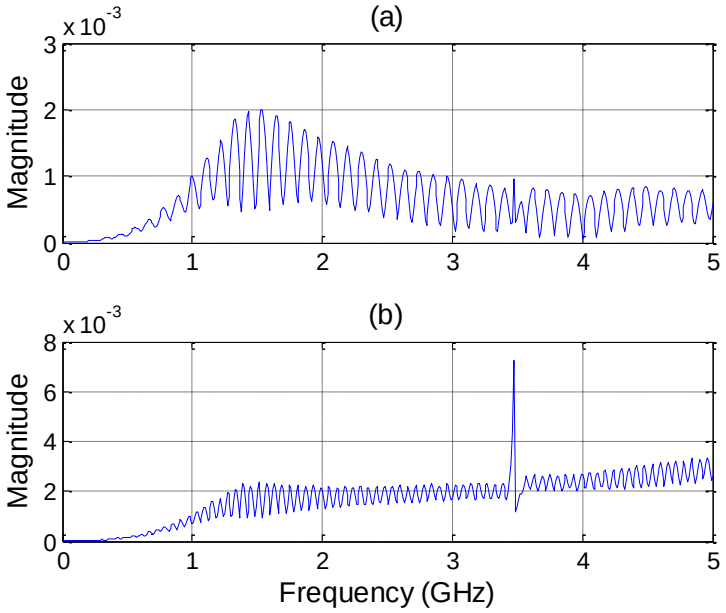

Figure 4.14 Frequency domain response of a PEC disk, and a PEC ellipsoid; (a) the left receiver, (b) the right receiver.

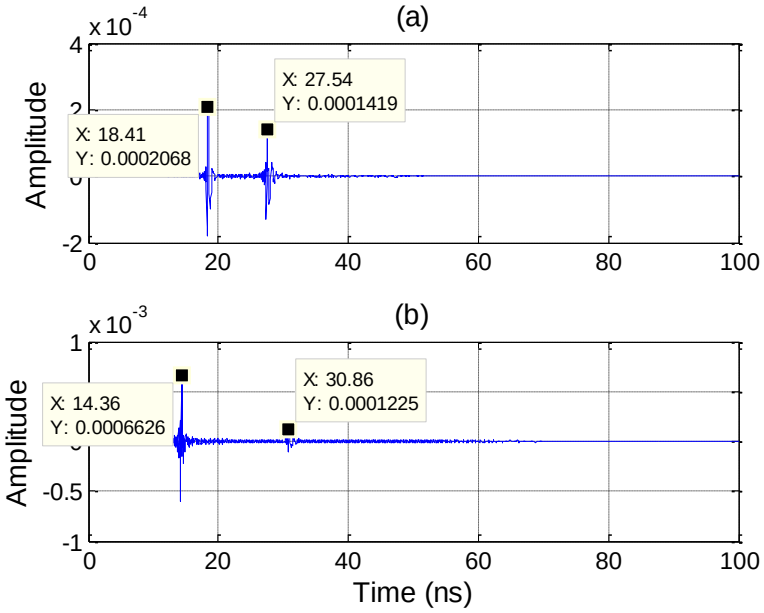

Figure 4.15 Time domain response of a PEC disk, and a PEC ellipsoid; (a) the left receiver, (b) the right receiver.

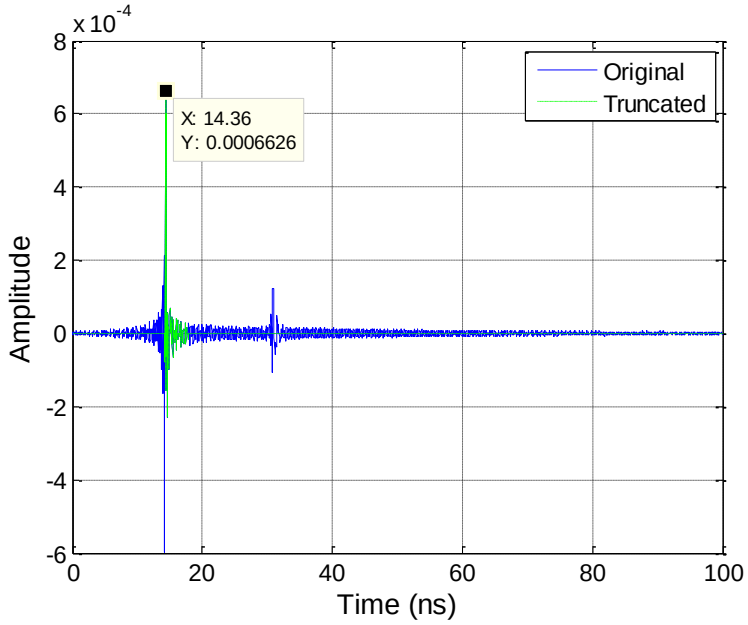

Figure 4.16 Truncated data from the first unknown target to apply the MP method from the right receiver (one disk and one ellipsoid model).

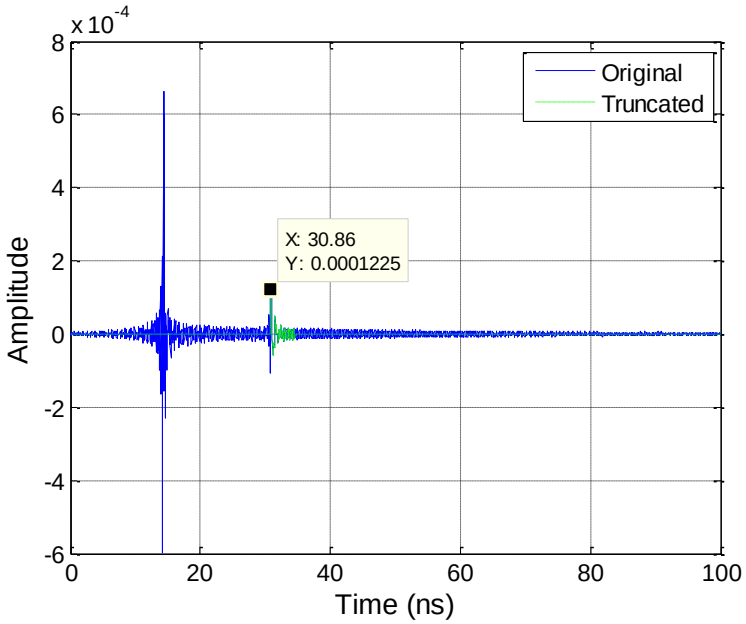

Figure 4.17 Truncated data from the second unknown target to apply the MP method from the right receiver (one disk and one ellipsoid model).

Table 4.3 Actual vs. Estimated Target Coordinates (Disk and Ellipsoid).

	Disk (D=0.1 m)		Ellipsoid (D=0.02 m, L=0.1 m)	
	R (m)	Angle (º)	*R* (m)	Angle (º)
Actual target coordinates	7.2469	15	9.2011	–12
Estimated target coordinates	7.2601	14.855	9.2199	–11.896

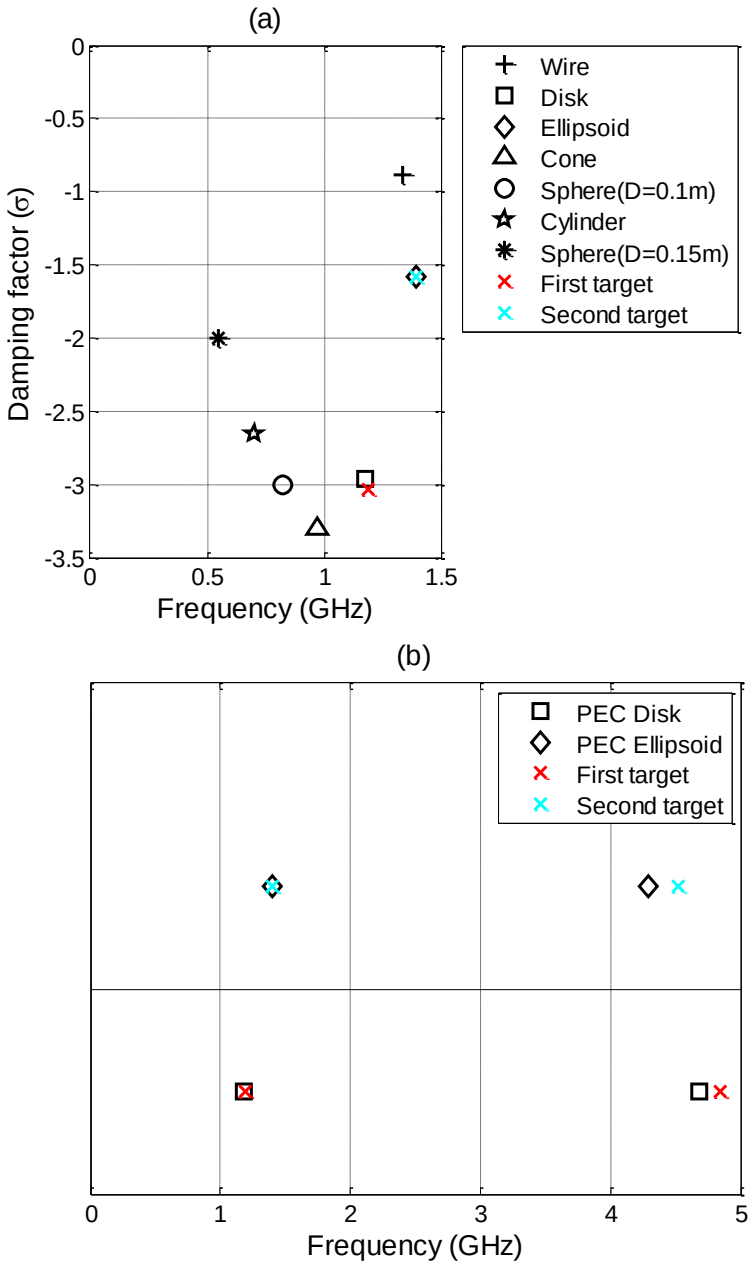

Figure 4.18 Pole Library vs. Computed poles of the unknown targets using the MP method (one disk and one ellipsoid model); (a) First order pole, (b) Resonant frequency.

4.5. One Cone and one Wire

For the next example displayed in Figure 4.19 we consider a PEC cone and a PEC wire located in free space. The diameter and height of the cone is 0.1 m and 0.1 m, respectively. The coordinates of the target from the origin is 7.2469 m and 15°, respectively. The length and radius of the wire is 0.1 m and 1 mm, respectively. Its coordinates from the origin are 8.0601 m and 7°, respectively. Figures 4.20-4.21 show the response from a cone and a wire as seen by the left and right receivers in the frequency domain and in the time domain, respectively.

Table 4.4 shows the actual vs. estimated coordinates of the targets (cone and wire) from the origin. For the first target, it has a relative 0.24 % error for the distance and 0.24 % error for the angle. For the second target, it has a 0.26 % error for the distance and 0.60 % error for the angle. Figures 4.22-4.23 show the truncated time domain data of the right receiver to apply the MP method. Figure 4.24 shows a library of poles for the PEC cone (0.1 m diameter, 0.1 m height), a PEC wire (0.1 m length, 1 mm radius) and the computed poles of the unknown objects. If we compare the library of poles with the ones computed in the time domain, we can clearly identify the two targets. The estimated errors of the resonant frequency are 3.41 % for the first target and 0.76 % for the second target, respectively as shown in Figure 4.24(b). Therefore, one can locate the 0.1-m-diameter & height PEC cone with approximate 97 % accuracy at 7.2642 m radial distance, 15.036° azimuthal angle and the 0.1-m-length, 1-mm-radius PEC wire with approximate 99 % accuracy at 8.0802 m radial distance, 7.0419° azimuthal angle.

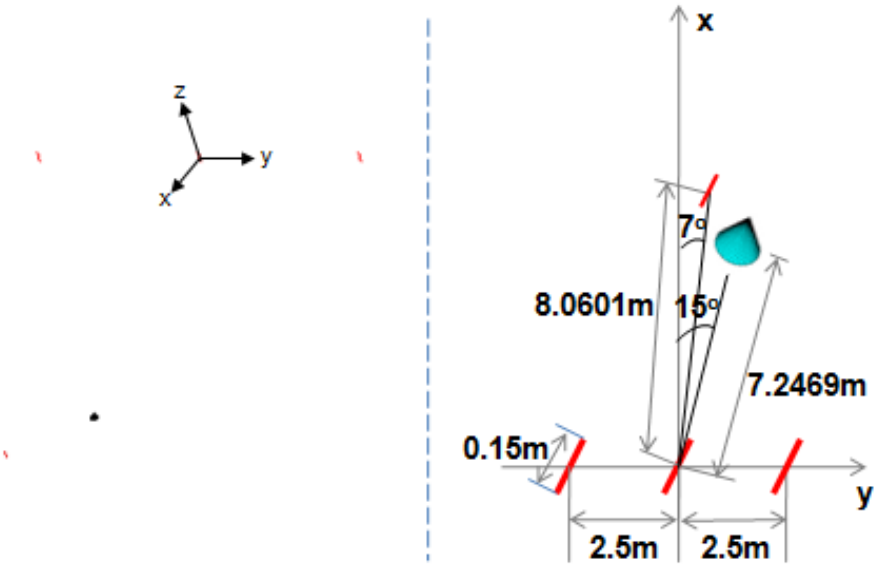

Figure 4.19 HOBBIES simulation model and its configuration with one transmitter, two receivers, a PEC cone, and a PEC wire.

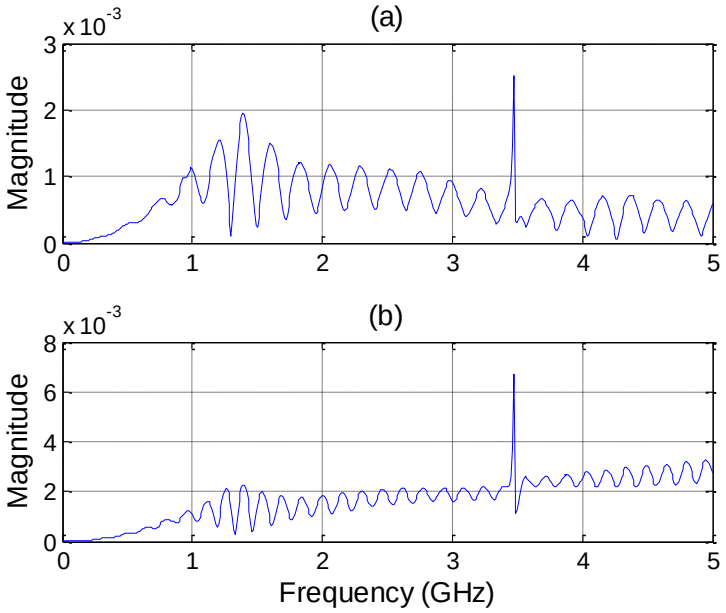

Figure 4.20 Frequency domain response of a PEC cone and a PEC wire; (a) the left receiver, (b) the right receiver.

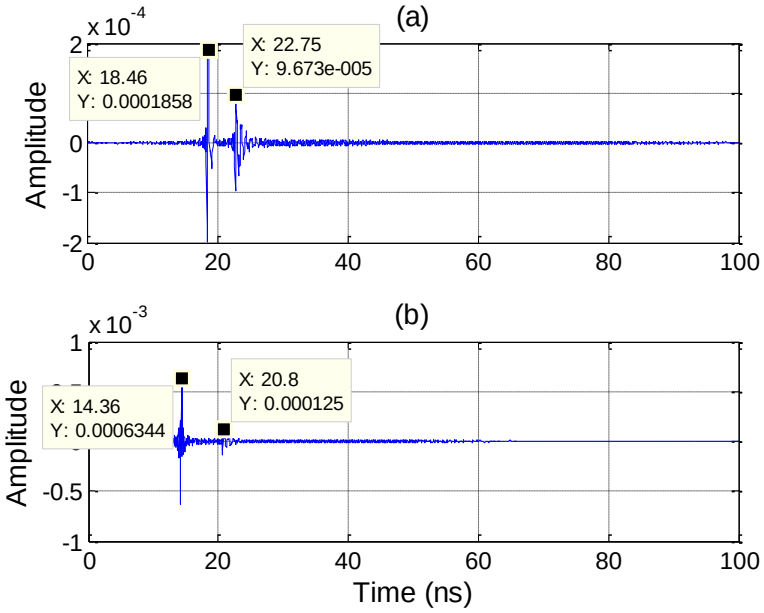

Figure 4.21 Time domain response of a PEC cone and a PEC wire; (a) the left receiver, (b) the right receiver.

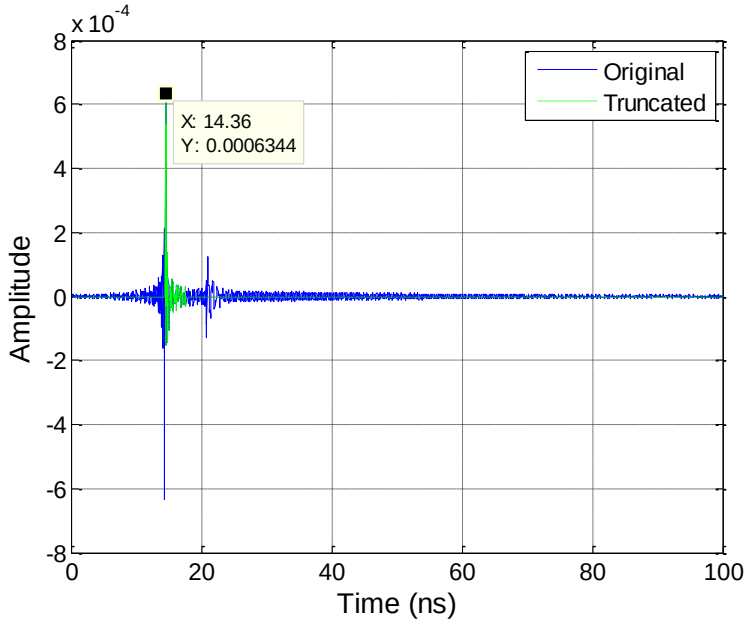

Figure 4.22 Truncated data from the first unknown target to apply the MP method from the right receiver (one cone and one wire model).

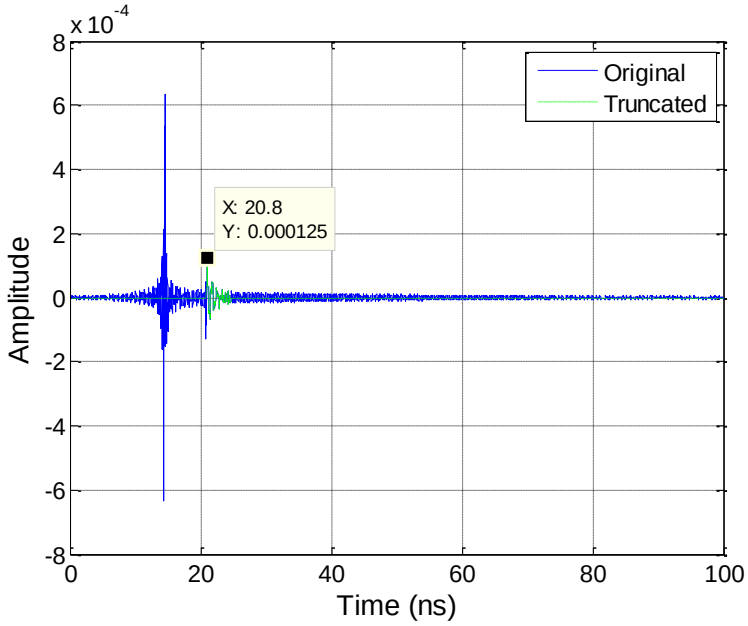

Figure 4.23 Truncated data from the second unknown target to apply the MP method from the right receiver (one cone and one wire model).

Table 4.4 Actual vs. Estimated Target Coordinates (Cone and Wire).

	Cone (D=0.1 m, H=0.1m)		Wire (L=0.1 m, r=1 mm)	
	R (m)	Angle (º)	*R* (m)	Angle (º)
Actual target coordinates	7.2469	15	8.0591	7
Estimated target coordinates	7.2642	15.036	8.0802	7.0419

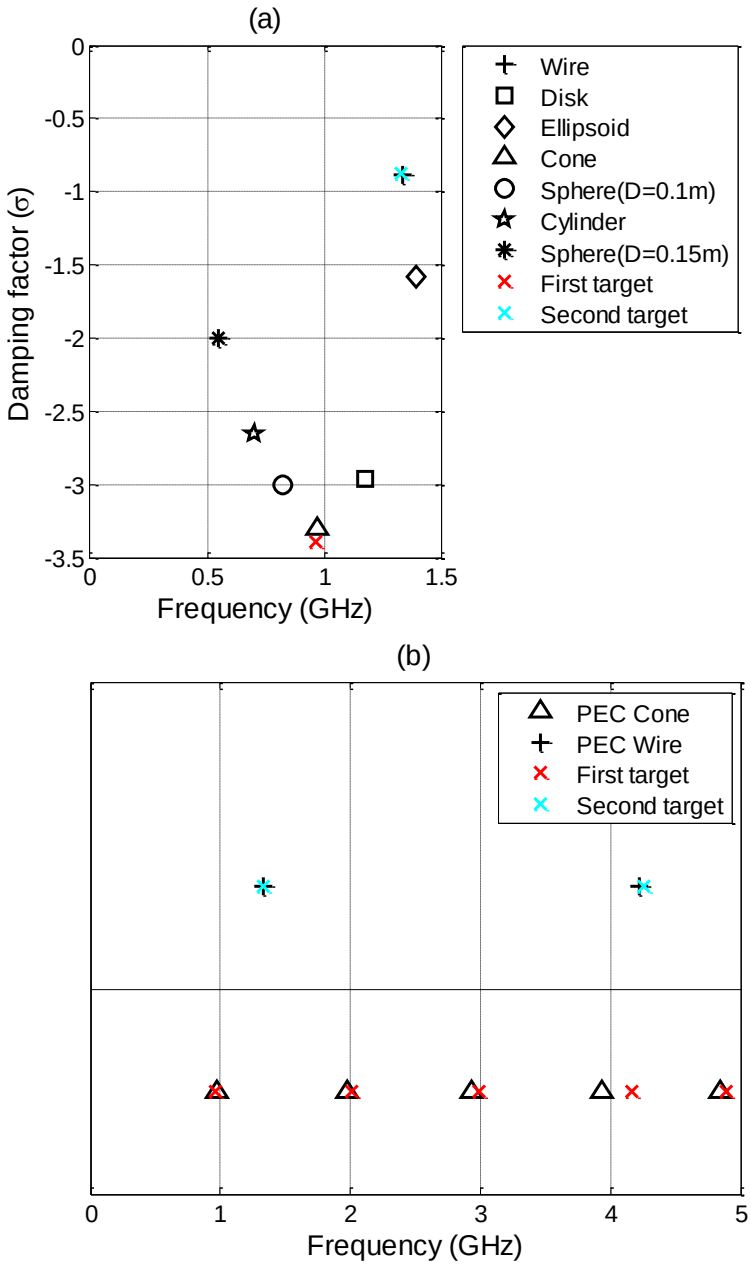

Figure 4.24 Pole Library vs. Computed poles of the unknown targets using the MP method (one cone and one wire model); (a) First order pole, (b) Resonant frequency.

4.6. One Cylinder and one Sphere

For the next example displayed in Figure 4.25 we consider a PEC cylinder and a PEC sphere located in free space. The diameter and height of the cylinder is 0.1 m and 0.1 m, respectively. The coordinates of the target from the origin is 8.0306 m and 5°, respectively. The diameter of the sphere is 0.1 m. Its coordinates from the origin are 9.0176 m and 7°, respectively. Figures 4.26-4.27 show the response from a cylinder and a sphere as seen by the left and right receivers in the frequency domain and in the time domain, respectively.

Table 4.5 shows the actual vs. estimated coordinates of the targets (cylinder and sphere) from the origin. For the first target, it has a relative 1.03 % error for the distance and 2.16 % error for the angle. For the second target, it has a 0.25 % error for the distance and 2.22 % error for the angle. Figures 4.28-4.29 show the truncated time domain data of the right receiver to apply the MP method. Figure 4.30 shows a library of poles for the PEC cylinder (0.1 m diameter, 0.1 m height), a PEC sphere (0.1 m diameter) and the computed poles of the unknown objects. If we compare the library of poles with the ones computed in the time domain, we can clearly identify the two targets. The estimated errors of the resonant frequency are 4.15 % for the first target and 5.87 % for the second target, respectively as shown in Figure 4.30(b). Therefore, one can locate the 0.1-m-diameter & height PEC cylinder with approximate 96 % accuracy at 7.9478 m radial distance, 5.1082° azimuthal angle and the 0.1-m-diameter PEC sphere with approximate 94 % accuracy at 9.0405 m radial distance, 7.1554° azimuthal angle.

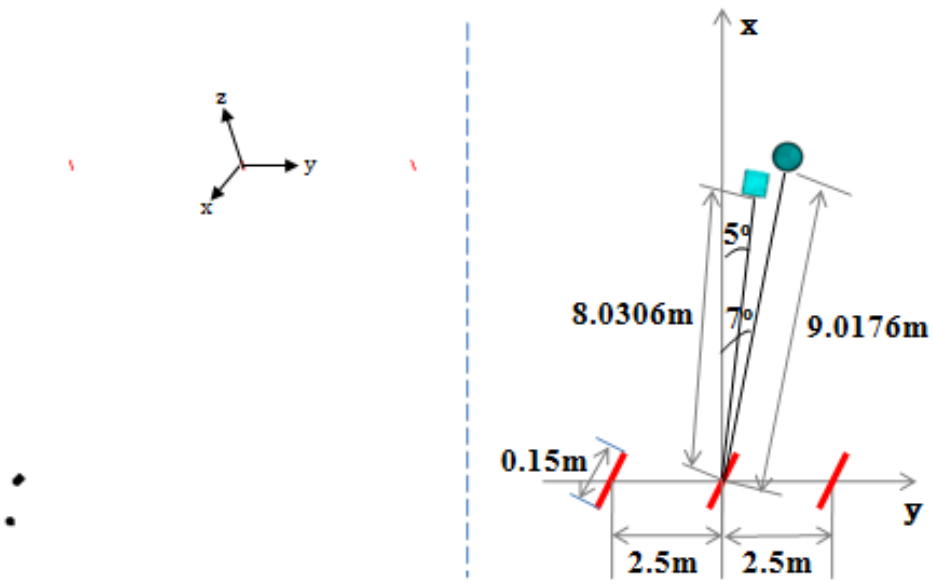

Figure 4.25 HOBBIES simulation model and its configuration with one transmitter, two receivers, a PEC cylinder, and a PEC sphere.

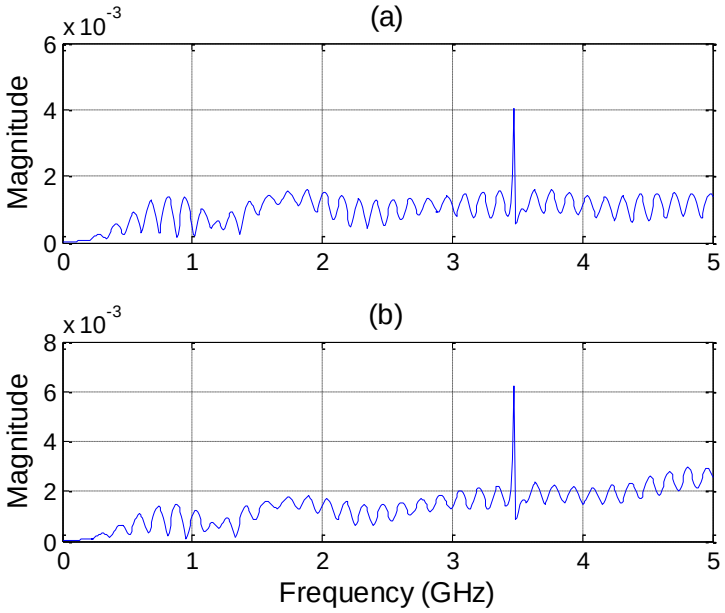

Figure 4.26 Frequency domain response of a PEC cylinder, and a PEC sphere; (a) the left receiver, (b) the right receiver.

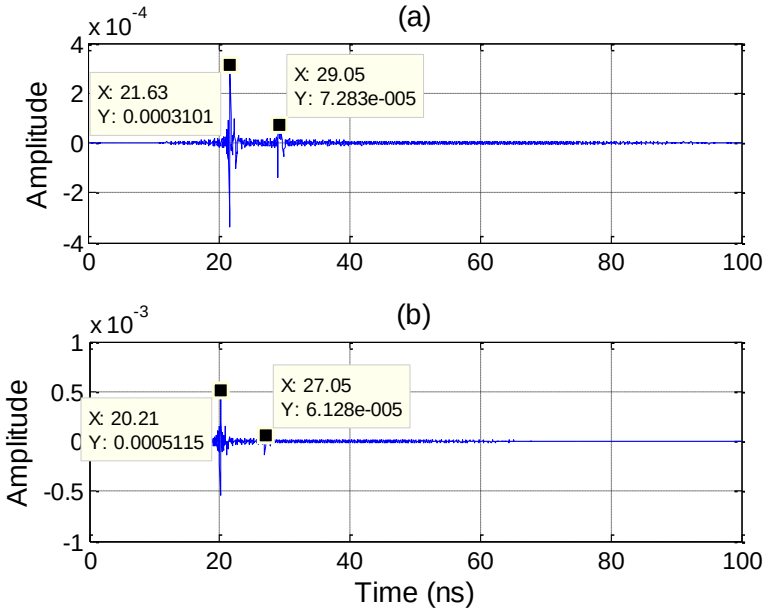

Figure 4.27 Time domain response of a PEC cylinder, and a PEC sphere; (a) the left receiver, (b) the right receiver.

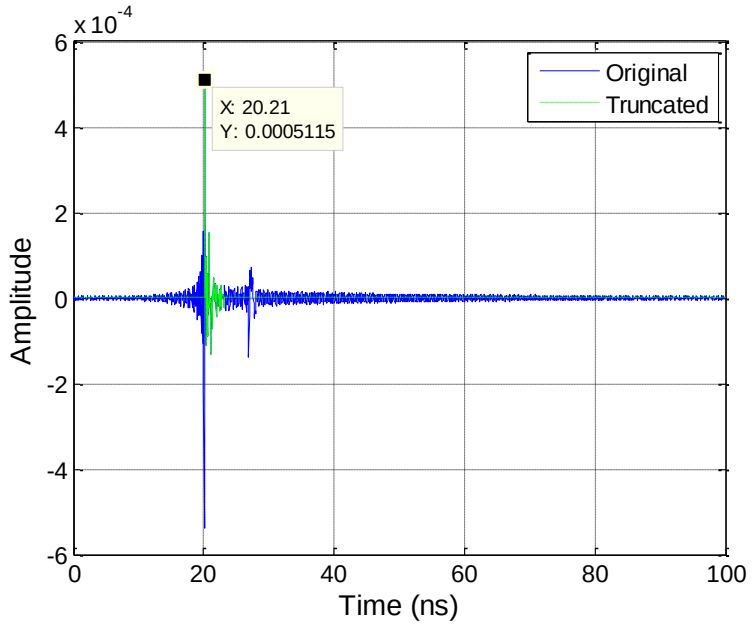

Figure 4.28 Truncated data from the first unknown target to apply the MP method from the right receiver (one cylinder and one sphere model).

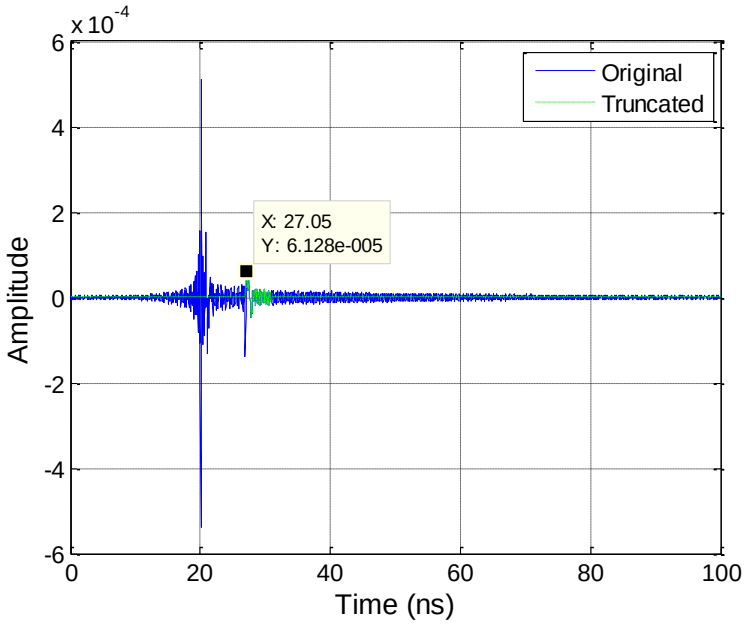

Figure 4.29 Truncated data from the second unknown target to apply the MP method from the right receiver (one cylinder and one sphere model).

Table 4.5 Actual vs. Estimated Target Coordinates (Cylinder and Sphere).

	Cylinder (D=0.1 m, H=0.1m)		Sphere (D=0.1 m)	
	R (m)	Angle (º)	*R* (m)	Angle (º)
Actual target coordinates	8.0306	5	9.0176	7
Estimated target coordinates	7.9478	5.1082	9.0405	7.1554

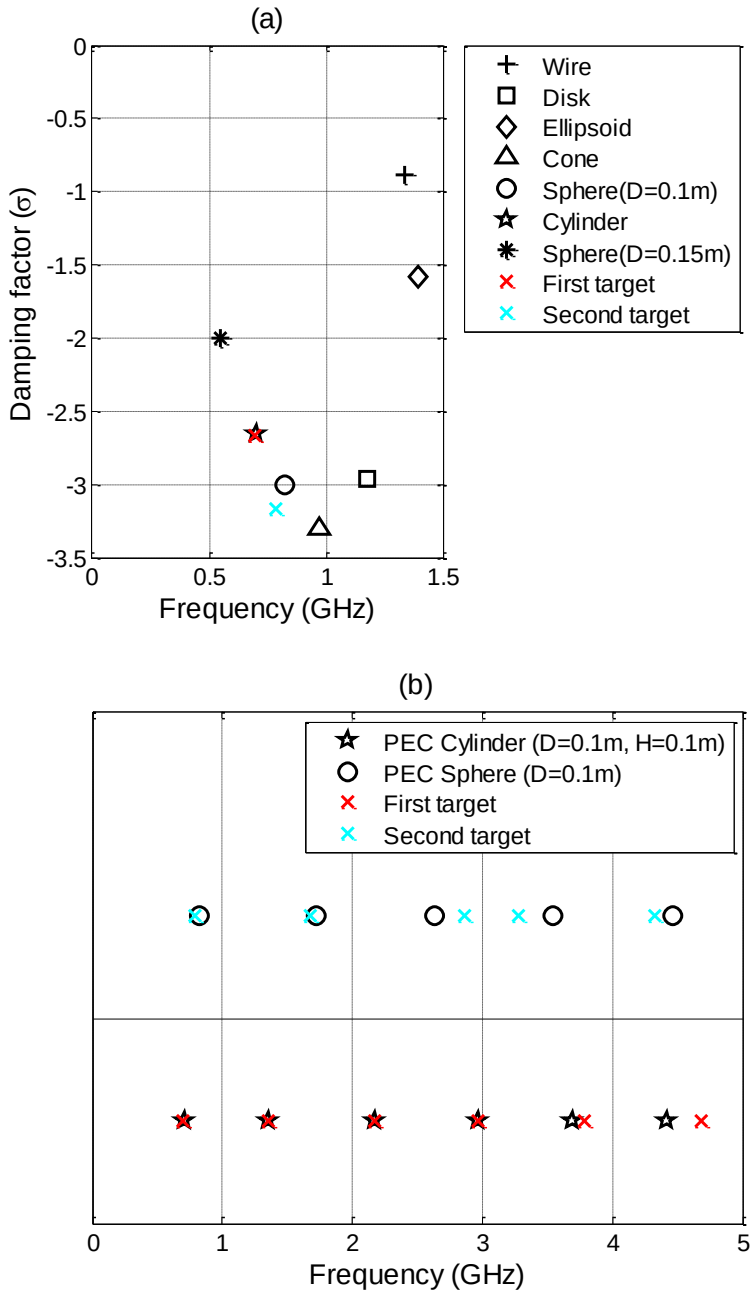

Figure 4.30 Pole Library vs. Computed poles of the unknown targets using the MP method (one cylinder and one sphere model); (a) First order pole, (b) Resonant frequency.

4.7. One Cone, one Wire, and one Sphere

For the last example displayed in Figure 4.31 we consider a PEC cone, a PEC wire, and a PEC sphere located in free space. We add an additional PEC sphere to the simulation model of chapter 4.5. The diameter of the sphere is 0.1 m. Its coordinates from the origin is 9 m and 0°, respectively. Figure 4.32 shows the response from a cone, a wire, and a sphere as seen by the left and right receivers in the frequency domain. Figure 4.33 shows their time domain response. Table 4.6 shows the actual vs. estimated coordinates of the targets from the origin. For the first and second targets, they have the same errors for the radial distance and for the azimuthal angle as Table 4.4. For the third target, it has a 0.28 % relative error for the radial distance and 0 % error for the azimuthal angle.

The MP method is applied to the truncated time domain data of the right receiver as shown in Figures 4.34, 4.35, and 4.36. Figure 4.37 shows a library of poles for the PEC cone (0.1 m diameter, 0.1 m height), a PEC wire (0.1 m length, 1 mm radius), a PEC sphere (0.1 m diameter) and the computed poles of the targets. If we compare the library of poles with the computed poles of the three detected targets, one can clearly identify the detected targets. The estimated errors of the resonant frequency are 3.51 % for the first target, 1.15 % for the second target, and 9.49 % for the third target respectively as shown in Figure 4.37(b).

Therefore, one can locate the PEC cone (0.1 m diameter, 0.1 m height) with approximate 96 % accuracy at 7.2642 m radial distance, 15.036° azimuthal angle, the PEC wire (0.1 m length, 1 mm radius) with approximate 99 % accuracy at 8.0802 m radial distance, 7.0419° azimuthal angle, and the PEC sphere (0.1 m diameter) with approximate 90 % accuracy at 8.9747 m radial distance, 0° azimuthal angle. For the third

target, it has a 10 % error in identifying the target as a 0.1-m-diameter sphere because of the relatively strong interaction effects between the various targets. From Figures 4.24 and 4.37, one can recognize that the first (front) target and the second (middle) target have almost the same accuracy of the identification procedure, as there are relatively weak interaction effects. However, for the third (last) target, the accuracy decreases from 99 % (Figure 4.6), 98 % (Figure 4.12) to 90 % because the amplitude of the late time response of the last target might increase or decrease from overlapping with the late time response of the first and the second targets. It means that if there are more than two targets, the accuracy of the identification for the rear target might decrease because of interaction effects between the various targets. For this case, identification accuracy for the third target is still acceptable.

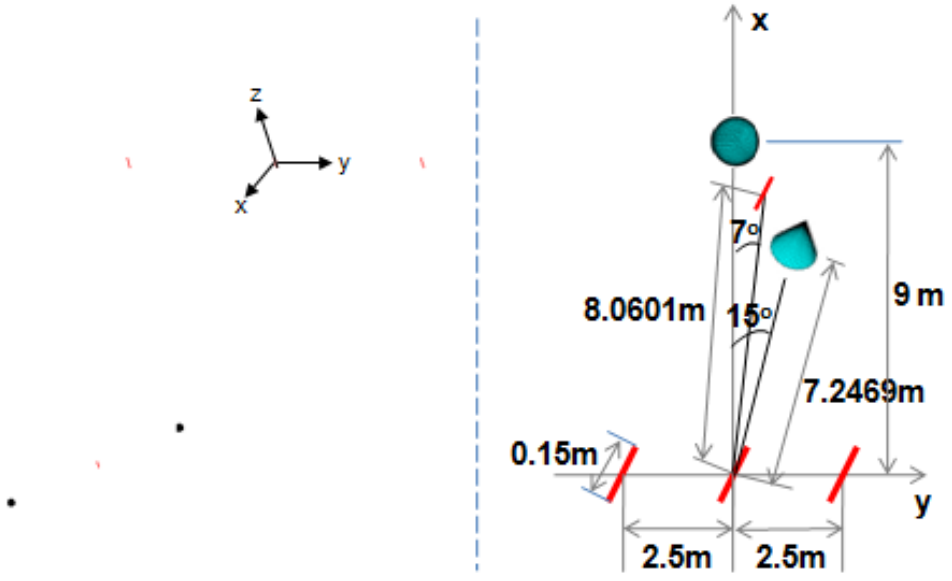

Figure 4.31 HOBBIES simulation model and its configuration with one transmitter, two receivers, a PEC cone, a PEC wire, and a PEC sphere.

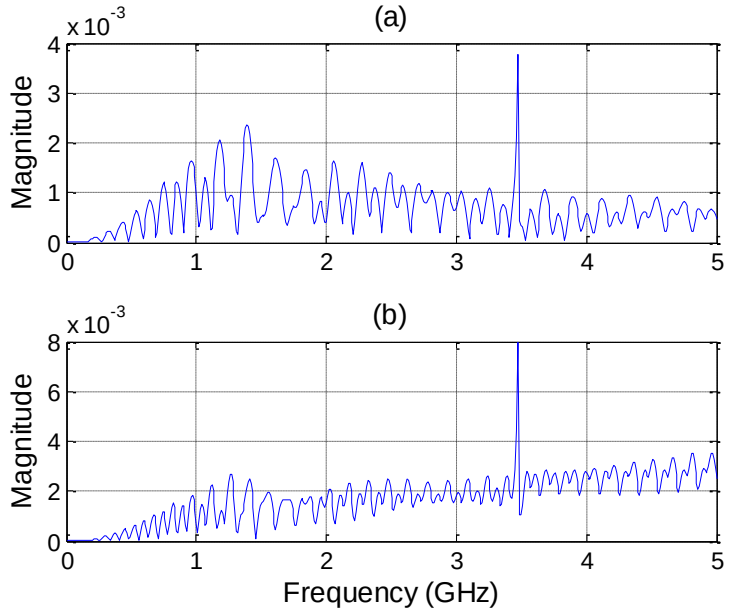

Figure 4.32 Frequency domain response of a PEC cone, a PEC wire, and a PEC sphere; (a) the left receiver, (b) the right receiver.

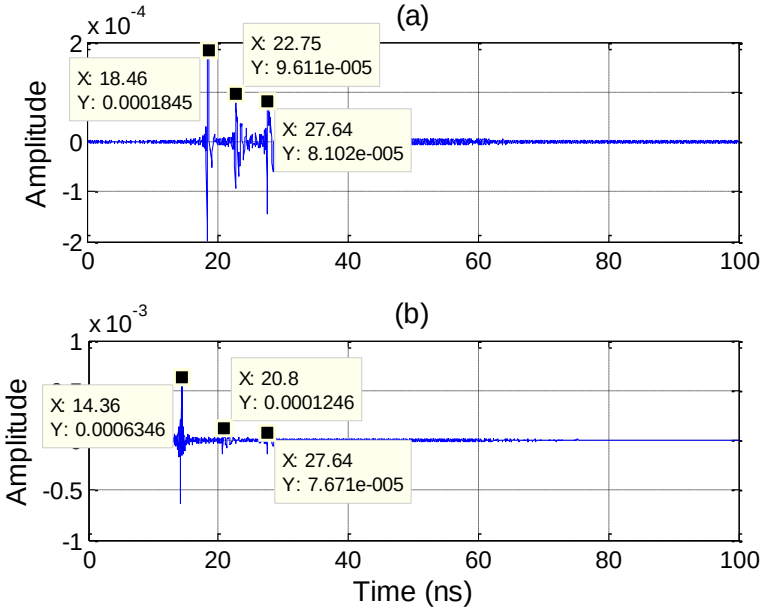

Figure 4.33 Time domain response of a PEC cone, a PEC wire, and a PEC sphere; (a) the left receiver, (b) the right receiver.

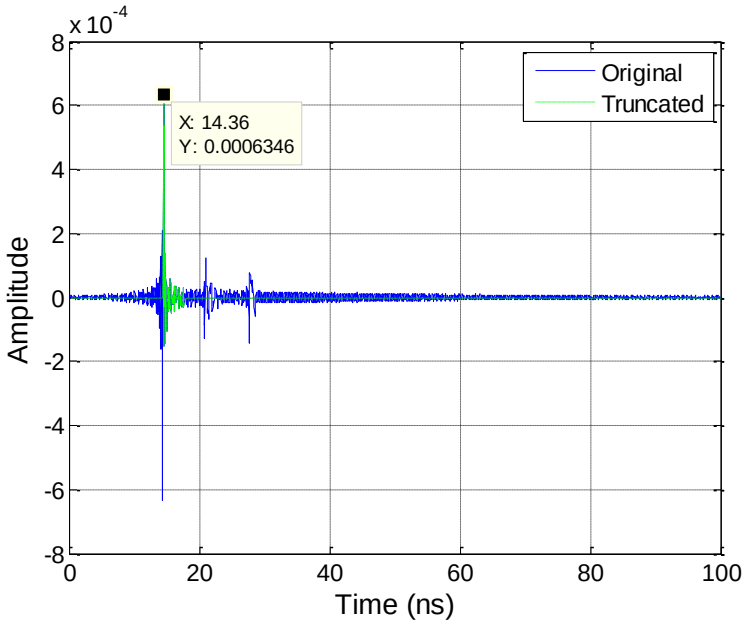

Figure 4.34 Truncated data from the first unknown target to apply the MP method from the right receiver (one cone, one wire, and one sphere model).

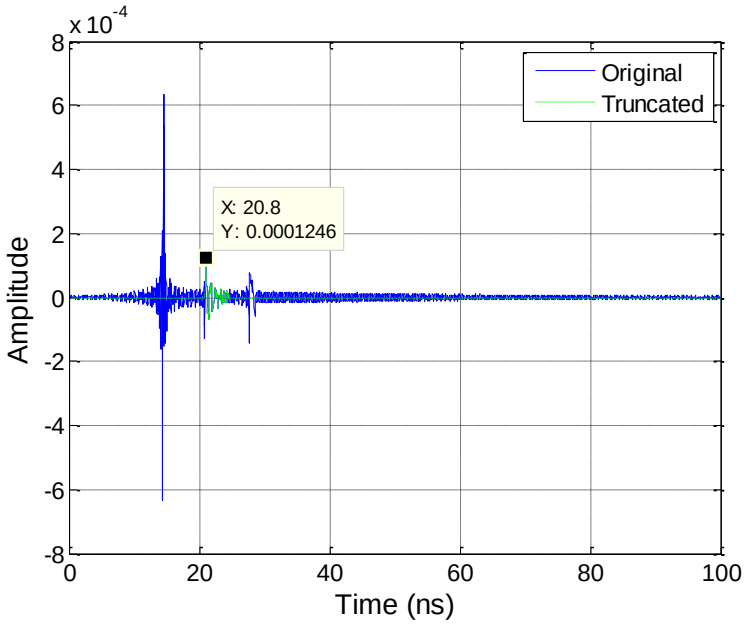

Figure 4.35 Truncated data from the second unknown target to apply the MP method from the right receiver (one cone, one wire, and one sphere model).

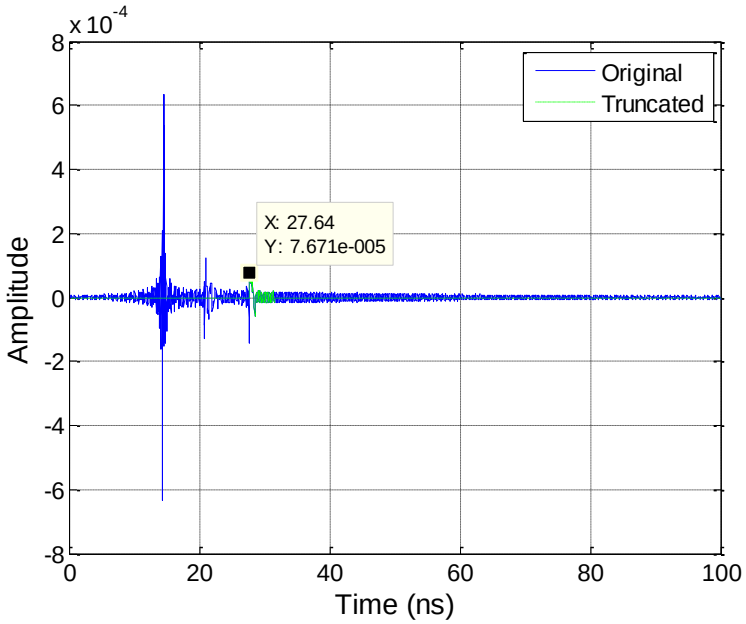

Figure 4.36 Truncated data from the third unknown target to apply the MP method from the right receiver (one cone, one wire, and one sphere model).

Table 4.6 Actual vs. Estimated Target Coordinates (Cone, Wire, and Sphere).

	Cone (D=0.1 m, H=0.1m)		Wire (L=0.1 m, r=1 mm)		Sphere (D=0.1 m)	
	R (m)	Angle (º)	*R* (m)	Angle (º)	*R* (m)	Angle (º)
Actual target coordinates	7.2469	15	8.0591	7	8.950	0
Estimated target coordinates	7.2642	15.036	8.0802	7.0419	8.9747	0

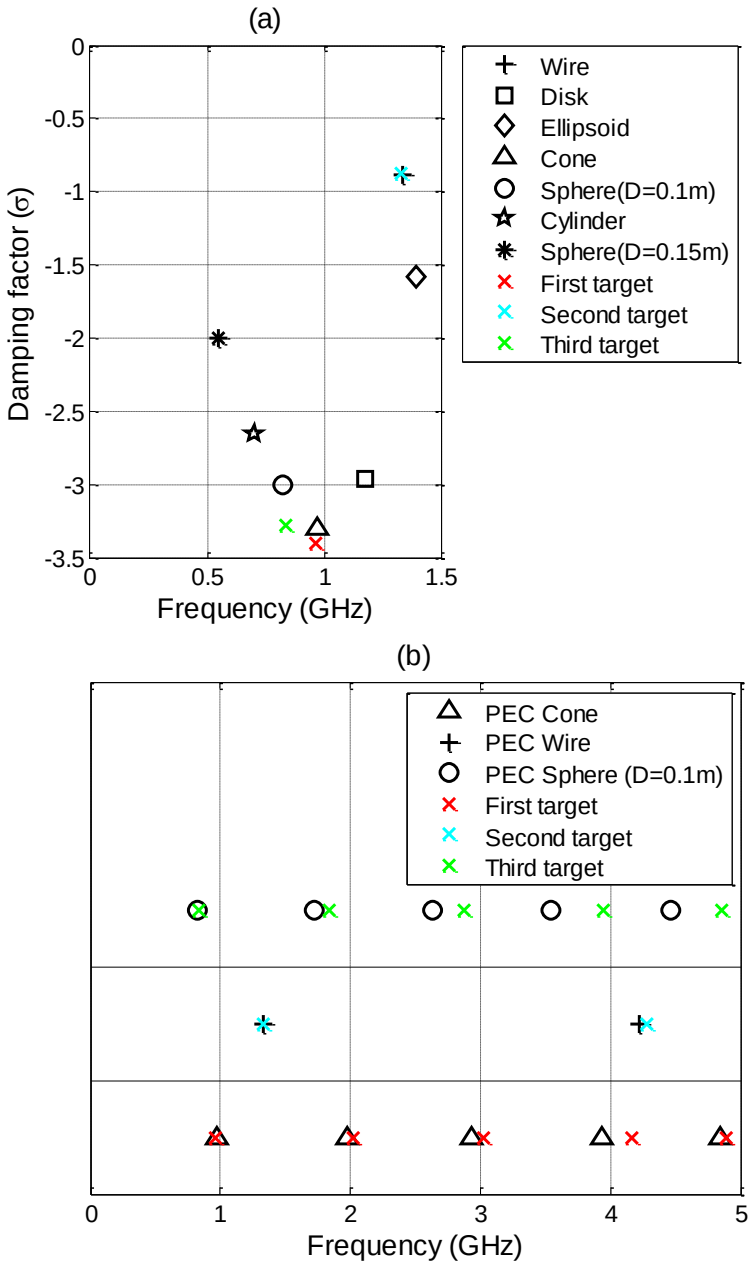

Figure 4.37 Pole Library vs. Computed poles of the unknown targets using the MP method (one cone, one wire, and one sphere model); (a) First order pole, (b) Resonant frequency.

5. SIMULATION EXAMPLE WITH AN OBJECT ON OR UNDER A DIELECTRIC MEDIUM

5.1. Overview

In this chapter, the application using the proposed methodology is extended from identification of an unknown object in free space to identification of an unknown object on urban ground or under an urban ground or under a sandy soil. Several examples are presented to clarify the proposed methodology for extended applications. For the simulation, we applied the same methodology as described for the PEC sphere example in the specified frequency range as outlined in chapter 3.3. The only different setup is adding a dielectric medium (urban ground: ε_r = 4, σ = 0.0002, sandy soil: ε_r = 10, σ = 0.002 [36]), the operating frequency range, spacing between the transmitter and the receiver considering the computation time (the number of unknown), and the limited spectrum band for the penetrating terrain [37]. The operating frequency ranges for examples in the chapter 5.2 and 5.3 are 0.01 GHz to 3 GHz (Δf = 0.01 GHz) and 0.01 GHz to 2 GHz (Δf = 0.01 GHz), respectively.

The first (5.2. one PEC sphere above an urban ground) example illustrates that even though there is effect of the ground in the scattered field data, the proposed methodology can be applied for identification of the unknown object on urban ground. The next (5.3. air cavity located under the ground) example also show that one can guess the unknown object located under an urban ground or under a sandy soil using the proposed methodology.

5.2. One PEC sphere above an Urban Ground

Figure 5.1 shows the configuration of the HOBBIES simulation model. The configuration is with one transmitter (center antenna), two receivers (left and right antennas), and one PEC sphere object located on urban ground (ε_r = 4, σ = 0.0002). The specification for each of the antenna for transmitter and receiver are 0.15 m in length and 1.5 mm radius. Each antenna is located at 2 m above an urban ground. Spacing between the transmitter and the receiver is 1.25 m to minimize the effects of the antenna coupling. The diameter of the sphere is 0.15 m. The sphere target is located above an urban ground and is oriented by 0° from the axis of the transmitting antenna. We applied a 1 V excitation to the transmitting antenna. The response of the object is computed from 0.01 GHz to 3 GHz (sampling frequency Δf = 0.01 GHz), and the number of samples is 300. Figure 5.2 shows the deconvolved response of the sphere to the left and right receiving antennas in the frequency domain. Figure 5.3 displays the time domain response of the object on urban ground for the left and right receivers. Table 5.1 describes the actual vs. estimated coordinates of the target from the origin based on the TDOA in the time domain. For the detected target, the computed error for the location is 1.85 % for the distance and a 0 % error for the angle.

The MP method is applied to the truncated time domain data obtained at the right receiver as shown in Figure 5.4. Figure 5.5 shows a library of poles and the computed poles of the detected target. If we compare the library of poles with the computed poles from the actual scattered fields from the target, we can clearly identify the detected target. Since the estimated error of the resonant frequency is 4.93 %, one can locate the 0.15-m-diameter PEC sphere with approximate 95 % accuracy at 1.8843 m radial distance and 0°

azimuthal angle. Notice that the most of the errors of the resonant frequency is due to the ground effect.

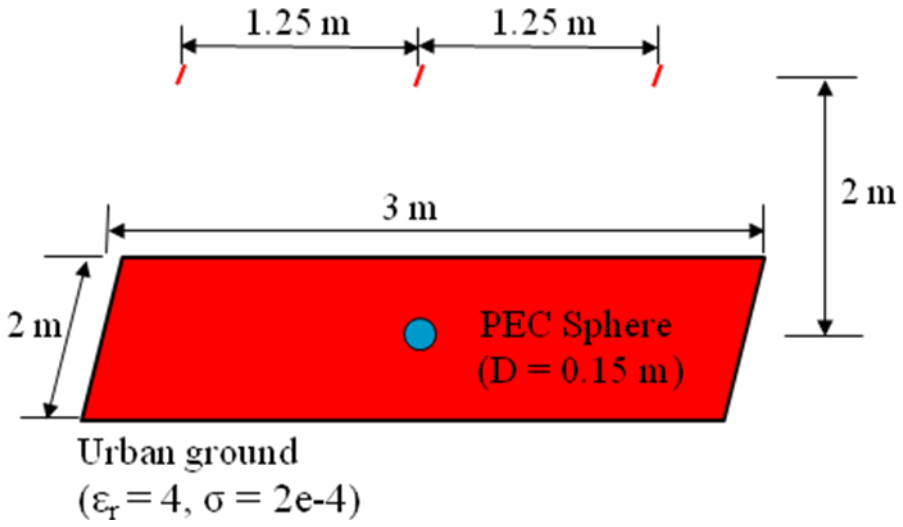

Figure 5.1 HOBBIES simulation model and its configuration with one transmitter, two receivers, and a 0.15-m-diameter PEC sphere on urban ground.

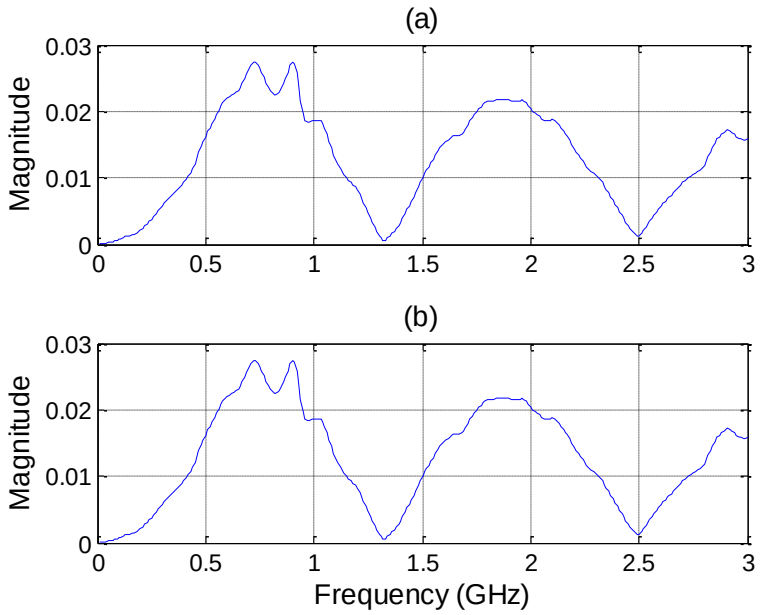

Figure 5.2 Frequency domain response of the 0.15-m-diameter PEC sphere on urban ground; (a) the left receiver, (b) the right receiver.

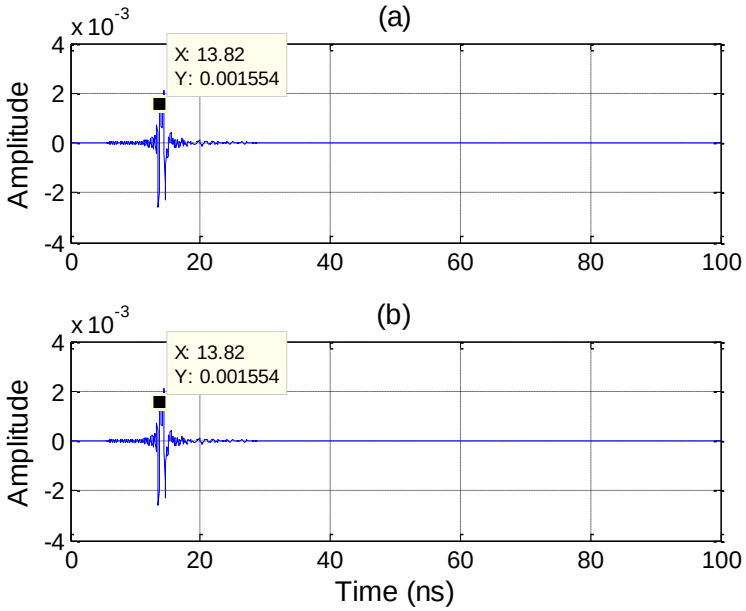

Figure 5.3 Time domain response of the 0.15-m-diameter PEC sphere on urban ground; (a) the left receiver, (b) the right receiver.

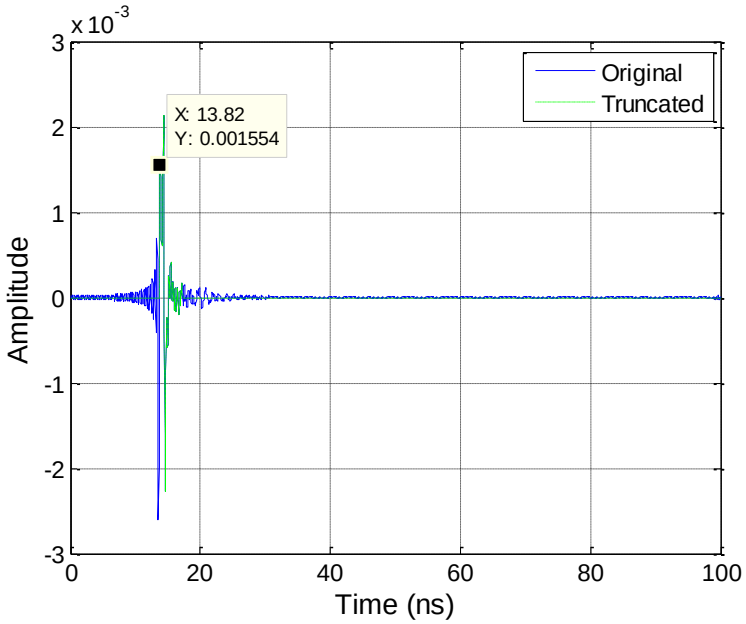

Figure 5.4 Truncated data from the unknown target to apply the MP method from the right receiver (sphere on urban ground).

Table 5.1 Actual vs. Estimated Target Coordinates (Sphere on urban ground).

	R (m)	Angle (°)
Actual target coordinates	1.85	0
Estimated target coordinates	1.8843	0

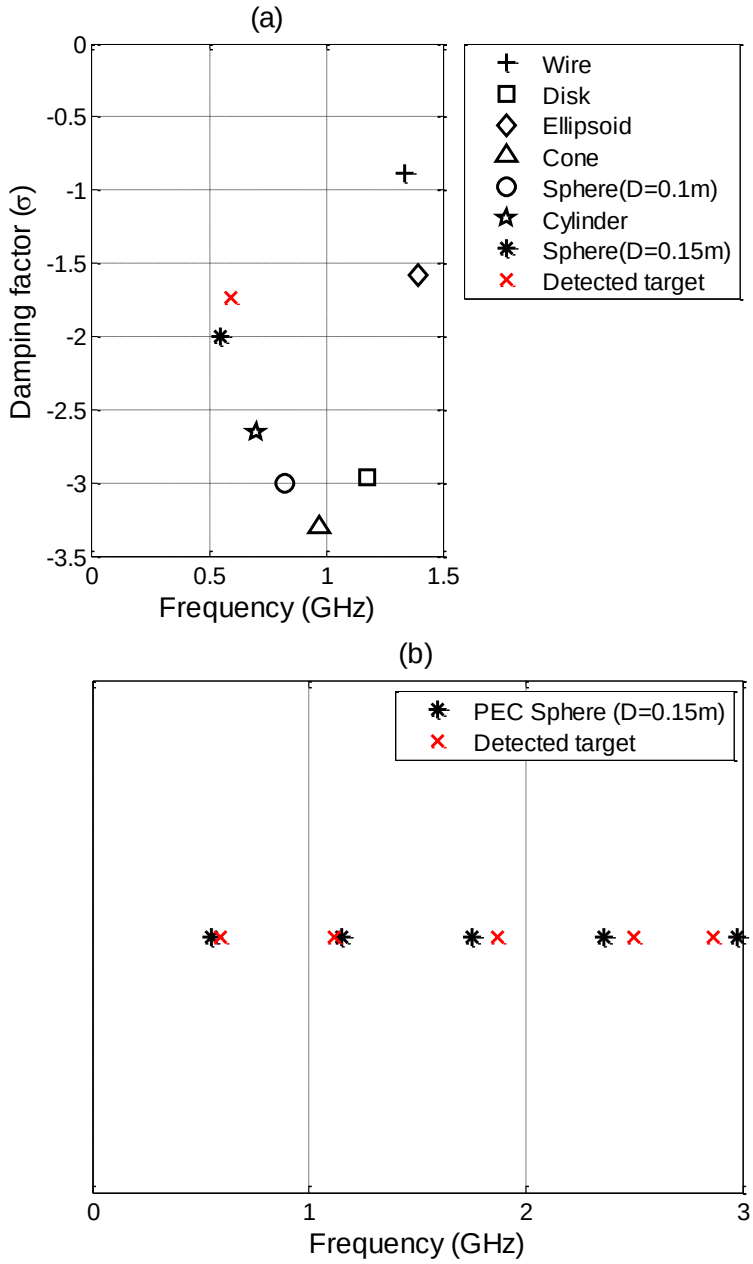

Figure 5.5 Pole Library vs. Computed poles of the unknown target using the MP method (sphere on urban ground); (a) First order pole, (b) Resonant frequency.

5.3. Air Cavity located under the Ground

For the next example we consider a spherical air cavity under an urban ground. Figure 5.6 shows the configuration of the HOBBIES simulation model. The configuration is with one transmitter (center antenna), two receivers (left and right antennas), and one spherical air cavity at a depth of 0.25 m under urban ground (ε_r = 4, σ = 0.0002). The specification for each of the antenna for transmitter and receiver and spacing between the transmitter and the receiver are the same as in the previous models. Distance between the transmitter and the surface of the urban ground is 0.5 m. The diameter of the spherical air cavity is 0.2 m. The spherical air cavity is located at a depth of 0.25 m under an urban ground and is oriented by 0° from the axis of the transmitting antenna. We applied a 1 V excitation to the transmitting antenna. The response of the object is computed from 0.01 GHz to 2 GHz (sampling frequency Δf = 0.01 GHz), and the number of samples is 200. Figure 5.7 shows the deconvolved response of the spherical air cavity to the left and right receiving antennas in the frequency domain. Figure 5.8 displays the time domain response of the object for the left and right receivers.

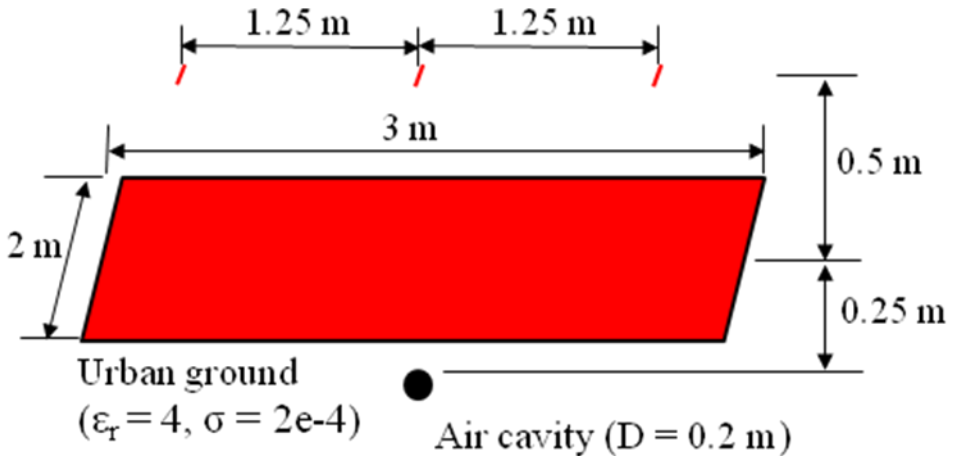

Figure 5.6 HOBBIES simulation model and its configuration with one transmitter, two receivers, a 0.2-m-diameter spherical air cavity at a depth of 0.25 m under urban ground.

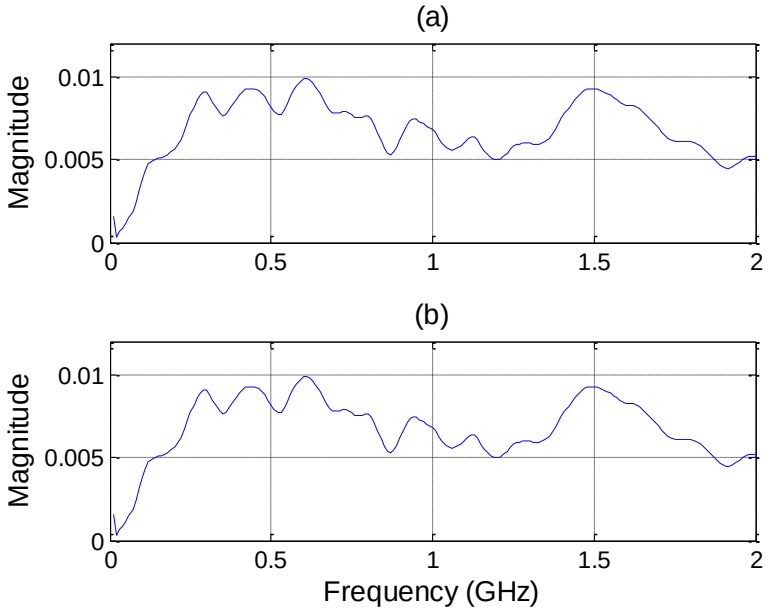

Figure 5.7 Frequency domain response of the 0.2-m-diameter spherical air cavity at a depth of 0.25 m under urban ground; (a) the left receiver, (b) the right receiver.

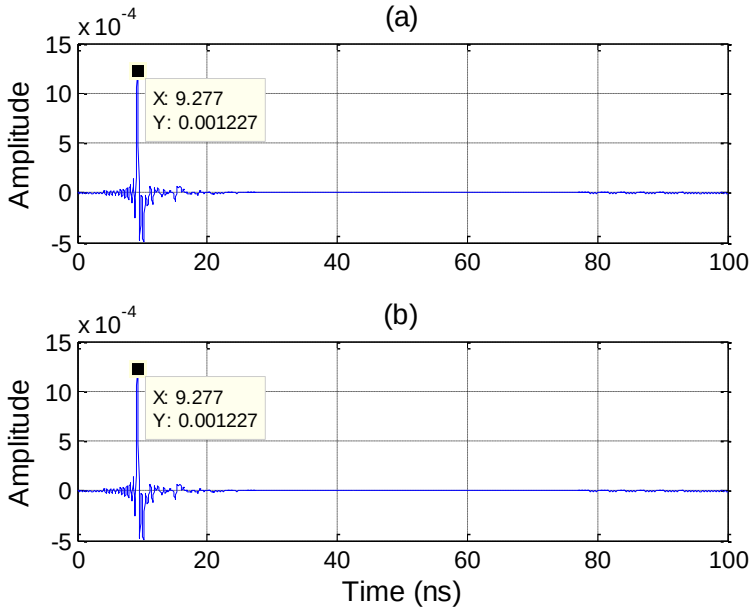

Figure 5.8 Time domain response of the 0.2-m-diameter spherical air cavity at a depth of 0.25 m under urban ground; (a) the left receiver, (b) the right receiver.

For the calculation of the target coordinates, if we assume that the locations of the left receiver, the right receiver, and the object are (0, –*d*, 0), (0, *d*, 0), and (*x*, *y*, *z*), respectively as shown in Figure 5.9. Since the object is oriented by 0° from the axis of the transmitting antenna,

$$R_L + R = R_R + R, \;\; R_L = R_R \tag{5.1}$$

where

$$R = \sqrt{x^2 + y^2 + z^2} = a_1 + b_1, \;\; R_R = \sqrt{x^2 + (y-d)^2 + z^2} = a_2 + b_2 \tag{5.2}$$

$$(a_1 + b_1)^2 + d^2 = (a_2 + b_2)^2 \tag{5.3}$$

$$\frac{b_1}{b_2} = \frac{(a_1 + b_1)}{(a_2 + b_2)} \Rightarrow a_1 b_2 = a_2 b_1 \tag{5.4}$$

where R is the radial distance of the surface of the unknown object from the transmitter. R_L and R_R are the distances of the surface of the object from the left receiver and right receiver, respectively.

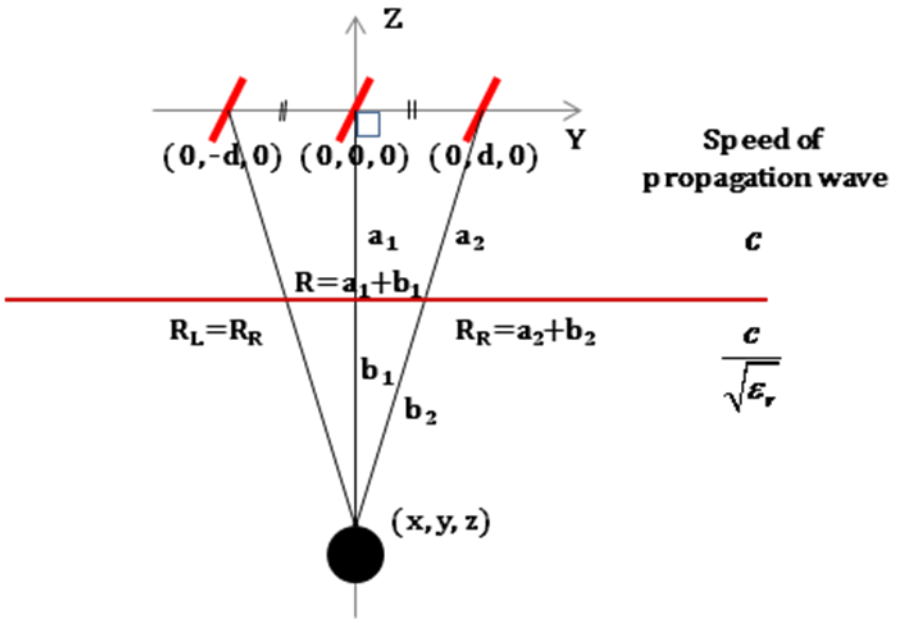

Figure 5.9 Configuration of one transmitter, two receivers, and one underground object for calculating object coordinates.

Considering different speed of propagation wave in air or in dielectric medium, the time delay (peak of the impulse response) of the left receiver (T_L) and the right receiver (T_R) can be formulated by

$$T_L = T_R = (a_1 + a_2)/c + (b_1 + b_2)/c \times \sqrt{\varepsilon_r} \tag{5.5}$$

One can calculate the detected underground target coordinates from (5.1-5.5) as shown in Table 5.2. For the detected target, the computed relative error for the location is 5.3 % for the distance and a 0 % error for the angle.

Table 5.2 Actual vs. Estimated Target Coordinates (Air cavity under urban ground at 0.25 m depth).

	R (m)	Angle (º)
Actual target coordinates	0.75	0
Estimated target coordinates	0.71	0

The MP method is applied to the truncated time domain data of the right receiver as shown in Figure 5.10. Notice that if an air cavity is in a dielectric medium of ε_r, its response can be compared to the actual response of a conducting object in free space with the same shape of an air cavity irrespectively of the value of ε_r [38]. Figure 5.11 shows a library of poles and the computed poles of the detected target. The Natural poles of a 0.2-m-diameter PEC sphere are computed using the Cauchy method as described in chapter 2. If we compare the library of poles with the computed poles of the detected target, we can guess the detected target as a 0.2-m-diameter spherical air cavity at a depth of 0.21 m under urban ground. Perhaps, the large difference in the values of the natural frequency may be due to the interaction of the surface to the buried object.

For the next example displayed in Figure 5.12 we consider a spherical air cavity under urban ground at a different depth. All simulation setup is the exactly same as previous simulation model except for a depth of 0.65 m under urban ground. Figure 5.13 shows the deconvolved response of the spherical air cavity to the left and right receiving antennas in the frequency domain. Figure 5.14 displays their time domain response for the left and right receivers. For the detected target, the computed error for the location is 3.9 % for the distance and a 0 % error for the angle as shown in Table 5.3. The MP method is applied to the truncated time domain data of the right receiver as shown in Figure 5.15. Figure 5.16 shows a library of poles and the computed poles of detected target. If we compare the library of pole of them with computed poles of the detected target, we can also guess the detected target as a 0.2-m-diameter spherical air cavity at a depth of 0.61 m under urban ground. One can observe that the resonant frequency of the first order pole increases as the depth of an object increases as shown in Figure 5.17.

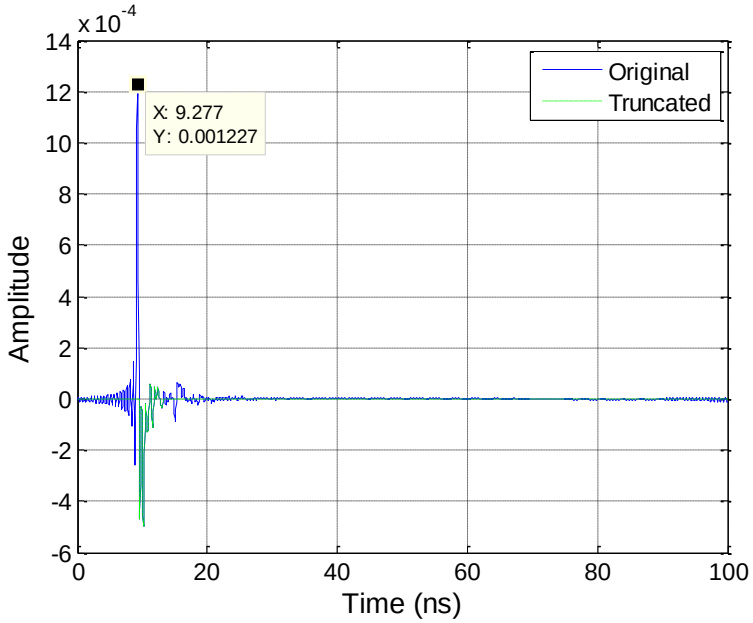

Figure 5.10 Truncated data from the unknown target to apply the MP method from the right receiver (air cavity under urban ground at 0.25 m depth).

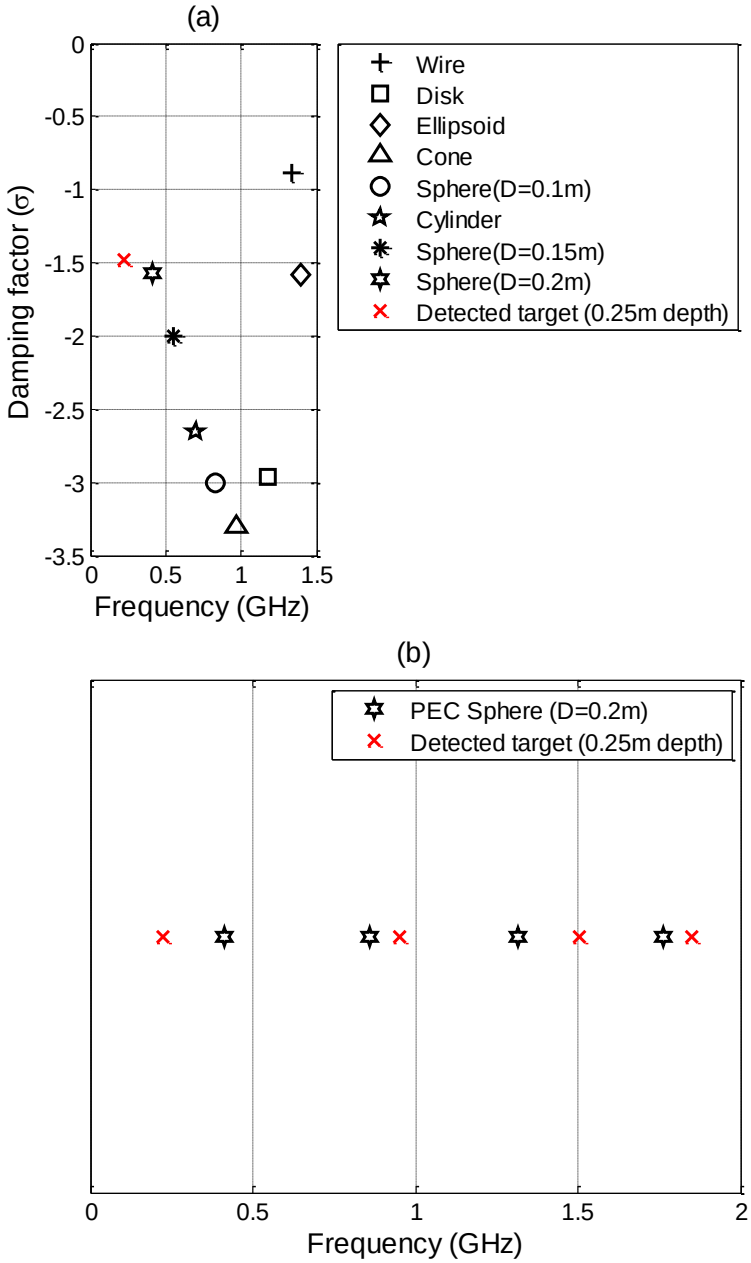

Figure 5.11 Pole Library vs. Computed poles of the unknown target using the MP method (air cavity under urban ground at 0.25 m depth); (a) First order pole, (b) Resonant frequency.

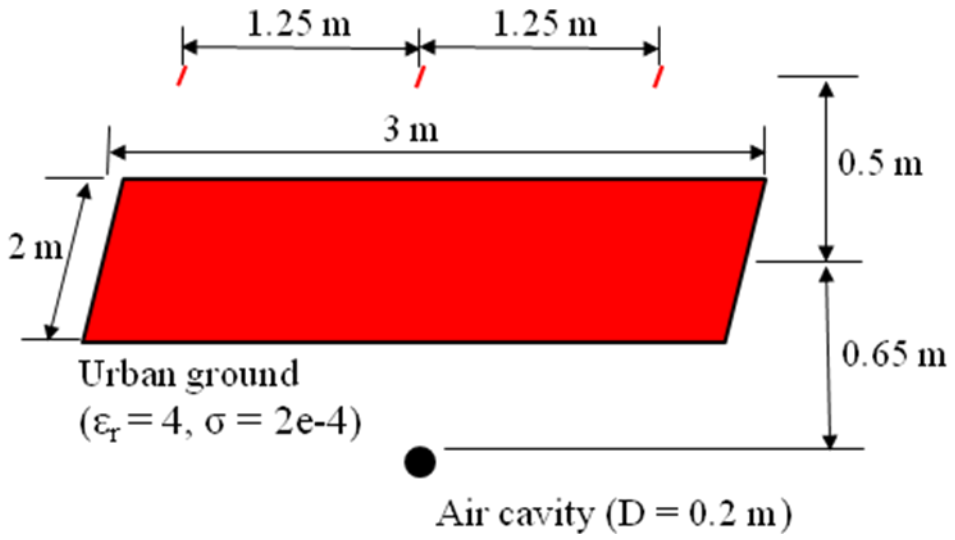

Figure 5.12 HOBBIES simulation model and its configuration with one transmitter, two receivers, a 0.2-m-diameter spherical air cavity at a depth of 0.65 m under urban ground.

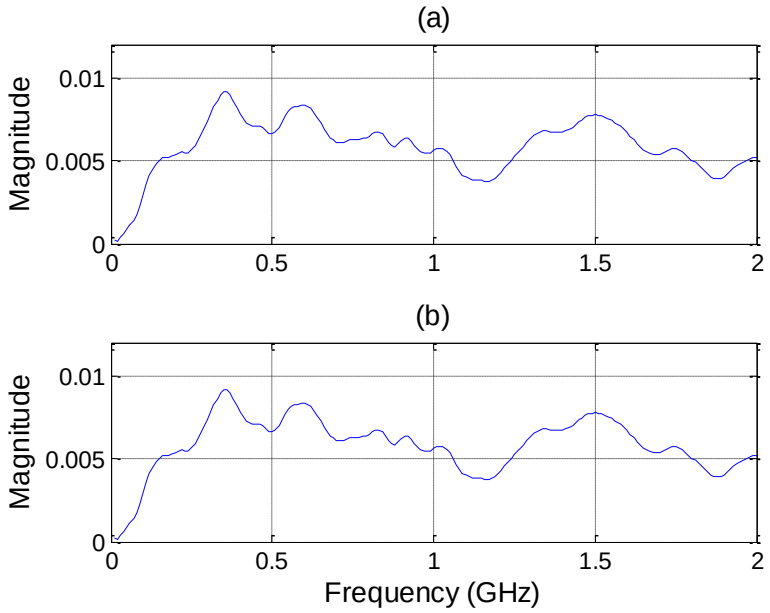

Figure 5.13 Frequency domain response of the 0.2-m-diameter spherical air cavity at a depth of 0.65 m under urban ground; (a) the left receiver, (b) the right receiver.

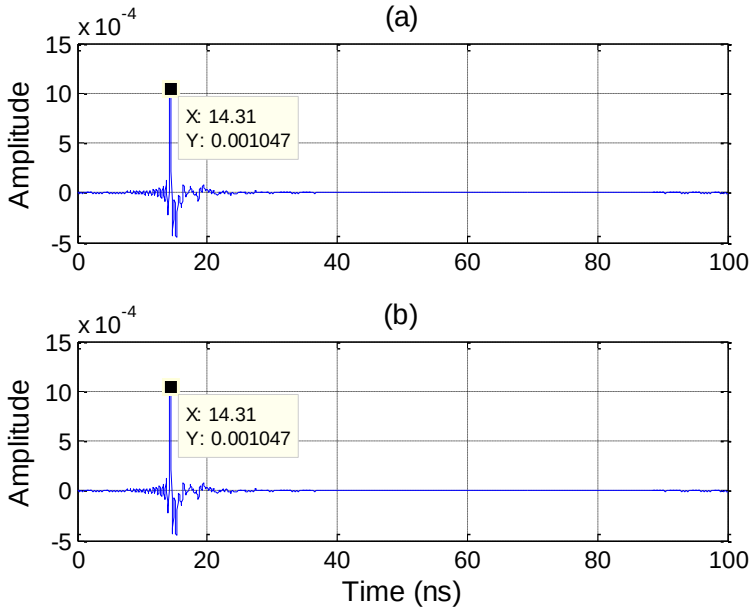

Figure 5.14 Time domain response of the 0.2-m-diameter spherical air cavity at a depth of 0.65 m under urban ground; (a) the left receiver, (b) the right receiver.

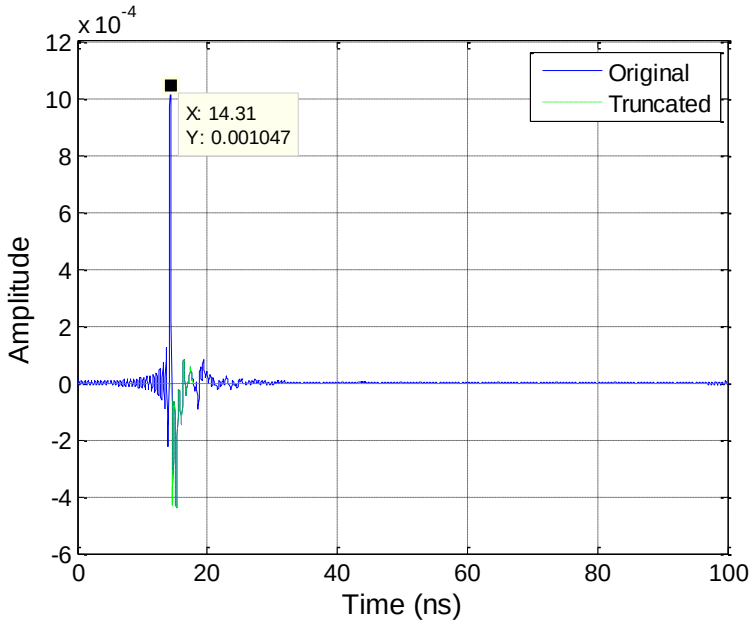

Figure 5.15 Truncated data from the unknown target to apply the MP method from the right receiver (air cavity under urban ground at 0.65 m depth).

Table 5.3 Actual vs. Estimated Target Coordinates (Air cavity under urban ground at 0.65 m depth).

	R (m)	Angle (º)
Actual target coordinates	1.15	0
Estimated target coordinates	1.1053	0

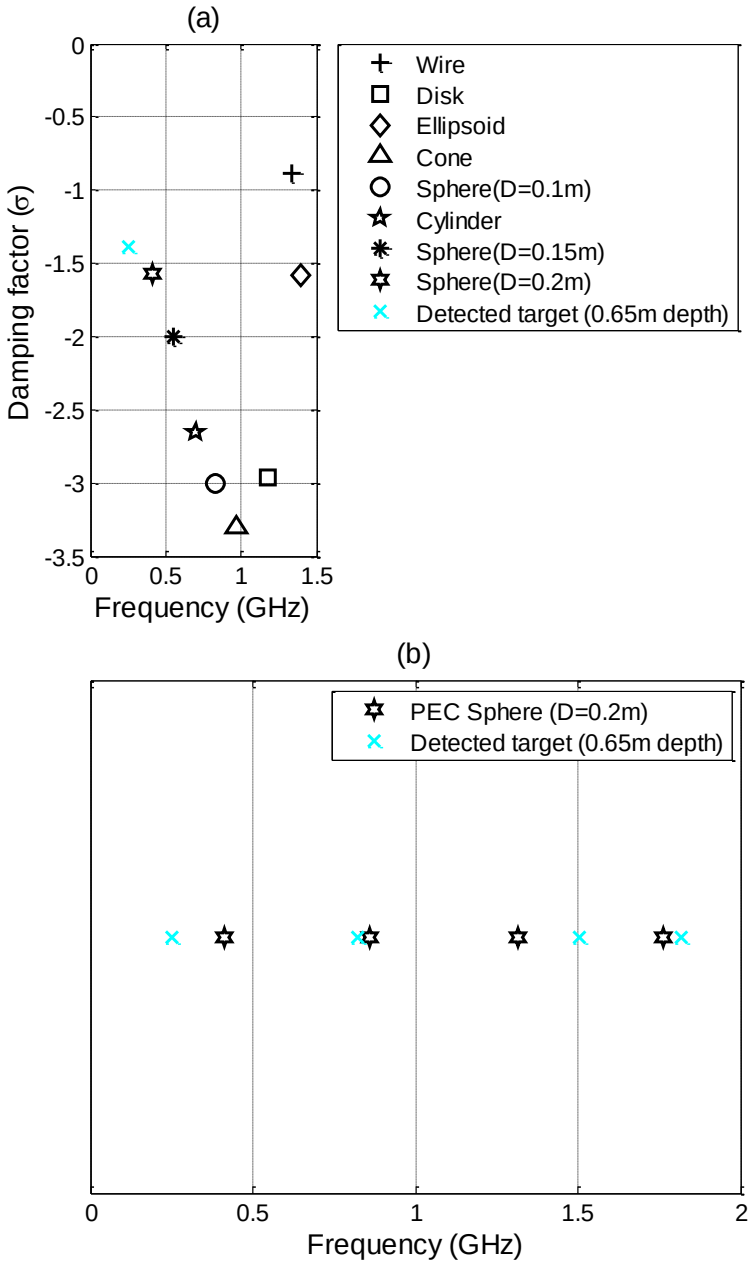

Figure 5.16 Pole Library vs. Computed poles of the unknown target using the MP method (air cavity under urban ground at 0.65m depth); (a) First order pole, (b) Resonant frequency.

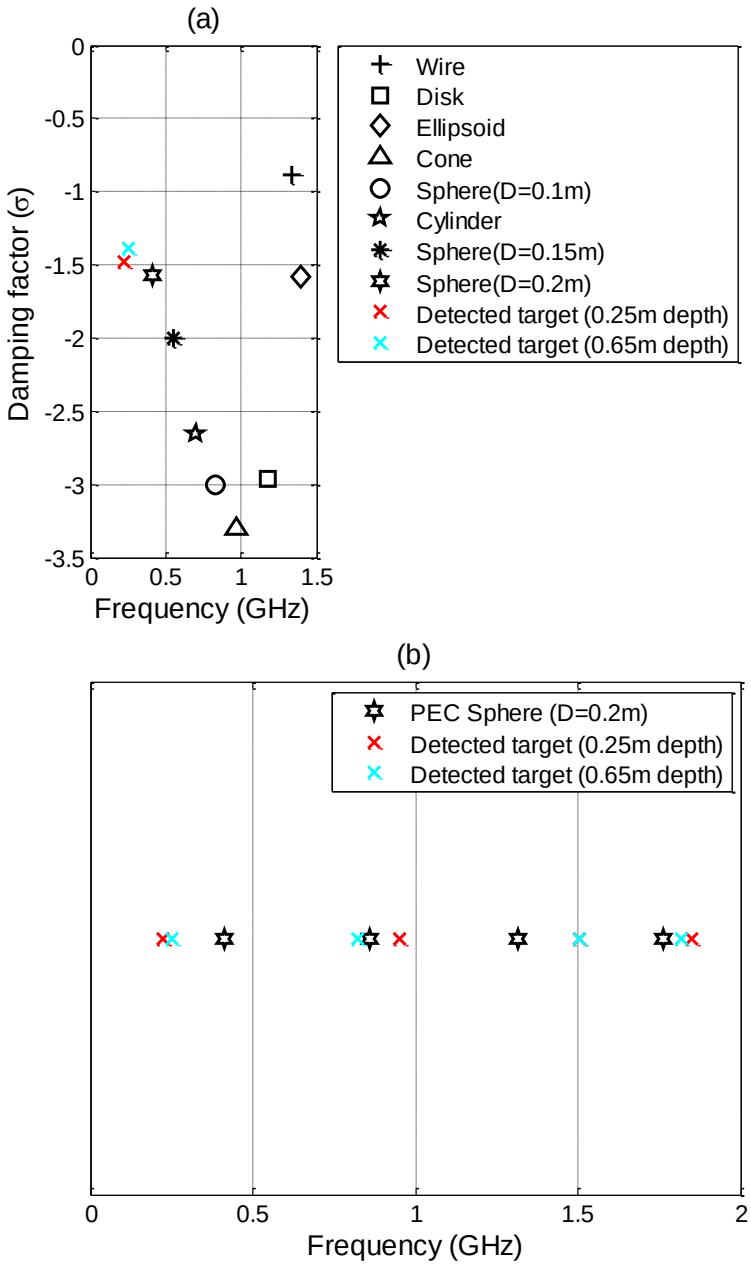

Figure 5.17 Pole Library vs. Computed poles of the unknown targets using the MP method (air cavities under urban ground at 0.25 m and 0.65m depth); (a) First order pole, (b) Resonant frequency.

For the next example we also consider a spherical air cavity under sandy soil at a depth of 0.65 m as shown in Figure 5.18. All simulation setup is the exactly same as previous simulation model except for different dielectric medium, sandy soil. (ε_r = 10, σ = 0.002). Figure 5.19 shows the deconvolved response of the spherical air cavity to the left and right receiving antennas in the frequency domain. Figure 5.20 displays their time domain response for the left and right receivers. For the detected target, the computed error for the location is 6.7 % for the distance and a 0 % error for the angle as shown in Table 5.4. The MP method is applied to the truncated time domain data of the right receiver as shown in Figure 5.21. Figure 5.22 shows a library of poles and the computed poles of detected target. If we compare the library of pole of them with computed poles of the detected target, we can also guess the detected target as a 0.2-m-diameter spherical air cavity at a depth of 0.57 m under sandy soil. One can observe that the response of an air cavity under a dielectric medium (ε_r) can be compared to the actual response of a conducting object in free space with the same shape of an air cavity irrespectively of the value of ε_r as shown in Figure 5.23.

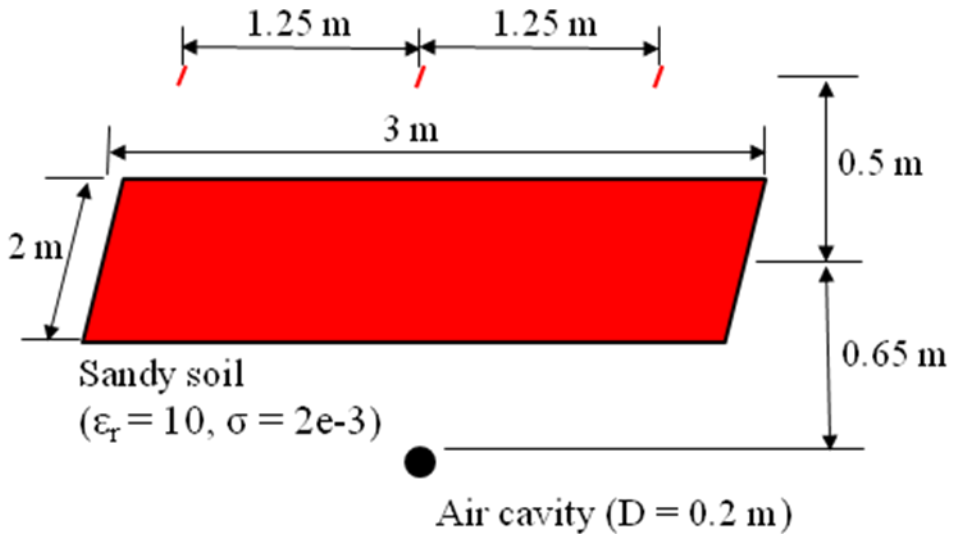

Figure 5.18 HOBBIES simulation model and its configuration with one transmitter, two receivers, a 0.2-m-diameter spherical air cavity at a depth of 0.65 m under sandy soil.

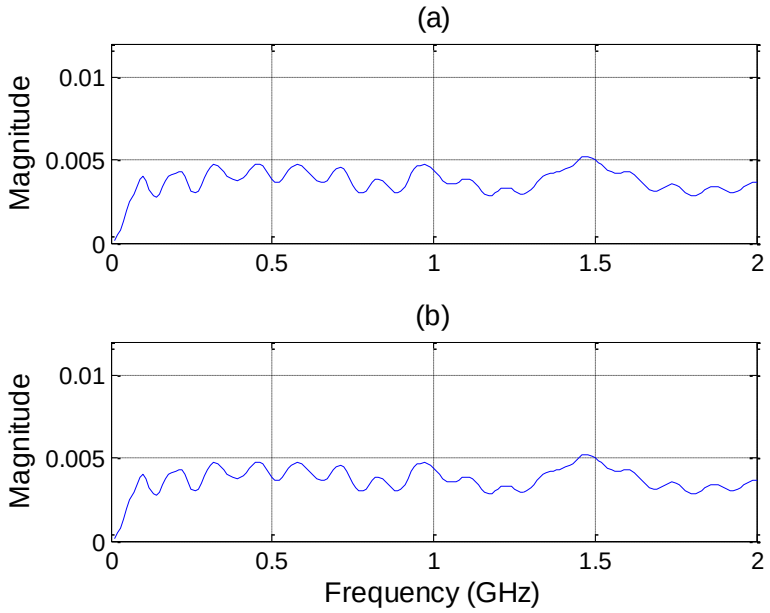

Figure 5.19 Frequency domain response of the 0.2-m-diameter spherical air cavity at a depth of 0.65 m under sandy soil; (a) the left receiver, (b) the right receiver.

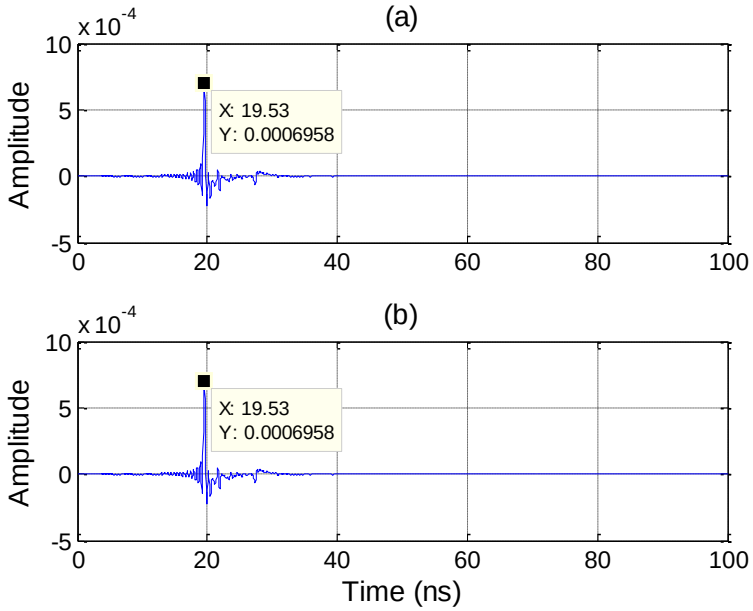

Figure 5.20 Time domain response of the 0.2-m-diameter spherical air cavity at a depth of 0.65 m under sandy soil; (a) the left receiver, (b) the right receiver.

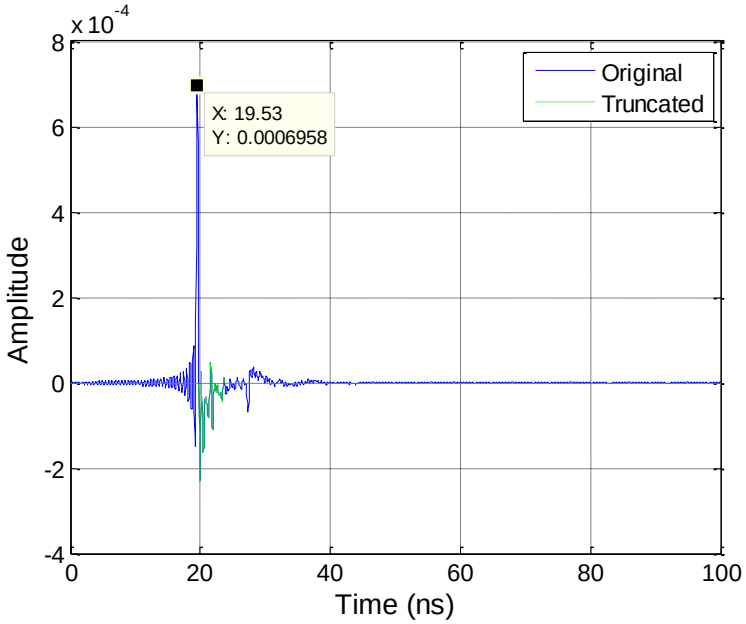

Figure 5.21 Truncated data from the unknown target to apply the MP method from the right receiver (air cavity under sandy soil at 0.65 m depth).

Table 5.4 Actual vs. Estimated Target Coordinates (Air cavity under sandy soil at 0.65 m depth).

	R (m)	Angle (º)
Actual target coordinates	1.15	0
Estimated target coordinates	1.0726	0

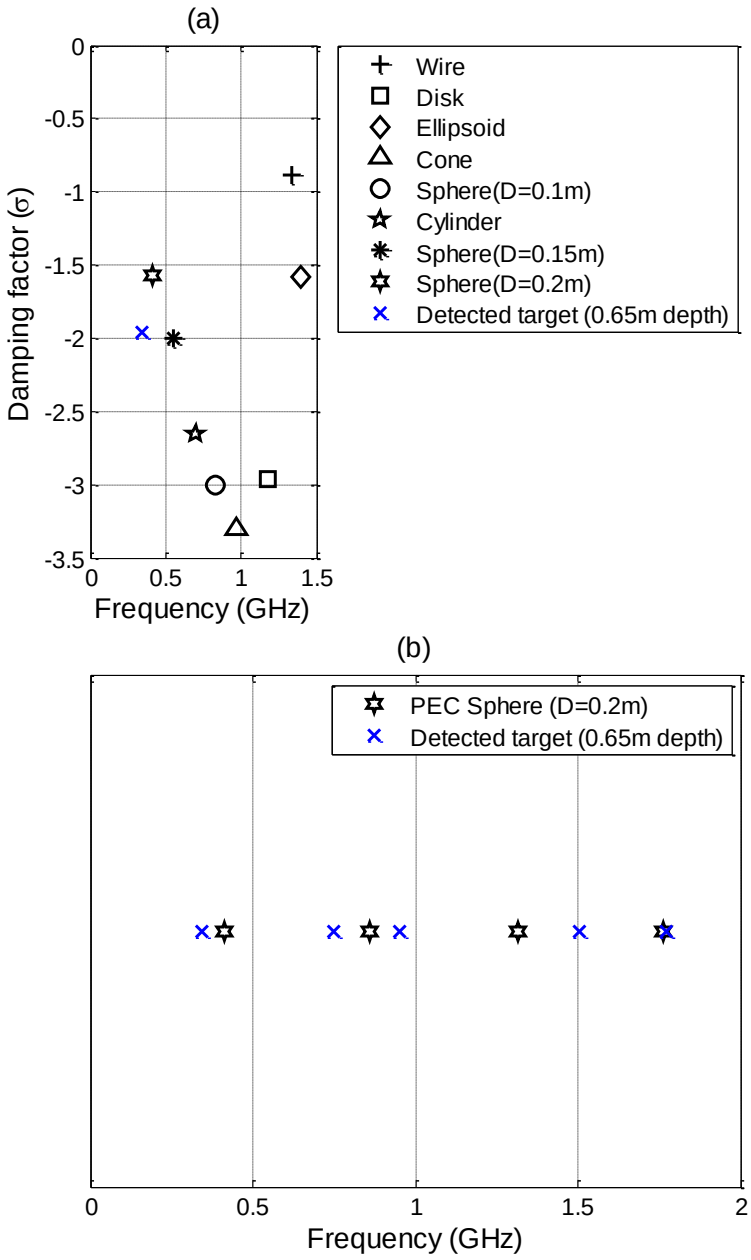

Figure 5.22 Pole Library vs. Computed poles of the unknown target using the MP method (air cavity under sandy soil at 0.65m depth); (a) First order pole, (b) Resonant frequency.

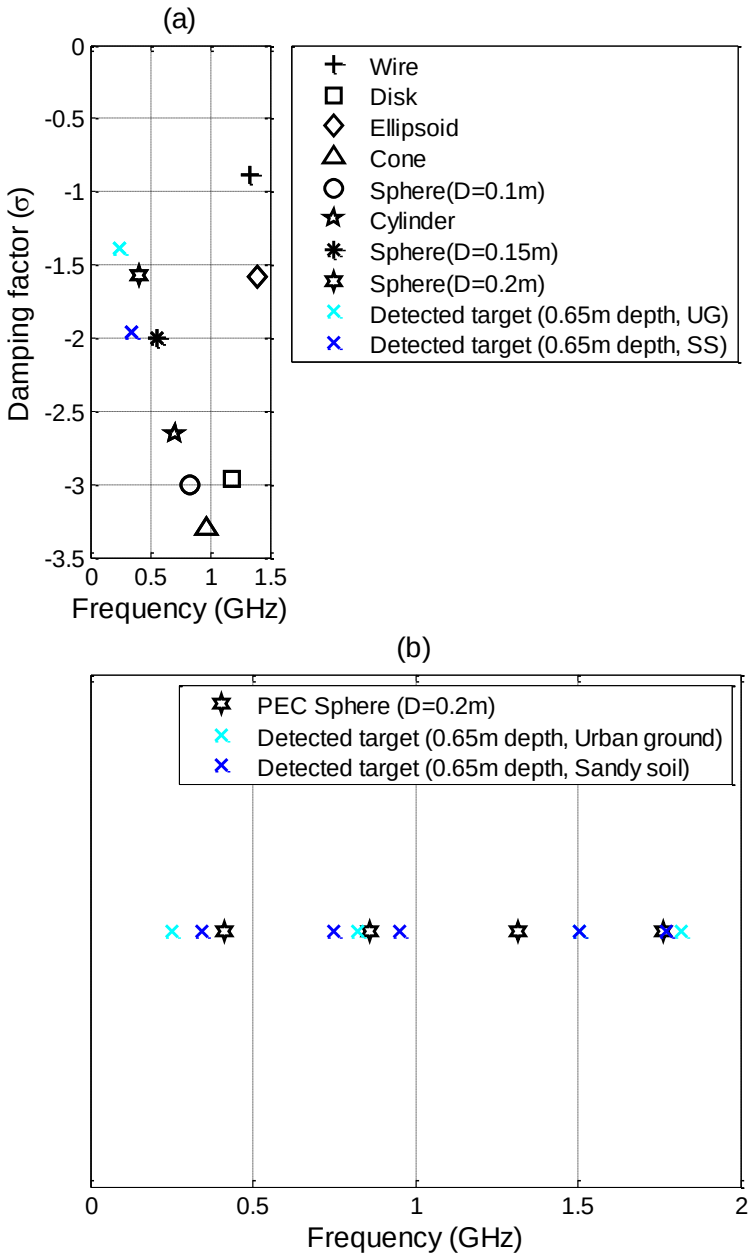

Figure 5.23 Pole Library vs. Computed poles of the unknown targets using the MP method (air cavities under urban ground and sandy soil at 0.65m depth); (a) First order pole, (b) Resonant frequency.

6. CONCLUSION

A new methodology for detection and identification of objects in free space or objects located above the ground, or under the ground has been developed. The main idea of the proposed methodology starts from finding the natural frequency of an object corresponding to its instinct characterization using the Singularity Expansion Method (SEM). Each object has its natural frequencies from the late time response in typical transient temporal response of scatterers with various shapes and constitutions, in free space, on ground, underground.

Among many techniques to extract singularities of the EM response of an object, the Cauchy method and the Matrix Pencil (MP) method have been chosen for identification of an unknown object. The unique feature of the Cauchy method is that it is not necessary to distinguish between the early time and the late time regions where the SEM formulation holds, and this may make this procedure accurate and efficient. Comparing the SEM poles of a PEC sphere and the computed poles from the Cauchy method, it is proved that one can use the natural poles of an object using the Cauchy method because the natural poles from both methods match each other. In this dissertation, a library of poles of the seven objects (two spheres, a wire, a disk, an ellipsoid, a cone, and a cylinder) are generated using the Cauchy method. The seven objects can be uniquely identified from their natural poles irrespectively with illuminated surface of the object for the different observation angle. The procedure to extract natural poles of objects using the Cauchy method in the frequency domain has illustrated in detail.

Another methodology has been also introduced for detecting and identifying the unknown object in the time domain. For the simulation model, one transmitter (dipole antenna) and two receivers (dipole antennas) are utilized to have the response of unknown object. One can obtain the received currents of the unknown object from the left and the right receivers after the deconvolving procedure. From the deconvolved response in the time domain, one can estimate the accurate coordinates (radial distance and azimuthal angle) of the unknown object using the time difference between the impulses of the left and the right receivers based on the Time-Difference-of-Arrival (TDOA). The MP method was applied to extract the natural poles of the unknown object using only late time response of its transient temporal response. By generating the pole library using frequency domain data and the actual poles computed using the time domain data, the correlation between the two pole sets obtained using totally different methodologies provides a robust identification procedure. The poles using responses from data generated in different domains can be used for comparison purpose. It is also proved that one can detect and identify the unknown object with high accuracy using library poles of objects, computed natural poles from the late time response of the unknown object, and the TDOA.

Even in the presence of noise the unknown object is identifiable by the proposed methodology because the MP method is the robust pole extraction technique in noisy environment. Several simulation examples in free space have explained this novel and accurate way for detection and identification of multiple objects. The drawback in this methodology is that if there are more than two objects, the accuracy of the identification for the rear object might decrease because of interaction effects between objects.

This dissertation also verifies that the proposed methodologies can be applied for not only an object in free space case but also an object on ground case or an object underground case. The extracted natural poles are compared with the natural poles of library poles of various objects. It gives very accurate result in the case even though the object is on urban ground. If the spherical air cavity is under urban ground or sandy soil then the extraction process is relatively less accurate but it can still guess the unknown object.

The main contributions of this dissertation are to illustrate that a target signature can be extracted using either the frequency domain technique or the time domain technique, separately. The proposed methodology can give us a robust identification procedure of the unknown objects using both the frequency domain (Cauchy method) and the time domain (Matrix Pencil method and TDOA) techniques, simultaneously. Also, the frequency sweeping radar using one transmitter and two receivers is the first proposed system to detect and identify the unknown objects. I think the frequency sweeping radar can be built on a truck using one transmitter, two receivers, and a network analyzer. The benefit of the dissertation is that the unknown object can be detected and identified for objects in free space or objects located above the ground, or under the ground cases using the proposed methodologies. For future work, I will study identification of a dielectric object.

BIBLIOGRAPHY

[1] M. I. Skolnik, *Introduction to Radar Systems*, 2nd ed. McGraw-Hill, 1981.

[2] C. E. Baum, "On the singularity expansion method for the solution of electromagnetic interaction problems," Air Force Weapons Laboratory, EMP Interaction Note 88, Dec. 11, 1971.

[3] K. Chen and D. Westmoreland, "Impulse response of a conducting sphere based on singularity expansion method," in *Proc. IEEE*, vol. 69, no. 6, pp. 747-750, June 1981.

[4] C. E. Baum, E. J. Rothwell, K. Chen, and D. P. Nyquist, "The singularity expansion method and its application to target identification," in *Proc. IEEE*, vol. 79, no. 10, pp. 1481-1492, Oct. 1991.

[5] G. H. Goldman, "Characterization of the effects of cavities and canopies on radar target signatures," Army Research Laboratory, ARL-TN-154, Feb. 2000.

[6] R. Prony, "Essai expérimental et analytique: sur les lois de la dilatabilité des fluides élastiques et sur celles de la force expansive de la vapeur de l'eau et de la vapeur de l'alkool, à différentes températures," Journal de l'École Polytechnique Floréal et Plairial, an III , vol. 1, cahier 22, pp. 24-76, 1795.

[7] A. S. Householder, "On Prony's method of fitting exponential decay curves and multiple-hit survival curves," Oak Ridge National Laboratory, ORNL-455, Sep. 1949.

[8] M. L. Van Blaricum and R. Mittra, "A technique for extracting the poles and residues of a system directly from its transient response," *IEEE Trans. Antennas Propag*., vol. AP-23, no. 6, pp. 777-781, Nov. 1975.

[9] M. A. Rahman and K. Yu, "Total least squares approach for frequency estimation using linear prediction," *IEEE Trans. Acoust., Speech Signal Process*., vol. ASSP-35, no. 10, pp. 1440-1454, Oct. 1987.

[10] J. Kergall, P. Pouliguen, M. Legoff, and Y. Chevalier, "Complex natural resonances extracted from radar signatures measured in time domain with UWB laboratory system," in *Proc. IEEE AP-S Int. Symp.*, pp.1346-1349, 1999.

[11] Y. Hua and T. K. Sarkar, "Generalized pencil-of-function method for extracting poles of an EM system from its transient response," *IEEE Trans. Antennas Propag*., vol. 37, no. 2, pp. 229-234, Feb. 1989

[12] Y. Hua and T. K. Sarkar, "Matrix pencil method for estimating parameters of exponentially damped/undamped sinusoids in noise," *IEEE Trans. Acoust., Speech Signal Process*., vol. 38, no. 5, pp. 814-824, May 1990.

[13] T. K. Sarkar and O. M. Pereira-Filho, "Using the matrix pencil method to estimate the parameters of a sum of complex exponentials," *IEEE Antennas Propag. Mag*., vol. 37, no.1, pp. 48-55, Feb. 1995.

[14] R. S. Adve, T. K. Sarkar, O. M. Pereira-Filho, and S. M. Rao, "Extrapolation of time-domain responses from three-dimensional conducting objects utilizing the matrix pencil technique," *IEEE Trans. Antennas Propag*., vol. 45, no. 1, pp. 147-156, Jan. 1997.

[15] Y. Wang and N. Shuley, "Complex resonate frequencies for the identification of simple objects in free space and lossy environments," *Prog. Electromagn. Res.*, vol. PIER 27, pp. 1-18, 2000.

[16] A. L. Cauchy, “Sur la formule de Lagrange relative a l’interpolation,” Analyse Albebrique, Paris, 1821.

[17] K. Kottapalli, T. K. Sarkar, Y. Hua, E. K. Miller, and G. J. Burke, “Accurate computation of wide-band response of electromagnetic systems utilizing narrow-band information,” *IEEE Trans. Microw. Theory Tech*., vol. 39, no. 4, pp. 682-687, Apr. 1991.

[18] J. Yang and T. K. Sarkar, “Interpolation/extrapolation of radar cross section (RCS) data in the frequency domain using the Cauchy method,” *IEEE Trans. Antennas Propag.*, vol. 55, no. 10, pp. 2844-2851, Oct. 2007.

[19] J. Chauveau, N. de Beaucoudrey, and J. Saillard, “Selection of contributing natural poles for the characterization of perfectly conducting targets in resonance region,” *IEEE Trans. Antennas Propag*., vol. 55, no. 9, pp. 2610-2617, Sep. 2007.

[20] W. Lee, T. K. Sarkar, H. Moon, and M. Salazar-Palma, “Computation of the natural poles of an object in the frequency domain using the Cauchy method,” *IEEE Antennas Wireless Propag. Lett.*, vol. 11, pp. 1137-1140, Oct. 2012.

[21] D. L. Moffatt and K. A. Shubert, “National resonance via rational approximants,” *IEEE Trans. Antennas Propag*., vol. AP-25, no. 5, pp. 657-660, Sep. 1977.

[22] C. K. Chui and A. K. Chan, “A two-sided rational approximation method for recursive digital filtering,” *IEEE Trans. Acoust., Speech Signal Process*., vol. ASSP-27, no. 2, pp. 141-145, April 1979.

[23] R. Kumaresan, “On a freqeuncy domain analog of Prony’s method,” *IEEE Trans. Acoust., Speech Signal Process*., vol. 38, no. 1, pp. 168-170, Jan. 1990.

[24] F. Schlagenhaufer, K. Fynn, "Rational approximation of transfer functions for radiating structures," *IEEE Int. Symp.*, vol. 2, pp.864-869, 2001.

[25] L. Li and C. H. Liang, "Analysis of resonance and quality factor of antenna and scattering systems using complex frequency method combined with model-based parameter estimation," *Prog. Electromagn. Res.*, PIER 46, pp. 165-188, 2004.

[26] W. Lee, T. K. Sarkar, H. Moon, and L. Brown, "Detection and identification using natural frequency of the perfect electrically conducting (PEC) sphere in the frequency domain and time domain," in *Proc. IEEE AP-S/URSI Int. Symp.*, pp.2334-2337, July 2011.

[27] W. Lee, T. K. Sarkar, H. Moon, and M. Salazar-Palma, "Identification of multiple objects using their natural resonant frequencies," *IEEE Antennas Wireless Propag. Lett.*, vol. 12, pp. 54-57, Mar. 2013.

[28] A. V. Oppenheim, R. W. Schafer, and J. R. Buck, Discrete-time Signal Processing, 2nd ed. Upper Saddle River, NJ: Prentice Hall, 1999.

[29] D. S. Watkins, *Fundamentals of Matrix Computation*, 3rd ed. Hoboken, NJ: Wiley, 2010.

[30] T. K. Sarkar, M. C. Wicks, M. Salazar-Palma, and R. J. Bonneau, *Smart Antennas*, Hoboken, NJ: Wiley, 2003, Appendix C.

[31] S. Van Huffel, "Analysis of the Total Least Squares Problem and its use in Parameter Estimations," Ph.D. dissertation, Dept. Elect. Eng., Katholieke Univ., Leuven, Belgium, 1990.

[32] Y. Zhang, T. K. Sarkar, X. Zhao, D. Garcia-Donoro, W. Zhao, M. Salazar-Palma, and S. Ting, *Higher Order Basis Based Integral Equation Solver* (*HOBBIES*), Hoboken, NJ: Wiley, 2012.

[33] K. W. Cheung, H. C. So, W. K. Ma, and Y. T. Chan, "Least squares algorithms for time-of-arrival-based mobile location," *IEEE Trans. Signal Process*., vol. 52, no. 4, pp. 1121-1128, Apr. 2004.

[34] C. A. Grosvenor, R. T. Johnk, J. Baker-Jarvis, M. D. Janezic, and B. Riddle, "Time-Domain Free-Field Measurements of the Relative Permittivity of Building Materials,", *IEEE Trans. Instrumentation and Measurement*, vol. 58, no. 7, pp. 2275-2282, July 2009.

[35] "Pappus's theorem", [Online]. Available: http://www.ies.co.jp/math/java/geo/pappus/pappus.html.

[36] J. D. Kraus, *Antennas*, 2nd ed. McGraw-Hill, 1988, Appendix A.

[37] M. Lazarus, "The great spectrum famine," *IEEE Spectrum Magazine*, pp. 26-31, Oct. 2010.

[38] D. Ghosh, "UWB Antenna Design for Signature Extraction of Buried Targets," Ph.D. dissertation, Dept. Elect. Eng. and Computer Sci., Syracuse Univ., NY, USA, 2008.

VITA

Name of Author: Woojin Lee

Education:

M.S., Gwangju Institute of Science and Technology, Republic of Korea February 2003

B.E., Korea Military Academy, Republic of Korea March 1998

Awards and Honors:

Member of the Phi Beta Delta International Honor Society March 2009

Experience: Army Officer of Republic of Korea

Planning officer for introducing the Signal Intelligence System Mar. 2005 to Sept. 2007

Tank Company Commander September 2003 to March 2005

Tank Platoon Leader July 1999 to October 2000

Armored Reconnaissance Platoon Leader July 1998 to July 1999

Publications:

Journal

[1] W. Lee, T. K. Sarkar, H. Moon, and M. Salazar-Palma, "Identification of multiple objects using their natural resonant frequencies," *IEEE Antennas Wireless Propag. Lett.*, vol. 12, pp. 54-57, Mar. 2013.

[2] W. Lee, T. K. Sarkar, H. Moon, and M. Salazar-Palma, "Computation of the natural poles of an object in the frequency domain using the Cauchy method," *IEEE Antennas Wireless Propag. Lett.*, vol. 11, pp. 1137-1140, Oct. 2012.

[3] W, Lee, T. K. Sarkar, J. Koh, H. Moon, and M. Salazar-Palma, "Generation of a wide-band response using early-time and middle-frequency data through the use of orthogonal functions," *Prog. Electromagn. Res.* M.(PIERM), Vol. 25, pp. 115–126, July 2012.

[4] W, Lee, T. K. Sarkar, J. Koh, H. Moon, and M. Salazar-Palma, "Generation of a wide-band response using early-time and middle-frequency data through the Laguerre functions," *Prog. Electromagn. Res.* Lett.(PIERL), Vol. 30, pp. 115–123, Mar. 2012.

Conference

[1] T. Tantisopharak, M. Krairiksh, H. Moon, W. Lee, and T. K. Sarkar, "Identification of maturity of fruit in the frequency domain using its natural frequencies," in Proc. IEEE APCAP, Aug. 2012.

[2] W. Lee, T. K. Sarkar, H. Moon, and L. Brown, "Detection and identification using natural frequency of the perfect electrically conducting (PEC) sphere in the frequency domain and time domain," in *Proc. IEEE AP-S/URSI Int. Symp.*, pp.2334-2337, July 2011.